

EXISTENCE OF THE TETRAGONAL AND RHOMBOHEDRAL DEFORMATION FAMILIES OF THE GYROID

HAO CHEN

ABSTRACT. We provide an existence proof for two 1-parameter families of embedded triply periodic minimal surfaces of genus three, namely the tG family with tetragonal symmetry that contains the gyroid, and the rGL family with rhombohedral symmetry that contains the gyroid and the Lidinoid, both discovered numerically in the 1990s. The existence was previously proved within a neighborhood of the gyroid and the Lidinoid, using Weierstrass data defined on branched rectangular tori. Our main contribution is to extend the technique to branched tori that are not necessarily rectangular.

1. INTRODUCTION

A triply periodic minimal surface (TPMS) is a minimal surface $M \subset \mathbb{R}^3$ that is invariant under the action of a 3-dimensional lattice Λ . The quotient surface M/Λ then lies in the flat 3-torus \mathbb{R}^3/Λ . The genus of M/Λ is at least three, and TPMSs of genus three are abbreviated as TPMSg3s.

Due to their frequent appearance in nature and science, the study of TPMSs enjoys regular contributions from physicists, chemists, and crystallographers. Their discoveries of interesting examples often precede the rigorous mathematical treatment. The most famous example would be the gyroid discovered in 1970 by Alan Schoen [Sch70], then a scientist at NASA. Unlike other TPMSs known at the time, the gyroid does not contain any straight line or planar curvature line, hence it cannot be constructed by the popular conjugate Plateau method [Kar89]. The second TPMSg3 with this property was discovered only twenty years later in 1990, by chemists Lidin and Larsson [LL90], and known nowadays as the Lidinoid. The gyroid and the Lidinoid were later proved to be embedded by mathematicians Große-Brauckmann and Wohlgemuth [GBW96].

By intentionally reducing symmetries of the gyroid and the Lidinoid, two 1-parameter families of TPMSg3s, which we call tG and rGL, were discovered in [FHL93, FH99]; see also [STFH06]. Both families contain the gyroid and retain respectively its rhombohedral and tetragonal symmetries. Remarkably, none of these surfaces contains straight lines or planar curvature lines. Moreover, tG and rGL surfaces are not contained in the 5-parameter family of TPMSg3s constructed by Meeks [Mee90]. Today, the only other explicitly known TPMSg3s outside Meeks' family are the recently discovered 2-parameter families oH (containing Schwarz' H) [CW18b] and o Δ [CW18a].

In [FHL93, FH99], periods were closed only numerically, producing convincing images that leave no doubt for the existence of tG and rGL. Although the importance of numerical discoveries could never be overestimated, the lack of a formal existence proof (that does not involve any numerics) often indicates room for better mathematical understanding. Indeed, our approach in the current paper brings new ways to visualize the tG and rGL surfaces.

Date: September 11, 2019.

2010 Mathematics Subject Classification. Primary 53A10.

Key words and phrases. Triply periodic minimal surfaces.

H. Chen is supported by Individual Research Grant from Deutsche Forschungsgemeinschaft within the project "Defects in Triply Periodic Minimal Surfaces", Projektnumer 398759432.

An attempt of existence proof for tG and rGL was carried out by Weyhaupt [Wey06, Wey08]. He used the flat structure technique first introduced by Weber and Wolf [WW98, WW02]. Unlike [FHL93, FH99] who parameterized TPMSg3s on branched spheres, Weyhaupt defined Weierstrass data on branched tori. In particular, the gyroid and the Lidinoid, as well as the classical Schwarz' surfaces, are parameterized on rectangular tori.

Weyhaupt showed that there exists a continuous 1-parameter family of tori that solve the period problems for tG. This family contains the rectangular torus of the gyroid and “does not deform too much from rectangular”. See [Wey08, Lemmas 4.3 & 4.5]¹ for precise statements. Similar results were obtained for an “rG” family near the gyroid and an “rL” family near the Lidinoid. These conclusions, in Weyhaupt’s own word [Wey06, §6.0.6], only asserted “the existence of an analytic family of possibly small parameter space”. In particular, it was not clear that rL and rG are part of the same family, which we call rGL in the current paper. Weyhaupt was aware that, to get away from small neighborhoods, one needs to deal with Weierstrass data defined on non-rectangular tori.

In the current paper, we provide an existence proof for the whole tG and rGL families. More precisely, our main results are

Theorem 1.1 (tG). *There is a 1-parameter family of TPMSg3s containing the gyroid, which we call tG, with the following properties:*

- *Each TPMSg3 in tG admits a screw symmetry of order 4 around a vertical axis and rotational symmetries of order 2 around horizontal axes.*
- *tG intersects the tD family and tends to 4-fold saddle towers in the limit.*

Theorem 1.2 (rGL). *There is a 1-parameter family of TPMSg3s containing the gyroid and the Lidinoid, which we call rGL, with the following properties:*

- *Each TPMSg3 in rGL admits a screw symmetry of order 3 around a vertical axis and rotational symmetries of order 2 around horizontal axes.*
- *rGL intersects the rPD family and tends to 3-fold saddle towers in the limit.*

Two properties are listed in each of the statements above. The first specifies the expected symmetries. Weyhaupt [Wey06, Wey08] has proved that TPMSg3s with these symmetries exist in a neighborhood of the gyroid and the Lidinoid. The significance of our work lies in the second property, which states that the 1-parameter family continues in one direction until intersecting Meeks’ family and, in the other direction, to degenerate limits where curvature blows up.

Let us give a preview of our approach.

We will use the same Weierstrass parameterization as Weyhaupt, only more explicit in terms of the Jacobi sn function. Explicit computations are not possible for non-rectangular tori. However, we notice from the Weierstrass data that the associate family of every tG or rGL surface contains a “twisted catenoid”. These are minimal annuli bounded by curved squares or triangles. Then we generalize a point of view from [GBW96]: As one travels along the associate family, the twisted catenoids open up into gyrating ribbons, and the surface is immersed if adjacent ribbons “fit exactly into each other”. This leads to two expressions for the associate angle, and the period problem asks to find tori for which the two expressions are equal.

It turns out that the torus of an rG or tGL surface is well defined up to a hyperbolic reflection group. The boundary of its fundamental domain corresponds to classical Schwarz’ TPMSg3s, which we understand very well. This already allows us to conclude the existence of the families, all the way to the degenerate limits. We then investigate the asymptotic behavior of the period problem at the limits of the tD or rPD family. This allows us to locate the intersections with Meeks’ family. A uniqueness statement hidden in Weyhaupt’s work [Wey06, Wey08] implies that the families must contain the gyroid, whose embeddedness then ensures the embeddedness of all TPMSg3s in the families.

The paper is organized as follows.

¹[Wey08, Lemma 4.4] is a typo. Weyhaupt meant $b > 0$ on B and $b < 0$ on Y .

In Section 2, we describe the symmetries of tG and rGL surfaces. This is done by relaxing a rotational symmetry of the classical tP, H and rPD surfaces to a screw symmetry of the same order. We will define a family \mathcal{T} of TPMSg3s with order-4 screw symmetries, which contains the tG family as well as Schwarz' classical tP, tD and CLP families; we also define a family \mathcal{R} of TPMSg3s with order-3 screw symmetries, which contains the rGL family as well as the classical H and rPD families.

In Section 3, we deduce the Weierstrass data for surfaces in \mathcal{T} and \mathcal{R} from their symmetries. We first prove that surfaces with screw symmetries can be represented as branched covers of flat tori. The symmetries then force the branch points at 2-division points of the tori. This allows us to write down the Weierstrass data explicitly in terms of the Jacobi elliptic function sn . In the end of this section, we establish a convention on the choice of the torus parameter.

In Section 4, we reduce the period problems to just one equation using the twisted catenoids and the ribbon picture. We then give the existence proof in Section 5. The asymptotic analysis is technical hence postponed to the Appendix.

Section 6 is dedicated to discussions. We point out that tG and rGL families provide bifurcation branches that were missing in [KPS14]. We also observe reflection groups that act on \mathcal{T} and \mathcal{R} , which provide new ways to visualize the known TPMSg3s. This motivates us to conjecture that the known surfaces are the only surfaces in \mathcal{T} and \mathcal{R} . The first step for proving the conjecture is to confirm a uniqueness statement for tG and rGL surfaces.

We assume some familiarity of the reader with classical TPMSg3s including Schwarz' surfaces, the gyroid, and the Lidinoid. If this is not the case, it is recommended to take a look into [FH92, GBW96, Wey06].

Acknowledgement. The author is grateful to Matthias Weber for constant and helpful conversations. I also thank the anonymous referee, whose useful suggestions to a preliminary version lead to significant improvement of the paper.

2. SYMMETRIES

The tG and rGL families were discovered by relaxing the symmetries of classical surfaces [FHL93, FH99]. It is then a good idea to first recall some classical TPMSg3s, namely the 1-parameter families tP, rPD and H. We recommend the following way to visualize.

tP: Consider a square catenoid, i.e. a minimal annulus bounded by two horizontal squares related by a vertical translation. Then the order-2 rotations around the edges of the squares generate a tP surface, and any tP surface can be generated in this way.

H: Consider a triangular catenoid, i.e. a minimal annulus bounded by two horizontal equiangular triangles related by a vertical translation. Then the order-2 rotations around the edges of the triangles generate an H surface, and any H surface can be generated in this way.

rPD: Similar to the H surfaces, the only difference being that one bounding triangle is reversed.

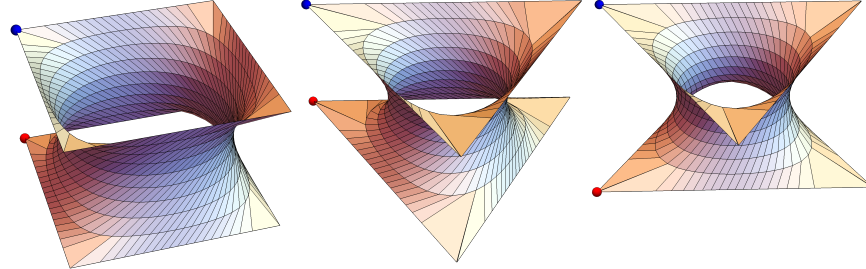


FIGURE 1. The catenoids that generate tP (left), H (middle) and rPD (right) surfaces.

The catenoids that generate tP, H and rPD surfaces are shown in Figure 1. The 1-parameter families are obtained by vertically “stretching” the catenoids. These families are, remarkably, already known to Schwarz [Sch90]. Reflections might be their most famous and obvious symmetries. But we highlight the following symmetries that will help understanding tG and rGL surfaces.

Inversions: These are orientation-reversing symmetries shared by every TPMSg3. Meeks [Mee90] proved that every TPMSg3 M/Λ has eight inversion centers at the points where Gaussian curvature vanishes. We will come back on that later.

For tP surfaces, the eight inversion centers are at the middle points of the eight bounding edges. For H and rPD surfaces, they are at the middle points of the six bounding edges and the two vertices (up to Λ) of the bounding triangles.

The catenoids above can be seen as the quotient of M/Λ over the inversions. So the fundamental unit M/Λ consists of two catenoids. See the top parts of Figures 2 and 3 for how their boundaries identify.

Order-2 rotations around horizontal axes: These are orientation-preserving symmetries that swap the bounding squares or triangles. So their axes lie in the middle horizontal plane, parallel to the edges and diagonals of the bounding squares or triangles. Up to the inversions, each tP surface has four such rotations, and each H or rPD surface has three.

Rotations around vertical axes: Up to the inversions, each of these TPMSg3s has exactly one such rotation. The vertical axis passes through the centers of the bounding squares or triangles. This symmetry is orientation-preserving. Its order is 4 for tP and 3 for H and rPD.

Roto-reflections: A roto-reflection is composed of a rotation around the normal vector at a vertex of the bounding squares or triangles, followed by a reflection in the tangent plane at this vertex. Note that these vertices have vertical normal vectors, hence are poles and zeros of the Gauss map. These symmetries are orientation-reversing. Their order is 4 for tP and 6 for H and rPD.

These symmetries are not independent.

- The rotation around the vertical axis is the composition of two order-2 rotations around horizontal axes.
- Conversely, in the presence of the rotation around the vertical axis, one order-2 rotational symmetry around a horizontal axis implies all the other.
- The roto-reflection arises from the screw symmetry and the inversions.
- For the H and rPD surfaces, [Wey06, Proposition 3.12] asserts that the order-3 rotation around the vertical axis implies the inversion symmetries in the vertices of the triangles.

Hence for TPMSg3s, the symmetries listed above can all be recovered from only two symmetries: the rotational symmetry (of order 3 or 4) around the vertical axis and an order-2 rotational symmetry around a horizontal axis.

It was observed in [GBW96, Lemma 4] that, as one travels along the associate family, all these symmetries are preserved, except for the rotational symmetry around the vertical axis, which is reduced to a screw symmetry. Recall that a screw transform is composed of a rotation and a translation in the rotational axis. The reduction of symmetry can be seen by noticing that the horizontal rotation axes are no longer in the same horizontal plane, hence their compositions induce screw transforms, instead of rotations. Note that the interdependences of the symmetries remain the same after this reduction. In particular, the argument for [Wey06, Proposition 3.12] applies word by word to the order-3 screw symmetry.

The gyroid is in the associate family of Schwarz’ P surface, which is in the intersection of tP and rPD families. Hence the gyroid admits a screw symmetry around a vertical axis and an order-2 rotational symmetry around a horizontal axis. The order of the screw symmetry is 3 or 4, depending on which rotational axes of P is placed vertically. Similarly, the Lidinoid is in the associate family of an H surface, hence admits an order-3 screw symmetry around a vertical axis and an order-2 rotational symmetry around a horizontal axis. As we have discussed, all other symmetries listed above can be recovered from these two.

Remark 2.1. Interestingly, no other embedded surface is contained in the associate families of the tP, H or rPD surfaces. This follows from a uniqueness statement hidden in the argument of Weyhaupt [Wey06], as we will explain in Section 6.

In the remaining of the paper, for the sake of a uniform treatment of Schwarz' surfaces and the deformations of the gyroid, we will see rotations as screw transforms with 0 translation. The paper aims at the following two sets of TPMSg3s

- \mathcal{T} consists of embedded TPMSg3s that admit order-4 screw symmetries around vertical axes and order-2 rotational symmetries around horizontal axes.
- \mathcal{R} consists of embedded TPMSg3s that admit order-3 screw symmetries around vertical axes and order-2 rotational symmetries around horizontal axes.

Schwarz' tP surfaces and the gyroid belong to \mathcal{T} . The conjugates of the tP surfaces, namely Schwarz' tD surfaces, belong to \mathcal{T} . We will see that Schwarz' CLP surfaces also belong to \mathcal{T} . Our main Theorem 1.1 states that there exists another 1-parameter family in \mathcal{T} , denoted by tG, that contains the gyroid.

Schwarz' rPD, H surfaces, as well as the gyroid and the Lidinoid belong to \mathcal{R} . Our main Theorem 1.2 states that there exists another 1-parameter family in \mathcal{R} , denoted by rGL, that contains the gyroid and the Lidinoid.

3. WEIERSTRASS PARAMETERIZATION

We use [Mee90] for general reference about TPMSg3.

Let M be a TPMS invariant under the lattice Λ . Meeks [Mee90] proved that M/Λ is of genus three if and only if it is *hyperelliptic*, meaning that it can be represented as a two-sheeted branched cover $M/\Lambda \rightarrow \mathbb{S}^2$ over the sphere. The Gauss map G provides such a branched covering. If M/Λ is of genus three, the Riemann-Hurwitz formula implies eight branch points of G . We call the corresponding ramification points on M/Λ *hyperelliptic points*. An inversion (in the ambient space \mathbb{R}^3) in any of the hyperelliptic points induces an isometry that exchanges the two sheets.

Let $z_1, \dots, z_8 \in \mathbb{C}$ be the stereographic projections of the Gauss map at the branch points. Now consider the hyperelliptic Riemann surface of genus three defined by

$$w^2 = P(z) = \prod_{i=1}^8 (z - z_i).$$

Then we have the following Weierstrass parameterization for M/Λ :

$$(1) \quad (z, w) \mapsto \operatorname{Re} \int^{(z,w)} \frac{(1-z^2, (1+z^2)i, 2z)}{w} dz.$$

This parameterization has been widely used for constructing TPMSg3s, ranging from the classical example of Schwarz' [Sch90] to the tG and rGL families discovered in [FHL93, FH99].

We use the following form of Weierstrass parameterization that traces back to Osserman [Oss64],

$$(2) \quad \Sigma \ni p \mapsto \operatorname{Re} \int^p (\omega_1, \omega_2, \omega_3) = \operatorname{Re} \int^p \left(\frac{1}{2} \left(\frac{1}{G} - G \right), \frac{i}{2} \left(\frac{1}{G} + G \right), 1 \right) dh \in \mathbb{R}^3.$$

Here Σ is a Riemann surface, on which $\omega_1, \omega_2, \omega_3$ must all be holomorphic. In particular, the holomorphic differential $\omega_3 = dh$ is called the *height differential*. G denotes (the stereographic projection of) the Gauss map. By comparing (1) and (2), one sees the correspondence $G = z$ and $dh = zdz/w$ (up to a scaling factor 2). The triple (Σ, G, dh) is called Weierstrass data.

The purpose of this section is to determine the Weierstrass data for surfaces in \mathcal{T} and \mathcal{R} from their symmetries. In particular, Σ will be a branched torus, whose branch points are determined in Lemmas 3.4 and 3.5. The height differential is determined in Lemma 3.2, and the Gauss map is explicitly given in Lemma 3.7.

3.1. Weierstrass data on tori. Surfaces in \mathcal{T} and \mathcal{R} all admit screw symmetries. The following proposition justifies our choice of branched tori for Σ .

Proposition 3.1. *If a TPMSg3 M admits a screw symmetry S , then $(M/\Lambda)/S$ is of genus one.*

Recall that we consider rotational symmetries as special screw symmetries, for which the proposition was proved in [Wey08, Proposition 2.8] but with minor flaws. Hence we include a proof here for completeness.

Proof. The height differential dh is invariant under S , hence descends holomorphically to the quotient $(M/\Lambda)/S$. Since there is no holomorphic differential on the sphere, the genus of $(M/\Lambda)/S$ cannot be 0.

Recall the Riemann–Hurwitz formula

$$g = n(g' - 1) + 1 + B/2.$$

In our case, $g = 3$ is the genus of M/Λ , g' is the genus of $(M/\Lambda)/S$, n is the degree of the quotient map, and B is the total branching number. Since the order of a screw symmetry is at least two, we conclude immediately that $g' < 3$.

It remains to eliminate the case $g' = 2$. Weyhaupt’s argument in [Wey08] did not accomplish this task. We proceed as follows². Without loss of generality, we may assume the screw axis to be vertical. As Weyhaupt argued, when $g' = 2$ we have necessarily $n = 2$, in which case $G \circ S = -G$. In the parameterization (1), since $dh = zdz/w$ is invariant under $z \mapsto -z$, so must the polynomial $w^2 = P(z)$, hence we can write $P(z) = Q(z^2)$, where Q is a polynomial of degree 4. Then $w^2 = Q(z)$ defines the quotient surface, whose genus is $g' = 1$. So $g' = 1$ is the only possibility. \square

The height differential dh , being a holomorphic 1-form on the torus, must be of the form $re^{-i\theta}dz$. Varying the modulus r only results in a scaling. Varying the argument θ gives the associate family, so we call θ the *associate angle*. The following lemma then applies to all TPMSg3s in \mathcal{T} and \mathcal{R} .

Lemma 3.2. *If a TPMSg3 M/Λ with a screw symmetry S is represented on the branched cover of the torus $(M/\Lambda)/S$, then up to the scaling, the height differential dh must be the lift of $e^{-i\theta}dz$ (note the sign!).*

3.2. Locating branch points. By [KK79, Lemma 2(ii)], we know that the order of the screw symmetry S must be 2, 3 or 4. This follows easily from a result of Hurwitz [Hur32], cited in [KK79] as Lemma 1. Moreover, if the order of S is prime, the following formula from [FK92] allows us to calculate the number of fixed points:

$$|\text{fix}(S)| = 2 + \frac{2g - 2g' \text{order}(S)}{\text{order}(S) - 1}.$$

In particular, a screw symmetry of order 2 fixes exactly four points, and a screw symmetry of order 3 fixes exactly two points. The following lemma follows from the same argument as in [Wey06, Lemmas 3.9, 3.13].

Lemma 3.3.

- If a TPMSg3 M/Λ admits a screw symmetry S of order 2, then G^2 descends to an elliptic function on the torus $(M/\Lambda)/S$ with two simple zeros and two simple poles.
- If M/Λ admits a screw symmetry S of order 3, then G^3 descends to an elliptic function on the torus $(M/\Lambda)/S$ with a double-order zero and a double-order pole.

We now try to locate the branch points of the covering map for surfaces in \mathcal{T} and \mathcal{R} . Since the ramification points on M/Λ are all poles and zeros of the Gauss map, our main tool is naturally Abel’s Theorem, which states that the difference between the sum of poles and the sum of zeros (counting multiplicity) is a lattice point.

A surface in \mathcal{T} admits a screw symmetry S of order 4, S^2 is then a screw symmetry of order 2. Recall that S and the inversions induce roto-reflectional symmetries of order 4 centered at the poles and zeros of the Gauss map. They descend to the quotient torus $(M/\Lambda)/S^2$ as inversions in the branch points of the covering map.

²This argument is communicated by Matthias Weber.

Lemma 3.4 (Compare [Wey06, Lemma 3.10]). *Let M be a TPMSg3 admitting a screw symmetry S of order 4, hence parameterized on a branched double cover of the torus $(M/\Lambda)/S^2$. If one branch point is placed at 0, then the other branch points must be placed at the three 2-division points of the torus.*

Proof. We may assume that the branch point at 0 corresponds to a zero of G^2 . If a pole p is not at any 2-division points, $-p$ must be a different pole by the roto-reflection. Then Abel's Theorem forces the other zero to be at a lattice point, which is absurd. So both poles must be placed at 2-division points. Then Abel's Theorem forces the other zero at the remaining 2-division point. \square

Note that the screw symmetry of order 4 descends to the quotient torus as the translation that swaps the zeros.

Lemma 3.5 ([Wey06, Lemma 3.13]). *Let M be a TPMSg3 admitting a screw symmetry S of order 3, hence parameterized on a branched triple cover of the torus $(M/\Lambda)/S$. If one branch point is placed at 0, then the other branch points must be placed at the three 2-division points of the torus.*

Proof. We may assume that the branch point at 0 corresponds to a double-order zero of G^3 . Then the Abel's Theorem forces the double-order pole to be at a 2-division point. \square

3.3. An explicit expression for the Gauss map. The locations of poles and zeros determine an elliptic function up to a complex constant factor. Elliptic functions with poles and zeros at lattice points and 2-division points are famously given by Jacobi elliptic functions. In particular, $\text{sn}(z; \tau)$ is an elliptic function with periods $4K$ and $2iK'$. Its zeros lie at 0 and $2K$, and poles at iK' and $2K + iK'$. Here, K is the complete elliptic integral of the first kind with modulus $m = \lambda(2\tau)$, λ is the modular lambda function, and $K' := -2i\tau K$.

We use [Law89] as the major reference for elliptic functions. Other useful references include [Bow61, BF71, BB98] and NIST's Digital Library of Mathematical Functions [DLMF].

Remark 3.6. Note that we do not define $K'(m) = K(1 - m)$, and our τ is half of the traditional definition but coincides with the definition on page 226 of [Law89].

Since sn has the expected zeros and poles, we may write the Gauss map G for a \mathcal{T} surface as

$$G^2 = \rho \text{sn}(4Kz; \tau).$$

In particular, the factor $4K$ on the variable z brings the defining torus to $\mathbb{C}/\langle 1, \tau \rangle$, which is more convenient for us. The zeroes of G^2 are at 0 and $1/2$, and the poles at $\tau/2$ and $(\tau + 1)/2$. The complex factor ρ is known as the López–Ros factor [LR91] in the minimal surface theory. Varying its argument only results in a rotation of the surface in the space, hence only the norm $|\rho|$ concerns us.

The multi-valued function on $\mathbb{C}/\langle 1, \tau \rangle$ is given by $G = [\rho \text{sn}(4Kz; \tau)]^{1/2}$. We take the branch cuts of the square root along the segments $[0, \tau/2]$ and $[(\tau+1)/2, \tau+1/2]$, compatible with [Wey06]; see Figure 2. None of the branch points is hyperelliptic point. Instead, the symmetry $\text{sn}(2K - z) = \text{sn}(z)$ reveals four other inversion centers at $1/4$, $3/4$, $1/4 + \tau/2$ and $3/4 + \tau/2$, and they lift to eight hyperelliptic points.

Similarly, we may write the Gauss map G for an \mathcal{R} surface as

$$G^3 = [\rho \text{sn}(4Kz; \tau)]^2$$

where ρ , again, is the López–Ros factor. This function is well defined on the torus $\mathbb{C}/\langle 1/2, \tau \rangle$, halving the defining torus of $\text{sn}(z; \tau)$. G^3 has a double-order zero at 0 and a double-order pole at $\tau/2$, as expected. The multi-valued function on $\mathbb{C}/\langle 1/2, \tau \rangle$ is given by $G = [\rho \text{sn}(4Kz; \tau)]^{2/3}$. We take the branch cuts of the cubic root along the segments $[0, \tau/2]$, $[\tau/2, \tau]$, $[1/2, (\tau + 1)/2]$ and $[(\tau + 1)/2, \tau + 1/2]$, compatible with [Wey06]; see Figure 3. This time, both branch points are hyperelliptic points; cf. [Wey06, Proposition 3.12]. We recognize two other inversion centers at $1/4$ and $1/4 + \tau/2$, which lift to six more hyperelliptic points.

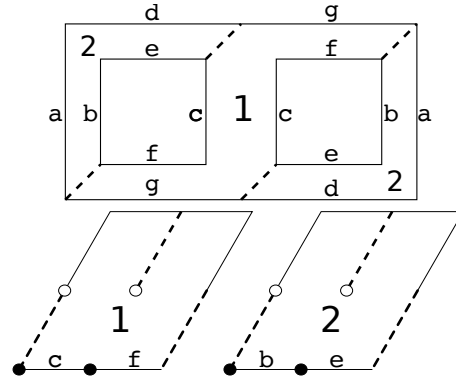


FIGURE 2. Top: Identifying segments with the same labels yields a surface of genus three. The numbered regions are fundamental domains of the screw symmetry of order 3. Bottom: Branch cuts in the branched torus for \mathcal{T} surfaces. Solid circles are zeros; empty circles are poles.

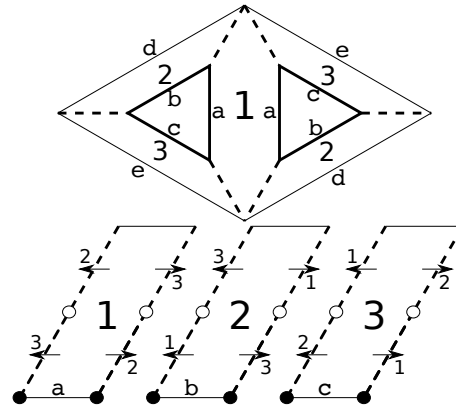


FIGURE 3. Top: Identifying segments with the same labels yields a surface of genus three. The numbered regions are fundamental domains of the screw symmetry of order 2. Bottom: Branch cuts in the branched torus for \mathcal{R} surfaces. Solid circles are zeros; empty circles are poles.

For surfaces in \mathcal{T} and \mathcal{R} , the López–Ros factor ρ can be determined by the order-2 rotational symmetries that swap the poles and zeros of the Gauss map. More specifically, G^2 and $1/G^2$ for \mathcal{T} must have the same residue at their respective poles, and G^3 and $1/G^3$ for \mathcal{R} must have the same principal parts at their poles. By the identity $\text{sn}(z + iK'; \tau) = 1/\sqrt{m} \text{sn}(z; \tau)$, we deduce that $\rho = m^{1/4}$ for both \mathcal{T} and \mathcal{R} .

We have shown that

Lemma 3.7. *Up to a rotation in \mathbb{R}^3 , the Gauss map G have the form*

$$\begin{aligned} G &= [m^{1/4} \text{sn}(4Kz; \tau)]^{1/2} && \text{for a surface in } \mathcal{T}, \text{ and} \\ G &= [m^{1/4} \text{sn}(4Kz; \tau)]^{2/3} && \text{for a surface in } \mathcal{R}. \end{aligned}$$

Remark 3.8. Equivalently, we can write the Gauss map for \mathcal{T} in the form

$$G^2 = \rho' \frac{\theta(z)\theta(z - 1/2)}{\theta(z - \tau/2)\theta(z - 1/2 + \tau/2)}$$

where θ is the Jacobi Theta function (actually one of them) for the lattice $\mathbb{C}/\langle 1, \tau \rangle$, and the López–Ros factor $\rho' = e^{-i\pi(\tau-1)/2}$. The Gauss map for \mathcal{R} may have a similar expression. This should help the readers to compare our computation with those in [Wey06, Wey08].

Remark 3.9. With a change of basis for the torus, one could, of course, use other Jacobi elliptic functions to express the Gauss map. We notice that the normalized Jacobi function $m^{1/4} \operatorname{sn}(z; \tau)$ is one of the three Jacobi-type elliptic functions constructed in [KWH93, § 3], where the symmetry is thoroughly investigated.

3.4. Conventions on the torus. Recall that the modular lambda function is invariant under the congruence subgroup $\Gamma(2)$. Hence $m = \lambda(2\tau)$ and $\operatorname{sn}(z; \tau)$ are invariant under the congruence subgroup $\Gamma_0(4)$ generated by the transforms $\tau \mapsto \tau + 1$ and $\tau \mapsto \tau/(1 - 4\tau)$. So the Weierstrass data is invariant under $\Gamma_0(4)$, and we have infinitely many choices of τ for each surface in \mathcal{T} or \mathcal{R} . In fact, using Jacobi sn function already limits the choice.

Surfaces in [Wey06, Wey08] all admit reflectional symmetries, making it possible to choose τ to be pure imaginary, so the torus is rectangular (and a different elliptic function should be used). We could not use this convention since, in general, the tG and rGL surfaces do not admit reflectional symmetry, nor do surfaces in their associated families.

The fundamental domain of $\Gamma(2)$ is usually taken as the region C bounded by the vertical lines $\operatorname{Re} \tau = \pm 1$ and the half circles $|\tau \pm 1/2| = 1/2$. It is then natural to choose 2τ in this region, so τ is in the region $C/2$ bounded by $\operatorname{Re} \tau = \pm 1/2$ and $|\tau \pm 1/4| = 1/4$, a fundamental domain of $\Gamma_0(4)$. Under this convention, our K' coincides with the standard *associated* elliptic integral of the first kind with modulus m ; then we can safely employ the formula in most textbooks.

This natural choice is, however, not convenient for analyzing the tG and rGL families. For instance, the tP and tD families correspond to the same vertical line $\operatorname{Re} \tau = 0$, and the gyroid also lies on this line. In fact, we will see that, for each $r \in (-1/2, 0) \cup (0, 1/2]$, there are two members of tG with $\operatorname{Re} \tau = r$ under the natural convention. The same happens for rGL. Hence we need a different convention.

We will see that, for a surface in \mathcal{T} or \mathcal{R} , the poles and zeros of the Gauss map are aligned along vertical lines, alternatingly arranged and equally spaced. For the sake of a uniform treatment, we make the following convention:

Convention. For surfaces in \mathcal{T} and \mathcal{R} , we assume that the Weierstrass parameterization maps $(1 + \tau)/2$ directly above 0.

Our convention should be seen as a marking on the surface. Although the Weierstrass data is invariant under the transform $\tau \mapsto \tau + 1$, the marked branch point $(1 + \tau)/2$ is however different. The marking then serves to distinguish, for instance, Schwarz' P, D surfaces and the gyroid. We will see that, under our convention, $\operatorname{Re} \tau = 0$ corresponds to the gyroid in \mathcal{T} and the Lidinoid in \mathcal{R} .

We list in Table 1 the Weierstrass data of classical TPMSg3 under our convention. For each family, we specify the possible τ for the torus and the associate angle θ . We also accompany a diagram, showing the possible τ (dashed curve), the fundamental parallelogram for a typical example, the poles (empty circles) and the zeros (solid circles) of $\operatorname{sn}(z; \tau)$ (whose defining torus could twice the shown quotient torus!), and an arrow indicating dh by pointing to the direction of increasing height. The bottom-left corner of the parallelogram is always 0, the bottom edge represents 1 for \mathcal{T} or $1/2$ for \mathcal{R} , and the left edge always represents τ . The tori used in [Wey06, Wey08] are shown as dotted rectangles for reference.

4. PERIOD CONDITIONS

Rectangular tori are convenient in many ways. For example, many straight segments in the branched torus correspond to geodesics on the surface, making it possible to compute explicitly [Wey06]. With general tori, we lose all the nice properties. An explicit computation is indeed hopeless, but we are still able to say something.

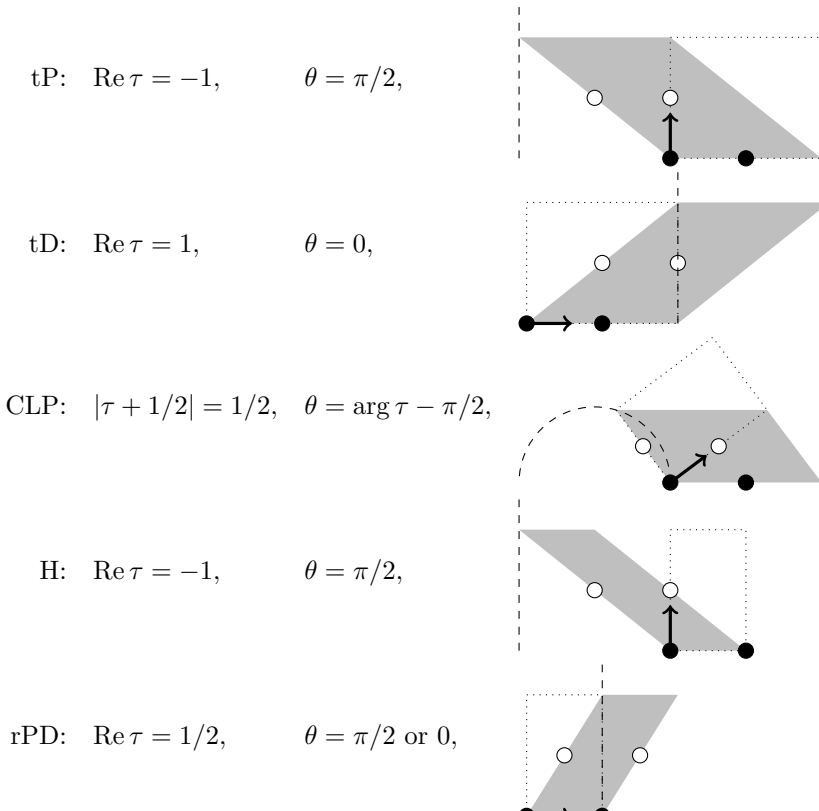


TABLE 1. Weierstrass data for classical TPMsG3.

4.1. Twisted catenoids. Assume $dh = e^{-i\pi/2} = -idz$ for the moment. We now study the image under the maps

$$\begin{aligned}\Phi_i : \mathbb{C} &\rightarrow \mathbb{C} \quad i = 1, 2 \\ \Phi_1 : z &\mapsto \int^z dh \cdot G \\ \Phi_2 : z &\mapsto \int^z dh/G.\end{aligned}$$

Let us first look at the lower half of the branched torus of \mathcal{T} , i.e. the part with $0 < \operatorname{Im} z < \operatorname{Im} \tau/2$. This is topologically an annulus and lifts to its universal cover $\{z \mid 0 < \operatorname{Im} z < \operatorname{Im} \tau/2\}$, which is a strip in \mathbb{C} . By analytic continuation, G lifts to a function of period 2 on the strip. The boundary lines $\operatorname{Im} z = 0^+$ and $\operatorname{Im} z = \operatorname{Im} \tau/2 - 0^+$ are then mapped by Φ_1 into periodic or closed curves.

By the same argument as in the standard proof of the Schwarz–Christoffel formula (see also [Wey06, FW09]), we see that the curves make an angle at each branch point. The interior angle is $\pi/2$ at the poles of G^2 and $3\pi/2$ at the zeros. By the symmetry $\operatorname{sn}(2K + z; \tau) = -\operatorname{sn}(z; \tau)$, the image of the segments $[n/2, (n+1)/2]$, $n \in \mathbb{Z}$, are all congruent, and images of adjacent segments only differ by a rotation of $\pi/2$ around their common vertex. Moreover, by the symmetry $\operatorname{sn}(2K - z; \tau) = \operatorname{sn}(z; \tau)$, the image of each segment admits an inversive symmetry. The inversion center is the image of the hyperelliptic points, at the midpoint of each segment. The same can be said about the segments $[(n+\tau)/2, (n+1+\tau)/2]$, $n \in \mathbb{Z}$.

Therefore, the boundaries of the strip are mapped to closed curves with a rotational symmetry of order 4. The curves look like “curved squares”, obtained by replacing the straight edges of the square by congruent copies of a symmetric curve. Moreover, the two twisted squares share the

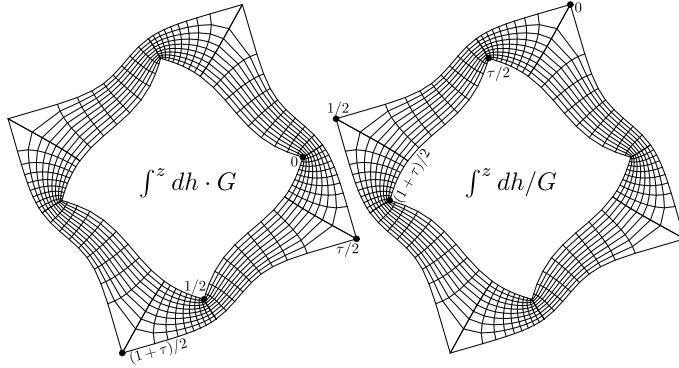


FIGURE 4. Plot of the lower annulus $0 < \operatorname{Im} z < \operatorname{Im} \tau/2$ under the maps Φ_1 and Φ_2 for \mathcal{T} , with $\tau = 0.3 + 0.2i$.

same rotation center. The strip is then mapped by Φ_1 to the twisted annulus bounded by the curved squares. See Figure 4.

A similar analysis can be carried out on the upper annulus $\operatorname{Im} \tau/2 < \operatorname{Im} z < \operatorname{Im} \tau$. However, the branch cuts ensure that the two annuli continuous into different branches (different signs of square root) when crossing the segments $[n/2, n/2 + \tau]$. As a consequence, the boundary curves is turning in the opposite direction. As one passes through the segment $[\tau/2, (\tau + 1)/2]$, the images of Φ_1 is extended by an inversion, which reverses orientation.

Because of our choice of the López–Ros parameter, the image of the lower annulus under Φ_2 is congruent to the image of the upper annulus under Φ_1 . The only difference is that the inner and the outer boundaries of the annulus are swapped. See Figure 4.

Combining the flat structures Φ_1 and Φ_2 gives us the image under the Weierstrass parameterization. Because of our choice of dh , we know that the lines $\operatorname{Im} z = 0$ and $\operatorname{Im} z = \operatorname{Im} \tau/2$ are mapped to two horizontal planar curves, at heights 0 and $\operatorname{Im} \tau/2$ respectively. The previous analysis tells us that these are two congruent closed curves that look like curved squares. In particular, they admit rotational symmetry of order 4. The strip $0 < \operatorname{Im} z < \operatorname{Im} \tau/2$ is then mapped to a “twisted square catenoid” bounded by these curves. Moreover, the twisted catenoid admits rotational symmetries of order 2 around horizontal axes that swap its boundaries. See Figure 5.

Inversion in the midpoint of a curved edge extends the surface with another twisted square catenoid, which is the image of the strip $\operatorname{Im} \tau/2 < \operatorname{Im} z < \operatorname{Im} \tau$. Repeated inversions in the midpoints of the curved edges extend the catenoid infinitely into the space \mathbb{R}^3 , but the result is usually not embedded.

The same argument applies to the Weierstrass data of \mathcal{R} . The lower annulus lift to a strip in \mathbb{C} of period $3/2$. We then obtain a twisted triangular catenoid with rotational symmetry of order 3, and repeated inversions in the midpoints of the curved edges extend the catenoid infinitely into \mathbb{R}^3 , but usually not embedded. See Figures 6 and 7.

It is interesting to observe the twisted catenoids when $\operatorname{Re} \tau$ increases.

Let us start from a tP surface with $\operatorname{Re} \tau = -1$. Its catenoid is the standard square catenoid, not twisted. As we increase $\operatorname{Re} \tau$, the square catenoid becomes “twisted” in two senses: on the one hand, the bounding squares become curved; on the other hand, horizontal projections of the squares form an angle. This “twist angle” seems to increase monotonically with $\operatorname{Re} \tau$ (we are not sure!); see Figure 5. Remarkably, when $\operatorname{Re} \tau = -1/2$, reflectional symmetry is restored in the Weierstrass data, and the catenoid is bounded by two straight squares forming a twist angle of $\pi/4$.

Then the catenoid is again “twisted” as we continue to increase $\operatorname{Re} \tau$ until 1. During the process, the twist angle increases from 0 at $\operatorname{Re} \tau = -1$ (tP), to $\pi/4$ at $\operatorname{Re} \tau = -1/2$, to $\pi/2$ at $\operatorname{Re} \tau = 0$ (gyroid), to $3\pi/4$ at $\operatorname{Re} \tau = 1/2$, until π at $\operatorname{Re} \tau = 1$ (tD). These are the only cases where reflectional symmetry is restored, and the bounding edges are straight. The term “twist angle”

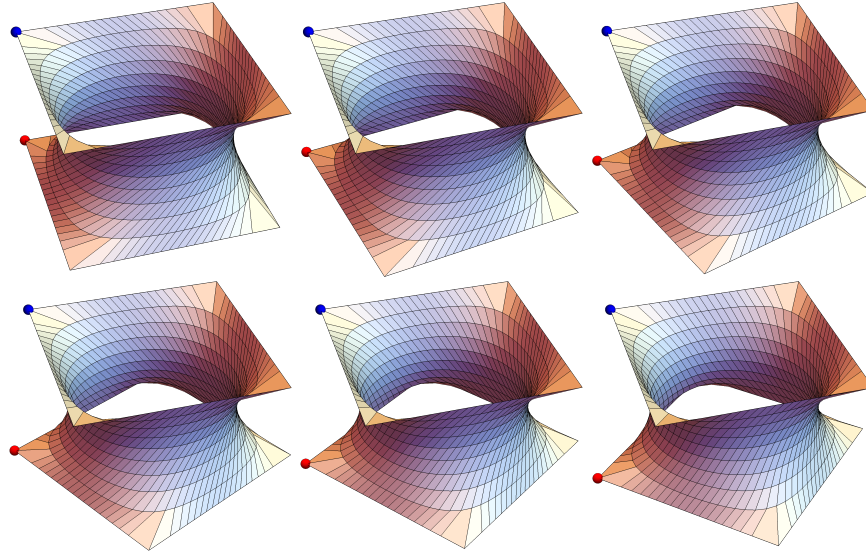


FIGURE 5. Plot of the annulus with $0 < \text{Im } z < \text{Im } \tau/2$ under the Weierstrass parameterization of \mathcal{T} , for $\text{Im } \tau = 1$ and $\text{Re } \tau = -1, -0.9, -0.8, -0.7, -0.6, -0.5$, in this order. The red and the blue points indicate the images of 0 and $(1 + \tau)/2$. An increasing “twist angle” is visible. Note that bounding edges are in fact slightly curved, except for $\text{Re } \tau = -1$ and -0.5 .

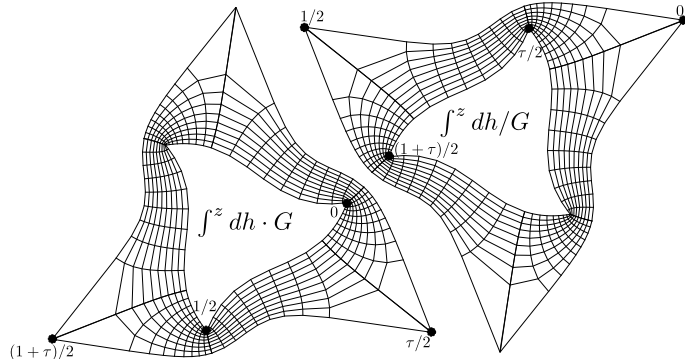


FIGURE 6. Plot of the annulus $0 < \text{Im } z < \text{Im } \tau/2$ under the maps Φ_1 and Φ_2 for \mathcal{R} , with $\tau = 0.3 + 0.2i$.

is in general ill-defined³, but carries a natural meaning in these cases. Note that, although the transform $\tau \mapsto \tau + 1$ leaves the catenoid invariant, the image of $(\tau + 1)/2$ (blue point in Figure 5) is however rotated by $\pi/2$. So the marked twisted catenoid is invariant under the transform $\tau \mapsto \tau + 4$.

Remark 4.1. The tG surfaces at $\text{Re } \tau = \pm 1/2$ deserve more attention, as the reflectional symmetries in their Gauss maps seem special.

Similarly, for \mathcal{R} , we can start from the triangular catenoid of H with $\text{Re } \tau = -1$, and increase $\text{Re } \tau$ until $1/2$. The bounding triangles become curved and form a twisted angle that seems to increase monotonically with $\text{Re } \tau$; see Figure 7. In particular, the “twist angle” increases from 0 at $\text{Re } \tau = -1$ (H), to $\pi/3$ at $\text{Re } \tau = -1/2$ (gyroid), to $2\pi/3$ at $\text{Re } \tau = 0$ (Lidinoid), until π at $\text{Re } \tau = 1/2$ (rPD). These are the only cases where the reflectional symmetry is restored, the

³ More precisely, I can think of several ways to define the “twist angle”. They seem inconsistent, and it is not clear which is more beneficial. Hence I prefer not to make the definition at the moment.

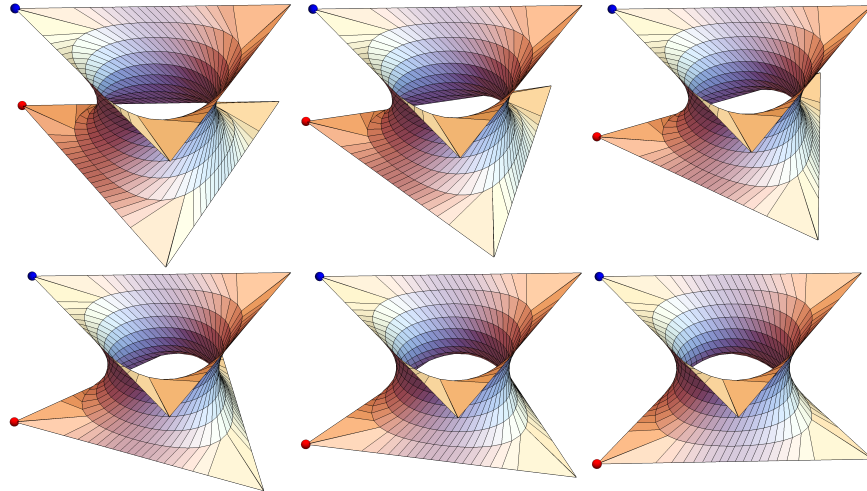


FIGURE 7. Plot of the annulus with $0 < \operatorname{Im} z < \operatorname{Im} \tau/2$ under the Weierstrass parameterization of \mathcal{R} , for $\operatorname{Im} \tau = 1$ and $\operatorname{Re} \tau = -1, -0.9, -0.8, -0.7, -0.6, -0.5$, in this order. The red and the blue points indicate the images of 0 and $(1 + \tau)/2$. An increasing “twist angle” is then visible. Note that bounding edges are in fact slightly curved, except for $\operatorname{Re} \tau = -1$ and -0.5 .

bounding edges are straight, and the meaning of the “twist angle” is clear. The marked twisted catenoid is invariant under the transform $\tau \mapsto \tau + 3$.

4.2. Vertical and horizontal associate angles. The Weierstrass parameterization defines an immersion only if the period problems are solved. That is, the integrations around closed curves on Σ should all vanish (up to Λ). The period problems for Schwarz’ surfaces were explicitly solved in [Wey06].

Große–Brauckmann and Wohlgemuth [GBW96] proposed a convenient way to visualize the gyroid, which we now generalize to all surfaces in \mathcal{T} and \mathcal{R} . This will reduce the period problems to just one equation.

We have demonstrated a twisted catenoid in the associate family of every surface in \mathcal{T} or \mathcal{R} . As one travels from the twisted catenoids along the associate family, the bounding twisted squares or triangles become “twisted helices”, and the twisted catenoid opens up into a ribbon bounded by these helices.

For an embedded TPMSg3 M/Λ , Meeks [Mee90] proved that its hyperelliptic points can be identified to the lattice and half-lattice points of Λ . Then the symmetries of \mathcal{T} and \mathcal{R} imply that the poles and zeros of the Gauss map are

- aligned along vertical lines arranged in a square or triangular lattice and
- alternatingly arranged and equally spaced on each vertical line.

Conversely, if these are the cases, then the two ribbons forming the fundamental unit “fit exactly into each other”. That is, their boundaries are identified in the same pattern as the twisted catenoids (see Figures 2 and 3). This is guaranteed by the screw and the inversional symmetries. So the properties listed above form a sufficient condition for the immersion.

To be more precise, we define the pitch of a helix to be the increase of height after the helix makes a full turn. Then the poles and zeros are alternatingly arranged and equally spaced on each vertical line if the pitch of each helix is an even multiple of the minimum vertical distance between the poles and the zeros. In particular, for the gyroid, the pitch doubles the minimum vertical distance. So we expect the same property for tG and rGL surfaces.

Remark 4.2. The ratio of the pitch over the minimum vertical distance can also take other values. They will be discussed in Section 6.

For tG surfaces, this means that the integral of the height differential dh from 0 to 2 doubles the integral from 0 to $(1+\tau)/2$. Or equivalently, the integral from 0 to 1 equals the integral from 0 to $(1+\tau)/2$. This can be easily achieved by adjusting the associate angle θ to (compare [Wey08, Definition 4.2])

$$\theta = \theta_v(\tau) = \arg(\tau - 1) - \pi/2 \quad \text{for tG.}$$

Similarly, for rGL surfaces, this means that the integral of dh from 0 to $3/4$ equals the integral from 0 to $(1+\tau)/2$. Then we deduce that

$$\theta = \theta_v(\tau) = \arg(\tau - 1/2) - \pi/2 \quad \text{for rGL.}$$

We now calculate the associate angle in another way, using the fact that the images of 0 and $(1+\tau)/2$ are vertically aligned, i.e. have the same horizontal coordinates.

First note that, by the symmetry $\operatorname{sn}(2K + iK' - z; \tau) = 1/\operatorname{sn}(z; \tau)$, we have the identity

$$\int_0^{(1+\tau)/2} dz/G = \int_0^{(1+\tau)/2} dz \cdot G =: \psi(\tau)$$

We may place the image of 0 at the origin. First look at the surface with $\theta = 0$, hence $dh = dz$. Then the horizontal coordinates of the image of $(1+\tau)/2$ are

$$\operatorname{Re} \int_0^{(1+\tau)/2} \left(\frac{1}{2} \left(\frac{1}{G} - G \right), \frac{i}{2} \left(\frac{1}{G} + G \right) \right) dz = (0, -\operatorname{Im} \psi(\tau)).$$

Then we look at the surface with $\theta = \pi/2$, hence $dh = e^{-i\pi/2} dz = -idz$ (the conjugate surface). Then the coordinates are

$$\operatorname{Re} \int_0^{(1+\tau)/2} \left(-\frac{i}{2} \left(\frac{1}{G} - G \right), \frac{1}{2} \left(\frac{1}{G} + G \right) \right) dz = (0, \operatorname{Re} \psi(\tau)).$$

So for the surface with associate angle θ , the first coordinate is always 0, while the second coordinate

$$-\cos \theta \operatorname{Im} \psi(\tau) + \sin \theta \operatorname{Re} \psi(\tau)$$

vanishes when

$$\theta = \theta_h(\tau) := \arg \psi(\tau).$$

We have shown that

Lemma 4.3. *The Weierstrass data given by Lemmas 3.2 and 3.7 define an immersion if and only if*

$$\theta_h(\tau) = \theta_v(\tau),$$

or more explicitly,

$$(3) \quad \arg \psi(\tau) = \begin{cases} \arg(\tau - 1) - \pi/2 & \text{for } \mathcal{T}; \\ \arg(\tau - 1/2) - \pi/2 & \text{for } \mathcal{R}. \end{cases}$$

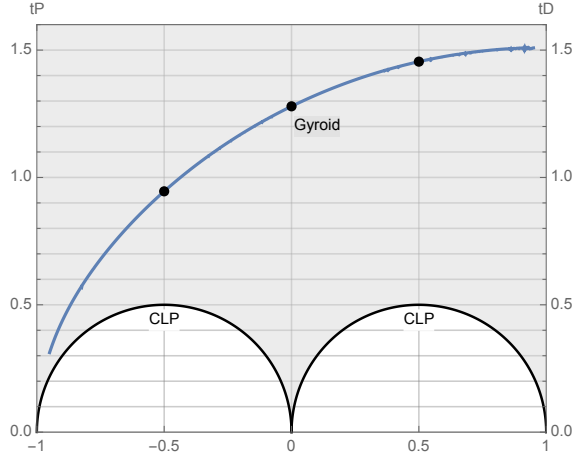
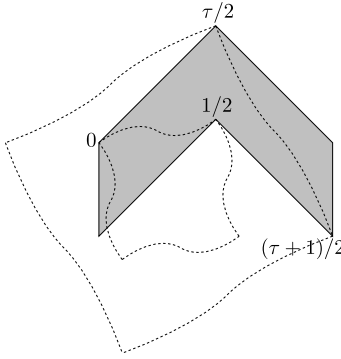
We are finally ready to give the existence proof.

5. EXISTENCE PROOF

5.1. tG family. In Figure 8, we show for \mathcal{T} the numerical solutions to (3) with $-1 < \operatorname{Re} \tau < 1$, accompanied by two half-circles representing the CLP family. Our task is to prove the existence of the continuous 1-parameter solution curve that we see in the picture, which we call the tG family. Let the shaded domain in the figure be denoted by

$$\Omega_t := \{\tau \mid \operatorname{Im} \tau > 0, -1 < \operatorname{Re} \tau < 1, |\tau \pm 1/2| > 1/2\}.$$

Proposition 5.1. *There exists a continuous 1-dimensional curve of τ in Ω_t that solves (3). This curve tends to -1 at one end and to $1 + ti$ for some $0 < t < \infty$ at the other end. Moreover, the TPMs g_3 s represented by points on the curve are all embedded.*

FIGURE 8. Solutions for \mathcal{T} to (3) with $-1 < \operatorname{Re} \tau < 1$.FIGURE 9. Image of the rectangle with vertices at $0, 1/2 - \tau/2, 1/2 + \tau/2, \tau$, under the map Φ_1 for a CLP surface (the grey area). The twisted square annulus is sketched (exaggeratedly) in dashed curves.

Proof. We examine the angles θ_v and θ_h on the boundaries of Ω_t .

On the vertical line $\operatorname{Re} \tau = -1$, we see immediately that $0 < \theta_v < \pi/2$. Since this line corresponds to the tP family, we know very well that the image of $(1 + \tau)/2$ is directly above the image of 0 when $dh = e^{-i\pi/2} dz$. Hence $\theta_h = \pi/2 > \theta_v$.

The half-circle $|\tau + 1/2| = 1/2$ corresponds to the CLP family. We know very well that the image of $(1 + \tau)/2$ is directly above the image of 0 when $dh = \exp(-i(\arg \tau - \pi/2)) dz$, so $\theta_h = \arg \tau - \pi/2$. Then the inequality $\theta_h < \theta_v$ follows from elementary geometry.

On the half-circle $|\tau - 1/2| = 1/2$, it follows from elementary geometry that $\theta_v = \arg \tau$. This half-circle corresponds again to the CLP family. When $dh = \exp(-i\theta_v) dz$, the image of $\tau/2$ is directly above the image of 0. In this case, we know very well that the flat structure of Φ_1 is as depicted in Figure 9; see [Wey06]. In particular, we have

$$\arg \int_0^{(1+\tau)/2} dh \cdot G = \arg \int_0^{(1+\tau)/2} dz \cdot G \exp(-i\theta_v) = \theta_h - \theta_v < 0,$$

hence $\theta_h < \theta_v$.

On the vertical line $\operatorname{Re} \tau = 1$, we see immediately that $\theta_v = 0$. Since this line corresponds to the tD family, we know very well that the image of $(1 + \tau)/2$ is directly above the image of 0 when $dh = dz$, so $\theta_h = 0$. Hence this line solves the period condition $\theta_h = \theta_v$, but not very helpful for our proof.

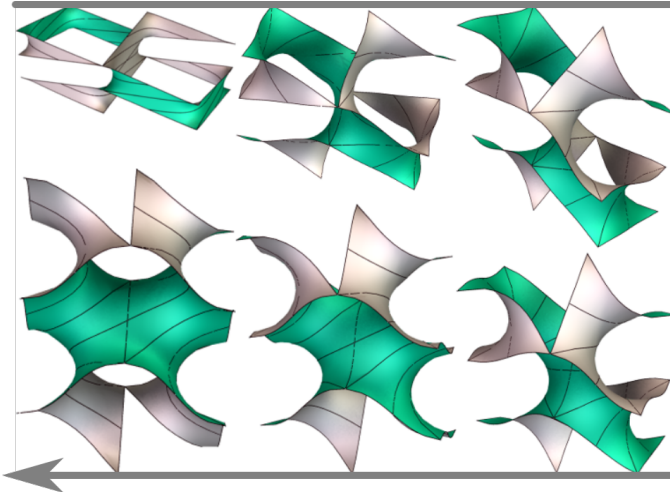


FIGURE 10. tG surfaces with $\operatorname{Re} \tau = -0.95, -0.6, -0.2, 0.2, 0.6$ and 0.95 , in the indicated order.

As $\operatorname{Im} \tau \rightarrow \infty$, we see immediately that $\theta_v \rightarrow 0$. Asymptotic behavior of θ_h is technical, so we postpone the details to Appendix, where Lemma A.2 states that $\theta_h \rightarrow \operatorname{Re}(1 - \tau)\pi/4$. Hence $\theta_h > \theta_v$ for $\operatorname{Im} \tau$ sufficiently large.

Now consider $\tau = 1 - \epsilon + i\eta$ for small ϵ . It is immediate that the derivative of θ_v with respect to ϵ at $\epsilon = 0$ is $1/\eta$, hence tends to 0 as $\eta \rightarrow \infty$. Meanwhile, the asymptotic behavior of θ_h tells us that $\partial\theta_h/\partial\epsilon \rightarrow \pi/4 > 0$ as $\eta \rightarrow \infty$. Consequently, there exist two positive numbers H and δ such that $\theta_h(1 - \epsilon + \eta i) > \theta_v(1 - \epsilon + \eta i)$ for all $\eta > H$ and $\epsilon < \delta$.

As $\tau \rightarrow 1$ within Ω_t , Lemma A.3 in Appendix claims that $\theta_h(\tau) \rightarrow 0$ from the negative side, but one sees immediately that $\theta_v(\tau) \rightarrow 0$ from the positive side. Consequently, there exists a neighborhood U of 1 such that $\theta_h(\tau) < \theta_v(\tau)$ for all $\tau \in U \cap \Omega_t$.

Note that θ_h and θ_v are both real analytic functions in the real and imaginary part of τ , hence the solution set of the period condition (3) is an analytic set. By the continuity, we conclude that the solution set contains a connected component that separates the half-circles $|\tau \pm 1/2| = 1/2$ from the line $\operatorname{Re} \tau = -1$ and the infinity. Moreover, this set must also separate a neighborhood U of 1 from the set $\{\tau \mid \operatorname{Re} \tau > 1 - \delta, \operatorname{Im} \tau > H\}$. Because of the analyticity, we may extract a continuous curve from the connected component, which is the tG family. In particular, this curve must tend to the common limit of CLP and tP (a saddle tower of order 4 at $\tau \rightarrow -1$), and intersect the tD family at a finite, positive point.

The proof of [Wey08, Lemma 4.4] implies that the gyroid is the only embedded TPMG3 on the vertical line $\operatorname{Re} \tau = 0$ that solves the period condition. Hence the tG family must contain the gyroid, whose embeddedness then ensures the embeddedness of all TPMG3s in the tG family. This follows from [Wey06, Proposition 5.6], which was essentially proved in [Mee90]. \square

In Figure 10, we show two adjacent ribbons for some tG surfaces. They form a fundamental unit for the translational symmetry group.

5.2. rGL family. In picture 8, we show for \mathcal{R} the numerical solutions to (3) with $-1 < \operatorname{Re} \tau < 1/2$. The two half-circle represents an order-3 analogue of the CLP surface, termed hCLP in [LL90], but already known to Schwarz [Sch90]; see also [FH92, EFS15]. Surfaces in hCLP are not embedded, but also not dense in the space. It is very easy to visualize and behaves very much like CLP. In particular, its Weierstrass data is as shown in Figure 12; compare CLP in Table 1.

Our task is to prove the existence of the continuous 1-parameter solution curve that we see in the picture, which we call the rGL family. Let the shaded domain in the figure be denoted by

$$\Omega_r = \{\tau \mid \operatorname{Im} \tau > 0, -1 < \operatorname{Re} \tau < 1/2, |\tau \pm 1/2| > 1/2\}.$$

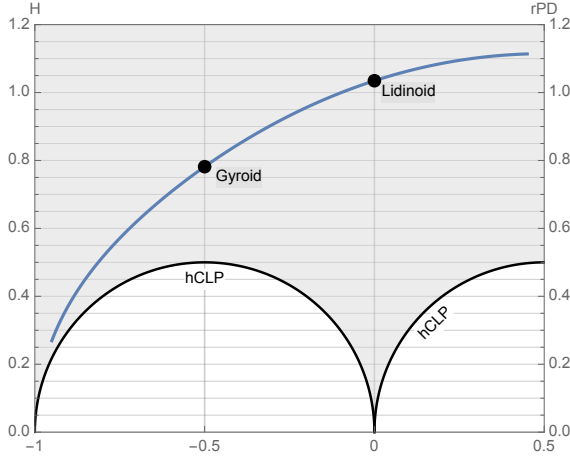
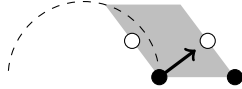
FIGURE 11. Solutions for \mathcal{R} to (3) with $-1 < \operatorname{Re} \tau < 1/2$.

FIGURE 12. Weierstrass data for hCLP.

Proposition 5.2. *There exists a continuous 1-dimensional curve of τ in Ω_r that solves (3). This curve tends to -1 at one end and to $1/2 + ti$ for some $0 < t < \infty$ at the other end. Moreover, the triply periodic minimal surfaces of genus three represented by points on the curve are all embedded.*

Proof. Part of the proof is very similar to tG, so we just provide a sketch.

The line $\operatorname{Re} \tau = -1$ corresponds to the H family, and we have $\theta_h = \pi/2 > \theta_v$.

The half-circle $|\tau + 1/2| = 1/2$ corresponds to the hCLP family, and we have $\theta_h < \theta_v$.

The line $\operatorname{Re} \tau = 1/2$ correspond to the rPD family, and we have $\theta_h = \theta_v = 0$. This solves the period condition, but not helpful for us.

As $\operatorname{Im} \tau \rightarrow \infty$, we have $\theta_h \rightarrow \operatorname{Re}(1/2 - \tau)\pi/3 > \theta_v = 0$. The argument for the asymptotic behavior is very similar as in the proof of Lemma A.2, so we will not repeat it.

By the same argument as for tG, we conclude that $\theta_h > \theta_v$ for $\tau = 1/2 - \epsilon + i\eta$ as long as $\eta > H$ and $\epsilon < \delta$ for some positive constants H and δ .

More care is however needed on the half-circle $|\tau - 1/2| = 1/2$. It corresponds again to the hCLP family. When $dh = \exp(-i \arg \tau) dz$, the image of $\tau/2$ is directly above the image of 0. In this case, we know very well that the flat structure of Φ_1 is as depicted in Figure 13. We see that

$$\arg \int_0^{(1+\tau)/2} dh \cdot G = \arg \int_0^{(1+\tau)/2} dz \cdot G \exp(-i \arg \tau) = \theta_h - \arg \tau < 0.$$

Let a denote the length of the tilted segments (e.g. from 0 to $\tau/2$) in the flat structure, and b the length of the vertical segments (e.g. from $1/2$ to $\tau/2$). It follows from an extremal length argument that the ratio a/b increases monotonically as τ travels along the half-circle with increasing $\operatorname{Re} \tau$. Then we see that $\theta_h - \arg \tau$ increases monotonically from $-\pi/2$ to 0.

On the other hand, it follows from elementary geometry that $\theta_v - \arg \tau = \arg \tau - \pi/2$, which decreases monotonically as τ travels along the half-circle with increasing $\operatorname{Re} \tau$. Consequently, there is a unique τ on the half-circle for which $\theta_v = \theta_h$, and we know very well that this occurs at $\tau = (1+i)/2$. At this point, it is interesting to verify that $a = b$, hence $\theta_h - \arg \tau = -\pi/4 = -\arg \tau$.

Therefore, by monotonicity, we have $\theta_h < \theta_v$ on the left quarter of this half-circle.

We then conclude the existence of a continuous curve of τ , namely the rG family, that solves $\theta_h = \theta_v$ and separates the half-circles $|\tau \pm 1/2| = 1/2$ from the line $\operatorname{Re} \tau = -1$ and the infinity.

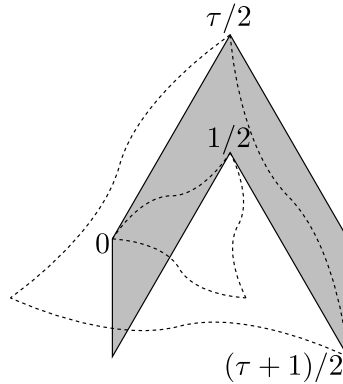


FIGURE 13. Image of the rectangle with vertices at $0, 1/2 - \tau/2, 1/2 + \tau/2, \tau$, under the map Φ_1 for an hCLP surface (the grey area). The twisted triangular annulus is sketched (exaggeratedly) in dashed curves.

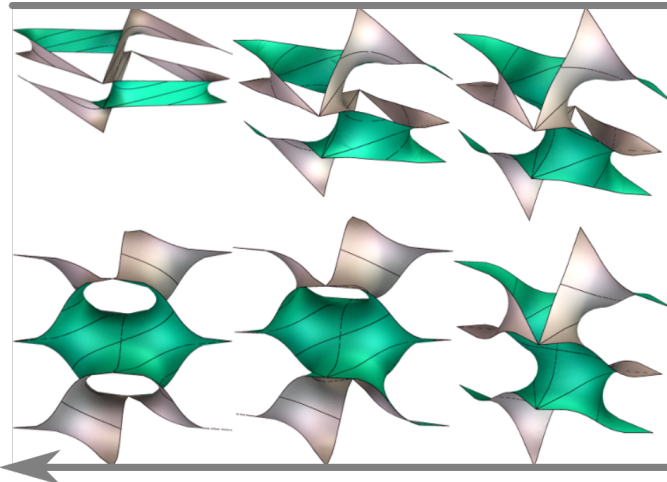


FIGURE 14. rGL surfaces with $\text{Re } \tau = -0.95, -0.7, -0.4, -0.1, 0.2$ and 0.45 , in the indicated order.

This curve must tend to the common limit of hCLP and H (a saddle tower of order 3 at $\tau \rightarrow -1$) and intersect rPD at a finite point.

Moreover, the Lidinoid and the gyroid are the unique solutions on their respective vertical lines. Hence the rGL family must contain them both. Their embeddedness then ensures the embeddedness of all TPMG3s in the rGL family. \square

In Figure 14, we show two adjacent ribbons for some rGL surfaces. They form a fundamental unit for the translational symmetry group.

6. DISCUSSION

6.1. Bifurcation. A TPMG3 is a *bifurcation instance* if the same deformation of its lattice could lead to different deformations (bifurcation branches) of the surface. Both the tG–tD and the rGL–rPD intersections are bifurcation instances.

Bifurcation instances among classical TPMG3s are systematically investigated in [KPS14], but some of them had no explicit bifurcation branch at the time. Two bifurcation instances were discovered in tD [KPS14]. The recently discovered tΔ family provides the missing bifurcation branch to one of them [CW18a]. The other bifurcation instance seems to escape the attention. Its conjugate is identified as the tP surface obtained from the square catenoid of maximum height,

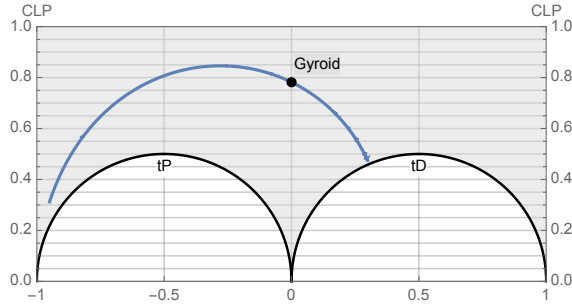


FIGURE 15. Transform of Figure 8 under the inversion $\tau' = 1/\bar{\tau}$.

but no bifurcation branch was previously known for itself. Numerics from [KPS14] and [FH99] (see also [STFH06]), which we can confirm with the help of (6) in Appendix, shows that this is exactly the tG–tD intersection with $\tau \approx 1 + 1.51019i$. Hence tG provides the missing bifurcation branch.

Likewise, two bifurcation instances were discovered in rPD [KPS14]. One of them is identified as the rPD surface obtained from the triangular catenoid of maximum height. The other is its conjugate, for which no bifurcation branch was previously known. Numerics from [KPS14] and [FH99] (see also [STFH06]) shows that this is exactly the rGL–rPD intersection, hence rGL provides the missing bifurcation branch.

Therefore, all bifurcation instances discovered in [KPS14] have now an explicit bifurcation branch.

Remark 6.1. Curiously, both tG–tD and rGL–rPD intersections are conjugate to catenoids of maximum height. Numerics shows that the height of the twisted catenoid seems to increase monotonically with $\operatorname{Re} \tau$ along the tG and rGL families, and reaches the maximum at the intersection.

6.2. Reflection group. In this part, we point out that “reflections in classical TPMSg3 families” generate a reflection group that acts on \mathcal{T} and \mathcal{R} .

We have seen that each τ corresponds to a marked twisted catenoid. The marked square catenoid is invariant under $\tau \mapsto \tau + 4$, and the marked triangular catenoid is invariant under $\tau \mapsto \tau + 3$.

For a twisted square catenoid, as one increases $\operatorname{Re} \tau$ beyond 1, the twist angle increases beyond π . However, note that $\tau \mapsto 2 - \tau$ only results in a reflection of the marked catenoid. Consequently, their associate surfaces with the same associate angle differ only by handedness. So, if τ closes the period with associate angle θ and gives an embedded TPMSg3 in \mathcal{T} , then $2 - \tau$ gives the same TPMSg3 with the same associate angle. Similarly, one can decrease $\operatorname{Re} \tau$ below -1, but $\tau \mapsto -2 - \tau$ only results in a reflection, hence τ and $-2 - \tau$ gives the same TPMSg3 in \mathcal{T} .

So we have shown that \mathcal{T} is invariant under the reflections in the vertical lines $\operatorname{Re} \tau = \pm 1$ (tP and tD). The same argument applies to show that \mathcal{R} is invariant under the reflections in $\operatorname{Re} \tau = -1$ (H) and $\operatorname{Re} \tau = 1/2$ (rPD).

Now let us apply the transform $\tau' = 1/\bar{\tau}$, which exchanges the vertical lines $\operatorname{Re} \tau = \pm 1$ with the half-circles $|\tau \pm 1/2| = 1/2$. Then Figure 8 becomes Figure 15.

The vertical lines $\operatorname{Re} \tau' = \pm 1$ correspond to CLP surfaces. With such a τ' and associate angle $\pi/2$, we know very well that the strip $0 < \operatorname{Im} z < \operatorname{Im} \tau'/2$ is mapped by the Weierstrass parameterization to a minimal strip bounded by two periodic zig-zag polygonal curves related by a vertical translation. Each polygonal curve consists of segments of equal length, making $\pi/2$ angles in alternating directions.

As we increase $\operatorname{Re} \tau'$, the straight segments of the polygonal curves become symmetric curves. At the same time, the two boundaries begin to drift with respect to each other. When $\operatorname{Re} \tau' = 0$, the drift is exactly half of a period, then reflectional symmetry is restored and the segments become

straight again; this is a tD surface. When $\operatorname{Re} \tau' = 1$, the drift is exactly one period, and a CLP surface is restored.

In principle, we could have built the whole paper on “drifted strips” instead of “twisted catenoids”. We will not go too far in this direction. Nevertheless, the alternative view facilitates the following observation: the transforms $\tau' \mapsto 2 - \tau'$ and $\tau' \mapsto -2 - \tau'$ only result in a reflection of the drifted strip. Consequently, \mathcal{T} is invariant under the reflections in $\operatorname{Re} \tau' = \pm 1$ (CLP). Similarly, \mathcal{R} is invariant under the reflections in hCLP families ($\operatorname{Re} \tau' = \pm 1$).

If we parameterize \mathcal{T} and \mathcal{R} by τ in the upper half-plane, which can be seen as the hyperbolic space, then we have proved that

Proposition 6.2.

- \mathcal{T} is invariant under the discrete group generated by reflections in $\operatorname{Re} \tau = -1$ (tP), $\operatorname{Re} \tau = 1$ (tD) and $|\tau \pm 1/2| = 1/2$ (CLP).
- \mathcal{R} is invariant under the discrete group generated by reflections in $\operatorname{Re} \tau = -1$ (H), $\operatorname{Re} \tau = 1/2$ (rPD) and $|\tau \pm 1/2| = 1/2$ (hCLP).

6.3. Higher pitch. We have seen that a tG surface consists of ribbons bounded by helices, and the pitch of the helices doubles the vertical distance between them. In general, for any surface in \mathcal{T} and \mathcal{R} , the ratio of the pitch of the helices to the vertical distance between them must be an even integer, say $2p$; we call p the *pitch* of the surface. The vertical associate angle for a surface of pitch p is $\theta_v(\tau; p) = \arg(\tau + 1 - 2/p) - \pi/2$ for \mathcal{T} , and $\theta_v(\tau; p) = \arg(\tau + 1 - 3/2p) - \pi/2$ for \mathcal{R} . The period condition is again $\theta_h(\tau) = \theta_v(\tau; p)$.

It is immediate that $p = 0$ for tP. We have seen that tD and tG close the period with $p = 1$. It is also not difficult to see that CLP closes the period with $p = 2$. In this case, a catenoid and the one directly above it opens into two ribbons that occupy the same vertical cylinder. They interlace each other, and the vertical gap between them equals the vertical width of each single ribbon, allowing adjacent ribbons to fit exactly in.

More generally, for a surface of pitch p , p ribbons occupy the same vertical cylinder so that adjacent ribbons fit exactly in. When $p \equiv 0 \pmod{2}$, one easily verifies that the half-circle $|\tau + 1 - 1/p| = 1/p$ closes the period for \mathcal{T} surfaces with pitch p . By the reflection group, we see that this half-circle corresponds to tP if $p \equiv 0 \pmod{4}$ and to CLP if $p \equiv 2 \pmod{4}$. We now prove that

Lemma 6.3. *Let*

$$\tau' = -\frac{(2k-1)\bar{\tau} + (2k-2)}{2k\bar{\tau} + (2k-1)}$$

be the image of τ under the reflection in the half-circle $|\tau + 1 - 1/2k| = 1/2k$. If τ closes the period (for \mathcal{T} or \mathcal{R}) with pitch p , then τ' closes the period with pitch $q = 4k - p$.

Proof. Note that $2/q - 1$ and $2/p - 1$ are related by the reflection in the named half-circle. It then follows from elementary geometry that $\theta_v(\tau; p) + \theta_v(\tau'; q) = \arg(\tau + 1 - 1/2k)$. On the other hand, note that

$$\tau' + 1 = \frac{\bar{\tau} + 1}{2k\bar{\tau} + (2k-1)}.$$

Then a change of variable in the integration $\psi(\tau)$ shows that $\theta_h(\tau) + \theta_h(\tau') = -\arg(2k\bar{\tau} + (2k-1)) = \arg(\tau + 1 - 1/2k)$. So $\theta_h(\tau) = \theta_v(\tau; p)$ implies that $\theta_h(\tau') = \theta_v(\tau'; q)$. \square

In particular, by reflections in CLP (resp. hCLP), we see that tG and tD (resp. rGL and rPD) close the period for each $p \equiv 1 \pmod{2}$.

6.4. Uniqueness. We conjecture the following uniqueness statements.

Conjecture 6.4.

- For every $r \in (-1, 1)$, there is a unique τ with $\operatorname{Re} \tau = r$ that solves the period condition (3) for \mathcal{T} with pitch 1.
- For every $r \in (-1, 1/2)$, there is a unique τ with $\operatorname{Re} \tau = r$ that solves the period condition (3) for \mathcal{R} with pitch 1.

The uniqueness has been proved by Weyhaupt [Wey06] for \mathcal{T} with $\Re\tau = 0$ (gyroid) and for \mathcal{R} with $\Re\tau = -1/2$ (gyroid) and 0 (Lidinoid). This shows that

Theorem 6.5. *The gyroid and the Lidinoid are the only non-trivial embedded TPMSg3s in the associate families of tP, tD, rPD and H surfaces.*

Proof. Any other embedded TPMSg3 must, by construction, lie on the same vertical lines, hence contradict the uniqueness. \square

Our approach leads to a simple proof that works not only for the gyroid and the Lidinoid but also for the tG surfaces with $\operatorname{Re}\tau = \pm 1/2$. Here is a sketch: On the one hand, it is immediate that θ_v decreases monotonically with $\operatorname{Im}\tau$. On the other hand, by enlarging the outer square or triangle, and shrinking the inner square or triangle, one easily sees from the flat structure that θ_h increases monotonically with $\operatorname{Im}\tau$. This simple proof is possible because, for these cases, the twist angles take special values and do not vary with $\operatorname{Im}\tau$. This may not hold for other cases, for which even the meaning of “twist angle” is not clear.

We also conjecture the following classification statement.

Conjecture 6.6.

- The tP, tD, CLP and tG surfaces are the only members of \mathcal{T} .
- The H, rPD and rGL surfaces are the only members of \mathcal{R} .

For a proof, we need to prove the previous conjecture first, then also exclude the existence of new surface with pitch 0 or 2.

Moreover, note that the order-2 rotations around horizontal axes are only used to determine the López–Ros factor. We wonder if this is necessary and conjecture that

Conjecture 6.7.

- The tP, tD, CLP and tG surfaces are the only TPMSg3s with an order-4 screw symmetry.
- The H, rPD and rGL surfaces are the only TPMSg3s with an order-3 screw symmetry.

APPENDIX A. ASYMPTOTIC BEHAVIOR OF ASSOCIATE ANGLE

We now give a detailed asymptotic analysis of θ_h for \mathcal{T} .

We need to study the shape of the twisted square annulus with more care. For safety and convenience, we adopt the natural convention (see Section 3.4) for all computations involving Jacobi elliptic functions. So we define $\tilde{\tau} = \tau - r$ where $r := \lfloor \operatorname{Re}\tau + 1/2 \rfloor$, hence $-1/2 < \operatorname{Re}\tilde{\tau} \leq 1/2$. We write $\tilde{m} = \lambda(2\tilde{\tau})$, and correspondingly $\tilde{K} = K(\tilde{m})$ and $\tilde{K}' = -2i\tilde{\tau}\tilde{K}$. Note that $\tilde{K}' = K(1-\tilde{m})$ coincides with the usual definition of the associated complete elliptic integral of the first kind.

Remark A.1. The arguments of the Jacobi elliptic functions can be directly replaced by their tilde versions. This practice is however not safe elsewhere. In particular, the López–Ros factor $m^{1/4}$ can not be directly replaced by $\tilde{m}^{1/4}$. Instead, we must use the convention that

$$\arg m = 2\pi r + \arg \tilde{m}.$$

Let us first look at

$$\psi_1(\tau) := \int_0^{1/2} (m^{1/4} \operatorname{sn}(4\tilde{K}z; \tilde{\tau}))^{1/2} dz,$$

which is a vector pointing from $\Phi_1(0)$ to $\Phi_1(1/2)$, hence an straightened edge vector of the inner twisted square. With the change of variable $\zeta = \operatorname{sn}(4\tilde{K}z; \tilde{\tau})$, we have

$$(4) \quad \psi_1(\tau) = 2 \frac{m^{1/8}}{4\tilde{K}} \int_0^1 \frac{\zeta^{1/2} d\zeta}{\sqrt{(1-\zeta^2)(1-\tilde{m}\zeta^2)}}.$$

Here we used the identities

$$\begin{aligned}\frac{d}{dz} \operatorname{sn}(z; \tilde{\tau}) &= \operatorname{cn}(z; \tilde{\tau}) \operatorname{dn}(z; \tilde{\tau}); \\ \operatorname{cn}^2(z; \tilde{\tau}) &= 1 - \operatorname{sn}^2(z; \tilde{\tau}); \\ \operatorname{dn}^2(z; \tilde{\tau}) &= 1 - \tilde{m} \operatorname{sn}^2(z; \tilde{\tau}).\end{aligned}$$

Then we compute the integral

$$\begin{aligned}\psi_2(\tau) &:= \int_0^{\tilde{\tau}/2} (m^{1/4} \operatorname{sn}(4\tilde{K}z; \tilde{\tau}))^{1/2} dz, \\ &= \int_0^{1/2} (m^{1/4} \operatorname{sn}(4\tilde{K}\tilde{\tau}x; \tilde{\tau}))^{1/2} \tilde{\tau} dx \\ &= \int_0^{1/2} (m^{1/4} \operatorname{sn}(2i\tilde{K}'x; \tilde{\tau}))^{1/2} \tilde{\tau} dx.\end{aligned}$$

This is a vector pointing from $\Phi_1(0)$ to $\Phi_1(\tilde{\tau}/2)$, hence from an inner vertex to the nearest outer vertex of the twisted annulus. Then we use the Jacobi imaginary transformation $\operatorname{sn}(z; \tau) = -i \operatorname{sc}(iz; -1/\tau)$ and obtain

$$\begin{aligned}\psi_2(\tau) &= \int_0^{1/2} (-im^{1/4} \operatorname{sc}(-2\tilde{K}'x; -1/\tilde{\tau}))^{1/2} \tilde{\tau} dx \\ (5) \quad &= e^{3\pi i/4} \frac{m^{1/8}}{4\tilde{K}} \int_0^\infty \frac{\xi^{1/2} d\xi}{\sqrt{(1+\xi^2)(1+\tilde{m}\xi^2)}},\end{aligned}$$

where we changed the variable $\xi = -\operatorname{sc}(-2\tilde{K}'x; -1/\tilde{\tau})$ and used the identities

$$\begin{aligned}\frac{d}{dz} \operatorname{sc}(z; \tilde{\tau}) &= \operatorname{dc}(z; \tilde{\tau}) \operatorname{nc}(z; \tilde{\tau}); \\ \operatorname{dc}^2(z; \tilde{\tau}) &= 1 + (1 - \tilde{m}) \operatorname{sc}^2(z; \tilde{\tau}); \\ \operatorname{nc}^2(z; \tilde{\tau}) &= 1 + \operatorname{sc}^2(z; \tilde{\tau}).\end{aligned}$$

The two vectors $\psi_1(\tau)$ and $\psi_2(\tau)$ can determine the images of all branch points under Φ_1 .

Lemma A.2. $\theta_h(\tau) \rightarrow \operatorname{Re}(1 - \tau)\pi/4$ as $\operatorname{Im} \tau \rightarrow \infty$.

Proof. As $\operatorname{Im} \tau = \operatorname{Im} \tilde{\tau} \rightarrow \infty$, we have [Law89, (2.1.12)]

$$m(\tau) = \lambda(2\tau) \sim 16 \exp(2i\pi\tau),$$

so $|m| \rightarrow 0$. Recall that $\tilde{K}(0) = \pi/2$, and that the integral in (4) tends to

$$\int_0^1 \frac{\zeta^{1/2} d\zeta}{\sqrt{(1-\zeta^2)}}$$

which is bounded. Therefore, $\psi_1(\tau) \rightarrow 0$ as $\operatorname{Im} \tau \rightarrow \infty$. In other words, the size of the inner square tends to 0.

On the other hand, we have

$$\psi_2(\tau) \sim e^{3i\pi/4} \frac{m^{1/8}}{4\tilde{K}} \int_0^\infty \frac{d\xi}{\xi^{1/2} \sqrt{1+\tilde{m}\xi^2}} = e^{(r+3)i\pi/4} \frac{\tilde{m}^{-1/8}}{4\tilde{K}} \int_0^\infty \frac{du}{u^{1/2} \sqrt{1+u^2}},$$

where we changed the variable $u = \xi\sqrt{m}$ and used the convention that $\arg m = 2\pi r + \arg \tilde{m}$. Note again that the integral is bounded, hence $|\psi_2(\tau)| \sim |m|^{-1/8}$. In other words, the size of the outer square grows exponentially with $\operatorname{Im} \tilde{\tau}$.

Therefore, as $\operatorname{Im} \tau \rightarrow \infty$, the integral

$$\psi(\tau) = \int_0^{(1+\tau)/2} (m^{1/4} \operatorname{sn}(4Kz; \tau))^{1/2} dz$$

is dominated by

$$\begin{aligned}\psi(\tau) &\sim \int_{(r+1)/2}^{(\tau+1)/2} (m^{1/4} \operatorname{sn}(4Kz; \tau))^{1/2} dz \sim e^{-(r+1)i\pi/2} \psi_2(\tau) \\ &\sim e^{-(r+1)i\pi/2} e^{(r+3)i\pi/4} \frac{\tilde{m}^{-1/8}}{4\tilde{K}} \int_0^\infty \frac{du}{u^{1/2}\sqrt{1+u^2}},\end{aligned}$$

Now we can conclude that

$$\theta_h(\tau) = \arg \psi(\tau) \rightarrow (1 - r - \operatorname{Re} \tilde{\tau})\pi/4 = \operatorname{Re}(1 - \tau)\pi/4.$$

□

A similar argument applies to rGL, so we omit the proof. The conclusion is that

$$\theta_h \rightarrow \operatorname{Re}(1/2 - \tau)\pi/3 \quad \text{as } \operatorname{Im} \tau \rightarrow \infty.$$

Lemma A.3. $\theta_h(\tau) \rightarrow 0$ from the negative side as $\tau \rightarrow 1$ within Ω_t .

Proof. By the transformation $\lambda(-1/\tau) = 1 - \lambda(\tau)$ [Law89, (9.4.10)], we see that

$$\tilde{m} = m(\tilde{\tau}) = 1 - 16e^{-i\pi/2\tilde{\tau}} + O(e^{-i\pi/2\tilde{\tau}}) \quad \text{as } \tilde{\tau} \rightarrow 0.$$

Then [Law89, Exercise 8.13]

$$\tilde{K} = \int_0^1 \frac{d\zeta}{\sqrt{(1-\zeta^2)(1-\tilde{m}\zeta^2)}} \sim -\frac{1}{2} \ln(1-\tilde{m}) \sim \frac{i\pi}{4\tilde{\tau}}.$$

The standard proof for this also applies to prove that the integral in (4) satisfies

$$\int_0^1 \frac{\zeta^{1/2} d\zeta}{\sqrt{(1-\zeta^2)(1-\tilde{m}\zeta^2)}} \sim -\frac{1}{2} \ln(1-\tilde{m}) \sim \frac{i\pi}{4\tilde{\tau}}.$$

One can also quickly convince oneself by noting that the integrand in (4) differs from the integrand of \tilde{K} only by a factor $\zeta^{1/2}$, which can be neglected near 1, where the divergence occurs. In other words, the integral in (4) is asymptotically equivalent to \tilde{K} . So we have $\psi_1(\tau) \rightarrow \frac{1}{2}m^{1/8}$ as $\tau \rightarrow 1$.

On the other hand, the integral in (5) tends to

$$\int_0^\infty \frac{\xi^{1/2} d\xi}{1+\xi^2} = \frac{\pi}{\sqrt{2}}$$

which is bounded, hence $\psi_2(\tau) \rightarrow 0$. Therefore, as $\tau \rightarrow 1$, we see from the flat structure that $\psi(\tau) \rightarrow \frac{1-i}{2}m^{1/8}$, so

$$\theta_h(\tau) = \arg(m(\tau))/8 - \pi/4 = \arg(\tilde{m})/8 \rightarrow 0.$$

Note again that we used the convention $\arg m(\tau) = m(\tilde{\tau} + 1) = 2\pi + \arg m(\tilde{\tau})$.

We now prove that the convergence is from the negative side. A routine calculation shows that

$$\arg(e^{-i\pi/2\tilde{\tau}}) = -\frac{\pi \operatorname{Re} \tilde{\tau}}{2|\tilde{\tau}|^2} = \frac{\pi \sin \theta_v}{2|\tilde{\tau}|}.$$

When $\tau \in \Omega_t$, it follows from elementary geometry that $0 < \sin \theta_v < |\tilde{\tau}|$, hence $0 < \arg(e^{-i\pi/2\tilde{\tau}}) < \pi/2$. Therefore, when τ tends to 0 within Ω_t , we have $\arg(\tilde{m}) = \arg(1 - 16e^{-i\pi/2\tilde{\tau}}) < 0$. □

Remark A.4. The integrals arisen from \mathcal{T} surfaces (e.g. (4) and (5)) can be explicitly expressed in terms of elliptic integrals; see [Bow61, Chapter X] and [BF71, §595 et seq.]. For example, we have

$$\begin{aligned}\int_0^{1/2} (m^{1/4} \operatorname{sn}(4\tilde{K}z; \tilde{\tau}))^{1/2} dz &= \frac{e^{r\pi i/4}}{2\sqrt{2}} \frac{\tilde{m}^{-1/8}}{\sqrt{1+\tilde{m}^{1/2}}} \frac{K(\mu) - K'(\mu)}{K(\tilde{m})}, \\ \int_{\tau/2}^{1/2+\tau/2} (m^{1/4} \operatorname{sn}(4\tilde{K}z; \tilde{\tau}))^{1/2} dz &= \frac{e^{r\pi i/4}}{2\sqrt{2}} \frac{\tilde{m}^{-1/8}}{\sqrt{1+\tilde{m}^{1/2}}} \frac{K(\mu) + K'(\mu)}{K(\tilde{m})},\end{aligned}$$

for the inner and outer edge vectors of the twisted annulus, where

$$\mu = \frac{(1 + \tilde{m}^{1/4})^2}{2 + 2\tilde{m}^{1/2}}.$$

We then obtain that

$$(6) \quad \psi(\tau) = e^{r\pi i/4} \frac{1 - i}{2\sqrt{2}} \frac{\tilde{m}^{-1/8}}{\sqrt{1 + \tilde{m}^{1/2}}} \frac{K(\mu)}{K(\tilde{m})}.$$

This facilitates the numeric calculation for the tG-tD intersection but does not give an explicit expression.

We are not aware of equally explicit expressions for integrals arisen from \mathcal{R} surfaces.

REFERENCES

- [BB98] Jonathan M. Borwein and Peter B. Borwein. *Pi and the AGM*, volume 4 of *Canadian Mathematical Society Series of Monographs and Advanced Texts*. John Wiley & Sons, Inc., New York, 1998. A study in analytic number theory and computational complexity, Reprint of the 1987 original, A Wiley-Interscience Publication.
- [BF71] Paul F. Byrd and Morris D. Friedman. *Handbook of elliptic integrals for engineers and scientists*. Die Grundlehren der mathematischen Wissenschaften, Band 67. Springer-Verlag, New York-Heidelberg, 1971. Second edition, revised.
- [Bow61] F. Bowman. *Introduction to elliptic functions with applications*. Dover Publications, Inc., New York, 1961.
- [CW18a] Hao Chen and Matthias Weber. A new deformation family of Schwarz' D surface. page 15 pp., 2018. Preprint, [arXiv:1804.01442](https://arxiv.org/abs/1804.01442).
- [CW18b] Hao Chen and Matthias Weber. An orthorhombic deformation family of Schwarz' H surfaces. page 17 pp., 2018. Preprint, [arXiv:1807.10631](https://arxiv.org/abs/1807.10631).
- [DLMF] *NIST Digital Library of Mathematical Functions*. <http://dlmf.nist.gov/>, Release 1.0.19 of 2018-06-22. F. W. J. Olver, A. B. Olde Daalhuis, D. W. Lozier, B. I. Schneider, R. F. Boisvert, C. W. Clark, B. R. Miller and B. V. Saunders, eds.
- [EFS15] Norio Ejiri, Shoichi Fujimori, and Toshihiro Shoda. A remark on limits of triply periodic minimal surfaces of genus 3. *Topology Appl.*, 196(part B):880–903, 2015.
- [FH92] Andrew Fogden and Stephen T Hyde. Parametrization of triply periodic minimal surfaces. II. regular class solutions. *Acta Crystallographica Section A*, 48(4):575–591, 1992.
- [FH99] Andrew Fogden and Stephan T. Hyde. Continuous transformations of cubic minimal surfaces. *The European Physical Journal B-Condensed Matter and Complex Systems*, 7(1):91–104, 1999.
- [FHL93] Andrew Fogden, M. Haeberlein, and Sven Lidin. Generalizations of the gyroid surface. *J. Phys. I*, 3(12):2371–2385, 1993.
- [FK92] H. M. Farkas and I. Kra. *Riemann surfaces*, volume 71 of *Graduate Texts in Mathematics*. Springer-Verlag, New York, second edition, 1992.
- [FW09] Shoichi Fujimori and Matthias Weber. Triply periodic minimal surfaces bounded by vertical symmetry planes. *Manuscripta Math.*, 129(1):29–53, 2009.
- [GBW96] Karsten Große-Brauckmann and Meinhard Wohlgemuth. The gyroid is embedded and has constant mean curvature companions. *Calc. Var. Partial Differential Equations*, 4(6):499–523, 1996.
- [Hur32] Adolf Hurwitz. *Über algebraische Gebilde mit eindeutigen Transformationen in sich*, pages 391–430. Springer Basel, Basel, 1932.
- [Kar89] Hermann Karcher. The triply periodic minimal surfaces of Alan Schoen and their constant mean curvature companions. *Manuscripta Math.*, 64(3):291–357, 1989.
- [KK79] Akikazu Kuribayashi and Kaname Komiya. On Weierstrass points and automorphisms of curves of genus three. In *Algebraic geometry (Proc. Summer Meeting, Univ. Copenhagen, Copenhagen, 1978)*, volume 732 of *Lecture Notes in Math.*, pages 253–299. Springer, Berlin, 1979.
- [KPS14] Miyuki Koiso, Paolo Piccione, and Toshihiro Shoda. On bifurcation and local rigidity of triply periodic minimal surfaces in \mathbb{R}^3 . page 26 pp., 2014. Preprint, [arXiv:1408.0953](https://arxiv.org/abs/1408.0953), to appear in Annales de l'Institut Fourier.
- [KWH93] Hermann Karcher, Fu Sheng Wei, and David Hoffman. The genus one helicoid and the minimal surfaces that led to its discovery. In *Global analysis in modern mathematics (Orono, ME, 1991; Waltham, MA, 1992)*, pages 119–170. Publish or Perish, Houston, TX, 1993.
- [Law89] Derek F. Lawden. *Elliptic functions and applications*, volume 80 of *Applied Mathematical Sciences*. Springer-Verlag, New York, 1989.
- [LL90] Sven Lidin and Stefan Larsson. Bonnet transformation of infinite periodic minimal surfaces with hexagonal symmetry. *Journal of the Chemical Society, Faraday Transactions*, 86(5):769–775, 1990.
- [LR91] Francisco J. López and Antonio Ros. On embedded complete minimal surfaces of genus zero. *J. Differential Geom.*, 33(1):293–300, 1991.

- [Mee90] William H. Meeks, III. The theory of triply periodic minimal surfaces. *Indiana Univ. Math. J.*, 39(3):877–936, 1990.
- [Oss64] Robert Osserman. Global properties of minimal surfaces in E^3 and E^n . *Ann. of Math. (2)*, 80:340–364, 1964.
- [Sch90] Hermann A. Schwarz. *Gesammelte Mathematische Abhandlungen*, volume 1. Springer, Berlin, 1890.
- [Sch70] Alan H. Schoen. Infinite periodic minimal surfaces without self-intersections. Technical Note D-5541, NASA, Cambridge, Mass., May 1970.
- [STFH06] Gerd E Schröder-Turk, Andrew Fogden, and Stephen T Hyde. Bicontinuous geometries and molecular self-assembly: comparison of local curvature and global packing variations in genus-three cubic, tetragonal and rhombohedral surfaces. *The European Physical Journal B-Condensed Matter and Complex Systems*, 54(4):509–524, 2006.
- [Wey06] Adam G. Weyhaupt. *New families of embedded triply periodic minimal surfaces of genus three in euclidean space*. ProQuest LLC, Ann Arbor, MI, 2006. Thesis (Ph.D.)–Indiana University.
- [Wey08] Adam G. Weyhaupt. Deformations of the gyroid and Lidinoid minimal surfaces. *Pacific J. Math.*, 235(1):137–171, 2008.
- [WW98] M. Weber and M. Wolf. Minimal surfaces of least total curvature and moduli spaces of plane polygonal arcs. *Geom. Funct. Anal.*, 8(6):1129–1170, 1998.
- [WW02] Matthias Weber and Michael Wolf. Teichmüller theory and handle addition for minimal surfaces. *Ann. of Math. (2)*, 156(3):713–795, 2002.

(Chen) GEORG-AUGUST-UNIVERSITÄT GÖTTINGEN, INSTITUT FÜR NUMERISCHE UND ANGEWANDTE MATHEMATIK
Email address: h.chen@math.uni-goettingen.de

STACKING DISORDER IN PERIODIC MINIMAL SURFACES

HAO CHEN AND MARTIN TRAIZET

ABSTRACT. We construct 1-parameter families of non-periodic embedded minimal surfaces of infinite genus in $T \times \mathbb{R}$, where T denotes a flat 2-tori. Each of our families converges to a foliation of $T \times \mathbb{R}$ by T . These surfaces then lift to minimal surfaces in \mathbb{R}^3 that are periodic in horizontal directions but not periodic in the vertical direction. In the language of crystallography, our construction can be interpreted as disordered stacking of layers of periodically arranged catenoid necks. Limit positions of the necks are governed by equations that appear, surprisingly, in recent studies on the Mean Field Equation and the Painlevé VI Equation. This helps us to obtain a rich variety of disordered minimal surfaces. Our work is motivated by experimental observations of twinning defects in periodic minimal surfaces, which we reproduce as special cases of stacking disorder.

1. INTRODUCTION

1.1. Background. Triply periodic minimal surfaces (TPMSs) is a topic of trans-disciplinary interest. On the one hand, the mathematical notion has been employed to model many structures in nature (e.g. biological membrane) and in laboratory (e.g. lyotropic liquid crystals); we refer the readers to the book [HBL⁺96] for more information. On the other hand, natural scientists have been contributing with important mathematical discoveries, many long precede the rigorous mathematical treatment. Examples include the famous gyroid discovered in [Sch70] and proved in [GBW96], as well as its deformations discovered in [FHL93, FH99] and recently proved in [Che19a].

The current paper is another example in which mathematics is inspired by natural sciences. In [HXBC11], mesoporous crystals exhibiting the structure of Schwarz' D surface are synthesized. Remarkably, a twinning structure, which looks like two copies of Schwarz' D surface glued along a reflection plane, is observed. In other word, the periodicity is broken in the direction orthogonal to the reflection plane. Thereafter, many other crystal defects are experimentally observed in more TPMS structures, leading to a growing demand of mathematical understanding.

Recently, the first named author [Che19b] responded to this demand with numerical experiments in Surface Evolver [Bra92]. More specifically, periodic twinning defects are numerically introduced into rPD surfaces (see Figure 1) and the gyroid. Success of these experiments provide strong evidences for the existence of single twinning defects.

Moreover, he also became aware of the node-opening techniques developed by the second named author [Tra02]. The idea is to glue catenoid necks among horizontal planes. When

Date: October 27, 2020.

2010 Mathematics Subject Classification. Primary 53A10.

Key words and phrases. minimal surfaces.

H. Chen is supported by Individual Research Grant from Deutsche Forschungsgemeinschaft within the project “Defects in Triply Periodic Minimal Surfaces”, Projektnummer 398759432. M. Traizet is supported by the ANR project Min-Max (ANR-19-CE40-0014).

the planes are infinitesimally close, the necks degenerate to singular points termed nodes. It is proved that, if the limit positions of the nodes satisfy a balancing condition and a non-degeneracy condition, then it is possible to push the planes a little bit away from each other, giving a 1-parameter family of minimal surfaces along the way. The technique has been used to construct TPMSs [Tra08] by gluing necks among finitely many flat tori, and non-periodic minimal surfaces with infinitely many planar ends [MT12] by gluing necks among infinitely many Riemann spheres.

In this paper, we combine the techniques in [Tra08] and [MT12] to glue necks among infinitely many flat tori. Then each balanced and non-degenerate arrangement of nodes gives rise to a 1-parameter families of minimal surfaces. Seen in $T \times \mathbb{R}$, each of these family converges to a foliation of $T \times \mathbb{R}$ by T . Seen in \mathbb{R}^3 , the minimal surfaces are periodic in two independent horizontal directions but not periodic in any other independent direction.

Our motivation is to rigorously construct twinning defects, but the examples produced by our construction is far richer. In the language of crystallography, our construction can be seen as stacking layers of periodically arranged catenoid necks. In the case that T is the 60-degree torus, for example, we will see that any bi-infinite sequence of 5 stacking patterns gives arise to a 1-parameter family of minimal surfaces. These are then uncountably many families. In particular, a twinning defect arises from a stacking fault, which is not periodic but still quite ordered from a physics point of view. But most of our examples does not exhibit any order, hence should be considered as stacking disorders.

Back to the twinning, experiments and simulations have shown that TPMSs with twinning defects decay exponentially to the standard TPMSs. We will provide mathematical proof to this physics phenomenon, hence finally justify the term “TPMS twinning”. More specifically, we will prove that if a configuration is eventually periodic, then the corresponding minimal surface is asymptotic to a TPMS. The proof uses weighted Banach space as in [Tra13].

Our construction uses Implicit Function Theorem, hence only works near the degenerate limit of foliations, which is not physically plausible. However, physicists have proposed formation mechanisms for TPMSs in nature and in laboratory (e.g. [CF97, MBF94, CCM⁺06, TBC⁺15]) that are very similar to node-opening, some even with experiment evidences. Hence we may hope that some of the minimal surfaces constructed in this paper, including those with stacking disorders, would be one day observed in laboratory.

1.2. Mathematical setting. A doubly periodic minimal surface (DPMS) M is invariant by two independent translations, which we may assume to be horizontal. Let Γ be the two-dimensional lattice generated by these translations, then M projects to a minimal surface M/Γ in $\mathbb{R}^3/\Gamma = T \times \mathbb{R}$, where $T = \mathbb{R}^2/\Gamma$ denotes a flat 2-torus. Immediate examples of infinite genus are given by triply periodic minimal surfaces (TPMSs), if one ignores one of their three periods. Motivated by experimental observations mentioned above, we are particularly interested in non-periodic DPMS with infinite genus.

A flat torus in $T \times \mathbb{R}$ is *horizontal* if it has the form $T \times \{h\}$ for some $h \in \mathbb{R}$; then h is called the *height* of the torus. Informally speaking, we construct minimal surfaces that look like infinitely many horizontal flat tori in $T \times \mathbb{R}$, ordered by increasing height, with one catenoid neck between each adjacent pair. The tori are then labeled by $k \in \mathbb{Z}$ in the order of height. The catenoid necks are also labeled by $k \in \mathbb{Z}$, such that the k -th neck is between the k -th and the $(k+1)$ -th tori.

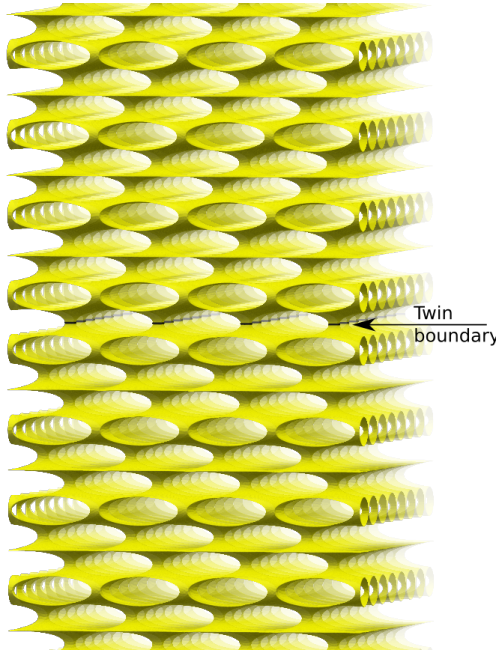


FIGURE 1. Twinning defects in an rPD surface near the catenoid limit, as described in Example 5. This is actually an approximation by a TPMS with large vertical period. The surface has a horizontal symmetry plane in the middle. The image was computed in Surface Evolver [Bra92] using the procedure in [Che19b].

Remark 1.1. Our construction can, in principle, handle finitely many necks between each adjacent pair of tori. But in view of the immediate interest from material sciences, we will only glue one catenoid neck between each adjacent tori. This also eases the notations and facilitates the proofs, but still produces a rich variety of examples.

More formally, we say that a minimal surfaces $M \in T \times \mathbb{R}$ is *stacked* if there is an increasing sequence of real numbers $(h_k)_{k \in \mathbb{Z}}$ satisfying

- $M \cap (T \times \{h_k\})$ has a single connected component that projects to a null-homotopic smooth simple closed curve in T ;
- $M \cap (T \times (h_k, h_{k+1}))$ is homeomorphic to T with two disks removed.

Then the k -th neck can be interpreted as an annular neighborhood of $M \cap (T \times \{h_k\})$.

Remark 1.2. The term “stacked” is borrowed from crystallography. Closed-packed structures are often described as a result of stacking layers of periodically arranged atoms, one on top of another. Analogously, a stacked minimal surface can be seen as obtained by stacking layers of periodically arranged catenoid necks.

We intend to construct 1-parameter families M_t , $t > 0$, of stacked minimal surfaces such that, in the limit $t \rightarrow 0$, every neck converges to a catenoid after suitable rescaling. If we rescale to keep the size of the torus, then M_t will converge to a foliation of $T \times \mathbb{R}$ by T , and necks converge to singular points, which we call *nodes*.

1.3. Definitions and main result.

Definition 1.1. A *node configuration* is a sequence $\mathbf{p} = (p_k)_{k \in \mathbb{Z}}$ such that $p_k \in T$ for all $k \in \mathbb{Z}$.

We use p_k to prescribe the limit position of the k -th node, and assume that

Hypothesis 1.2 (Uniform separation). There exists a constant $\varrho > 0$ such that p_k and p_ℓ are at least at distance ϱ apart whenever $|k - \ell| = 1$.

Assume that $2\omega_1 = 1$ and $2\omega_2 = \tau$ generate the lattice Γ , so $T = T_\tau = \mathbb{C}/(\mathbb{Z} + \tau\mathbb{Z})$. Without loss of generality, we also assume that $\text{Im } \tau > 0$. Then for $p \in T$, we use $x(p; \tau)$ and $y(p; \tau)$ to denote its coordinates in the basis 1 and τ , and define the function

$$\xi(p; \tau) = x(p; \tau)\eta_1(\tau) + y(p; \tau)\eta_2(\tau),$$

where $\eta_i(\tau) = \zeta(z + 2\omega_i; \tau) - \zeta(z; \tau) = 2\zeta(\omega_i; \tau)$ for $i = 1, 2$, and

$$\zeta(z; \tau) = \frac{1}{z} \sum_{0 \neq u \in \mathbb{Z} + \tau\mathbb{Z}} \left(\frac{1}{z-u} + \frac{1}{u} + \frac{z}{u^2} \right)$$

is the Weierstrass zeta function associated to Γ .

The following definitions are borrowed from [Tra08] and [MT12]. Given a node configuration \mathbf{p} , the *force* F_k exerted on the node p_k by other nodes is

$$(1) \quad F_k := \zeta(p_{k+1} - p_k; \tau) + \zeta(p_{k-1} - p_k; \tau) + 2\xi(p_k; \tau) - \xi(p_{k+1}; \tau) - \xi(p_{k-1}; \tau)$$

Definition 1.3. A node configuration is said to be *balanced* if $F_k = 0$ for all $k \in \mathbb{Z}$.

Since our construction uses the Implicit Function Theorem, we need the differential of the force to be invertible in some sense. As explained in [MT12], (p_k) is not the right parameter to formulate non-degeneracy and one needs to introduce the sequence $\mathbf{q} = (q_k)$ defined by

$$q_k = p_k - p_{k-1}.$$

Note that the uniform separation hypothesis can be reformulated as (q_k) being bounded away from 0. From now on, we use the term “configuration” for the infinite sequence (q_k) .

Under the new variables, (1) becomes

$$F_k := \zeta(q_{k+1}; \tau) - \zeta(q_k; \tau) + \xi(q_k; \tau) - \xi(q_{k+1}; \tau) = G_{k+1} - G_k.$$

where

$$G_k = G(q_k; \tau) = \zeta(q_k; \tau) - \xi(q_k; \tau).$$

A configuration is then balanced if (G_k) is a constant sequence, i.e. $G_k = G_0$ for all $k \in \mathbb{Z}$.

Definition 1.4. A configuration is said to be *non-degenerate* if the differential of $(G_k)_{k \in \mathbb{Z}}$ with respect to $(q_k)_{k \in \mathbb{Z}}$, as a map from ℓ^∞ to itself, is an isomorphism.

Note that $G(q; \tau)$ is periodic in q but not meromorphic. The function $G(q; \tau)$ is called the *Hecke form* in [Lan95]. It was proved by Hecke [Hec27] that, if $q = (k_1 + k_2\tau)/N$ with $\gcd(k_1, k_2, N) = 1$, then $G(q; \tau)$ is a modular form of weight 1 with respect to the congruence group $\Gamma(N)$. Recently, the Hecke form gained popularity for its importance in the study of PDEs, including the Mean Field Equation, the Painlevé VI Equation, and the (generalized) Lamé Equation; see [Lin16] for a survey. We will exploit some of the recent results [LW10, CKLW18, BE16] in our construction.

Now we are ready to state our main theorems

Theorem 1.5. *If a configuration \mathbf{q} is balanced, non-degenerate, and satisfies the uniform separation hypothesis, then there exists in $T \times \mathbb{R}$ a 1-parameter family $(M_t)_{0 < t < \epsilon}$ of embedded stacked minimal surfaces which, in the limit $t \rightarrow 0$, converges to a foliation of $T \times \mathbb{R}$ by T . Moreover, the necks have asymptotically catenoidal shape and their limiting positions in T are prescribed by \mathbf{p} .*

Theorem 1.6. *Let \mathbf{q} and \mathbf{q}' be two balanced and non-degenerate configurations that satisfy the uniform separation hypothesis. Assume that (q_k) is periodic (in the sense $q_{k+N} = q_k$) and $q'_k = q_k$ for all $k \geq 0$. Let (M_t) and (M'_t) denote the corresponding 1-parameter families of minimal surfaces. Then M_t is a TPMS and M'_t is asymptotic to a translation of M_t as $x_3 \rightarrow \infty$.*

The paper is organized by increasing technicality. After reviewing some examples in Section 2, we prove our main theorems in Section 3 and Section 4, respectively. Technical ingredients of the proofs are delayed to later sections. In Section 5 we prove the existence and smooth dependence on parameters of a holomorphic 1-form ω that we used in the Weierstrass data in Section 3. In Section 6, we study the asymptotic behavior of ω and other parameters, which is crucial for proving the TPMS asymptotic behavior in Section 4.

2. EXAMPLES

Given an infinite sequence of planes, if only one node is opened between each adjacent pair, the result is necessarily a Riemann minimal example [MT12]. We now show that opening nodes among flat tori is a sharp contrast. Although we only open one node between each adjacent pair of tori, we still obtain a rich variety of balanced configurations. We produce configurations using the following

Proposition 2.1. *Let $\tilde{q}_0, \tilde{q}_1, \dots, \tilde{q}_{n-1}$ be n solutions of the equation*

$$(2) \quad G(q; \tau) = C$$

for the same complex constant C . Assume that the differential of G with respect to q at \tilde{q}_k , as a function from \mathbb{R}^2 to \mathbb{R}^2 , is non-singular for each k . Then any bi-infinite sequence $(q_k)_{k \in \mathbb{Z}}$ of elements in the set $\{\tilde{q}_0, \tilde{q}_1, \dots, \tilde{q}_{n-1}\}$ is a balanced, non-degenerate configuration satisfying the uniform separation hypothesis.

Proof. The configuration is balanced by definition. Since there is only a finite number of points \tilde{q}_k , the uniform separation hypothesis is satisfied and the differentials of G with respect to q at \tilde{q}_k , as well as their inverses, are uniformly bounded. Then the differential of (G_k) with respect to (q_k) is clearly an automorphism of ℓ^∞ . \square

We can produce a rich variety of examples thanks to the fact that (2) often has several solutions, which we can combine in any arbitrary way to form stacking disorders. We first discuss the number of solutions of Equation (2).

2.1. Solutions with $C = 0$. The solutions to $G(q; \tau) = 0$ are critical points of the Green function on a flat torus. The number of critical points and their non-degeneracy has been investigated in [LW10, CKLW18, BE16]. Recall that the function G is odd and Γ -periodic in the variable q . Hence for any τ , the 2-division points $1/2, \tau/2$ and $(1 + \tau)/2$ are trivial solutions to $G(q; \tau) = 0$. Moreover, it is recently proved [CKLW18] (see also [BMMS17]) that

all three trivial solutions are non-degenerate for a generic τ , and at least two of them are non-degenerate for any τ . Using Proposition 2.1, any flat 2-torus T admits uncountably many balanced and non-degenerate configurations, giving rise to uncountably many 1-parameter families of non-periodic minimal surfaces in $T \times \mathbb{R}$.

Since $G(q; \tau)$ is odd in q , non-trivial solutions of $G(q; \tau) = 0$ must appear in pairs. Using a deep connection with the mean field equation, Lin and Wang proved that $G(q; \tau) = 0$ has at most one non-trivial solution pair for a fixed τ [LW10, Theorem 1.2]. In other words, $G(q; \tau) = 0$ has either three or five solutions. A direct and simpler proof was later provided by Bergweiler and Eremenko [BE16], who also give an explicit criterion distinguishing τ 's with three and five solutions. Moreover, in the case of five solutions, all solutions are non-degenerate [LW17]. For an explicit example, with $\tau = \exp(i\pi/3)$, the non-trivial pair of solutions are

$$(3) \quad q = \pm(1 + \tau)/3.$$

2.2. TPMS examples. For a fixed τ , any bi-infinite sequence of the solutions of $G(q; \tau) = 0$ is a balanced configuration, hence gives rise to a family of minimal surfaces. From a crystallographic point of view, most of these surfaces would be considered as disordered.

TPMSs with perfect periodic patterns, arising from periodic configurations, are certainly the most interesting cases for crystallographers. In the following, we list some TPMSs of genus three that arise from configurations with period 2 (namely $q_{2k} = q_0$ and $q_{2k+1} = q_1$ for all $k \in \mathbb{Z}$). This completes the discussion in Section 4.3.3 of [Tra08] which was incomplete.

Example 1. If $q_1 = q_0$ (so q is constant) the configuration is trivially balanced. These configurations give rise to TPMSs in Meeks' 5-parameter family. Some famous examples are:

- $\operatorname{Re} \tau = 0$, $q_0 = (1 + \tau)/2$, gives an orthorhombic deformation family of Schwarz' P surface (named oPa in [FH92]), which reduces to Schwarz' tP family when $\tau = i$.
- $|\tau| = 1$, $q_0 = (1 + \tau)/2$, gives another orthorhombic deformation family of Schwarz' P surface (named oPb in [FH92]), which reduces to Schwarz' tP family when $\tau = i$.
- $\operatorname{Re} \tau = 0$, $q_0 = 1/2$, gives an orthorhombic deformation family of Schwarz' CLP surface (named oCLP' in [FH92]).
- $\tau = \exp(i\pi/3)$, $q_0 = (1 + \tau)/3$, gives a rhombohedral deformation family of Schwarz' D and P surfaces (known as rPD).

Note that the first three examples are obtained from trivial solutions of $G(q; \tau) = 0$, and the fourth one is obtained from the non-trivial solutions (3).

Example 2. When $\operatorname{Re} \tau = 0$, $q_0 = 1/2$ and $q_1 = \tau/2$, gives the newly discovered $o\Delta$ surfaces [CW18a]. Note that this example is obtained by alternating two trivial solutions of the equation $G(q; \tau) = 0$.

Example 3. Examples with $q_1 = -q_0$ were studied in [CW18b]. In particular

- $\tau = \exp(i\pi/3)$, $q_0 = (1 + \tau)/3$, gives hexagonal Schwarz' H family. Note that this example is obtained by alternating the two non-trivial solutions (3).
- There exists a real number $\pi/2 > \theta^* > \pi/3$ such that whenever $\tau = \exp(i\theta)$ with $\theta < \theta^*$, the configuration is balanced with $q_0 = c(1 + \tau)$ for a unique $c < 1/2$. This leads to the orthorhombic deformations of Schwarz' H surfaces in [CW18b]. Existence and uniqueness of θ^* was essentially proved [Web02, WHW09], and independently

in [LW10]. Its value was computed in [CW18b] explicitly as

$$(4) \quad \theta^* = 2 \arctan \frac{K'(m)}{K(m)} \approx 1.23409,$$

where m is the unique solution of $2E(m) = K(m)$, and $K(m)$, $K'(m)$ and $E(m)$ are elliptic integrals of the first kind, associated first kind, and second kind, respectively.

- For general τ , non-trivial q_0 's that give balanced configurations are studied in [Web02, LW10, CKLW18] and numerically in [CW18b].

Remark 2.1. For crystallographers, the rPD and the H surfaces are analogous to, respectively, the cubic and hexagonal close-packing.

Remark 2.2. Interestingly, configurations in Examples 1 and 3 give rise to TPMSs no matter their degeneracy. Those in Example 1 form a 4-parameter family, and they are limits of Meeks 5-parameter family. Those in Example 3 are degenerate only if q_0 is a 2-division point, hence reduces to Example 1. In particular, the degenerate configuration with $\tau = \exp(i\theta^*)$ and $q_0 = q_1 = (1 + \tau)/2$ is considered in [CW18b]. It is the limit of a 1-parameter family of TPMSs that are degenerate in the sense that the same deformation of the lattices may lead to different deformations of the TPMSs. It is not clear to what extent does this phenomenon generalize.

2.3. Examples of TPMSs with defects. From the TPMS examples above, we obtain the following examples with asymptotic TPMS behavior by Theorem 1.6. From a crystallographic point of view, they are TPMSs with planar defects.

Example 4. We may combine oPa, oCLP' and o Δ surfaces using the trivial solutions of $G(q; \tau) = 0$ at the 2-division points. For example:

- The configuration $(q_k)_{k \in \mathbb{Z}}$ defined by

$$\operatorname{Re} \tau = 0, \quad q_k = \begin{cases} 1/2 & \text{if } k < 0, \\ (1 + \tau)/2 & \text{if } k \geq 0, \end{cases}$$

gives rise to non-periodic minimal surfaces in $T \times \mathbb{R}$ which are asymptotic to oPa surfaces as $x_3 \rightarrow +\infty$ and oCLP' surfaces as $x_3 \rightarrow -\infty$.

- The configuration $(q_k)_{k \in \mathbb{Z}}$ defined by

$$\operatorname{Re} \tau = 0, \quad q_k = \begin{cases} 1/2 & \text{if } k < 0, \\ \tau/2 & \text{if } k \geq 0, \end{cases}$$

gives rise to non-periodic minimal surfaces in $T \times \mathbb{R}$ which are asymptotic, as $x_3 \rightarrow +\infty$ and $x_3 \rightarrow -\infty$, to two different oCLP' surfaces. When $\tau = i$, the two oCLP' surfaces differ only by a 180-degree rotation with horizontal axis, hence can be seen as a rotation twin.

- The configuration $(q_k)_{k \in \mathbb{Z}}$ defined by

$$\operatorname{Re} \tau = 0, \quad q_k = \begin{cases} 1/2 & \text{if } k < 0 \text{ and odd,} \\ \tau/2 & \text{if } k < 0 \text{ and even,} \\ (1 + \tau)/2 & \text{if } k \geq 0, \end{cases}$$

gives rise to non-periodic minimal surfaces in $T \times \mathbb{R}$ which are asymptotic to oPa surfaces as $x_3 \rightarrow +\infty$ and the newly discovered o Δ surfaces [CW18a] as $x_3 \rightarrow -\infty$.

We certainly did not list all possible combinations. Note that these examples generalize to other τ 's in an obvious way, giving rise to non-periodic minimal surfaces that are asymptotic to unnamed TPMSs.

Example 5. We may combine H and rPD surfaces using the pair of non-trivial solutions (3). For example:

- The configuration defined by

$$\tau = \exp(i\pi/3), \quad q_k = \begin{cases} (1+\tau)/3 & \text{if } k < 0, \\ -(1+\tau)/3 & \text{if } k \geq 0, \end{cases}$$

gives rise to non-periodic minimal surfaces in $T \times \mathbb{R}$ which are asymptotic, as $x_3 \rightarrow +\infty$ and $x_3 \rightarrow -\infty$, to two Schwarz rPD surfaces that differ only by a reflection, hence are twins of Schwarz rPD-surfaces (see Figure 1). Such a D-twin has been observed experimentally.

- The configuration defined by

$$\tau = \exp(i\pi/3), \quad q_k = \begin{cases} (1+\tau)/3 & \text{if } k < 0 \text{ and even,} \\ -(1+\tau)/3 & \text{otherwise,} \end{cases}$$

gives rise to non-periodic minimal surfaces in $T \times \mathbb{R}$ which are asymptotic to Schwarz rPD surfaces as $x_3 \rightarrow +\infty$ and Schwarz' H surfaces as $x_3 \rightarrow -\infty$.

- The configuration defined by

$$\tau = \exp(i\pi/3), \quad q_k = \begin{cases} (1+\tau)/3 & \text{if } k < 0 \text{ and even or if } k > 0 \text{ and odd,} \\ -(1+\tau)/3 & \text{otherwise,} \end{cases}$$

gives rise to non-periodic minimal surfaces in $T \times \mathbb{R}$ which are asymptotic, as $x_3 \rightarrow +\infty$ and $x_3 \rightarrow -\infty$, to two different Schwarz' H surfaces that differ only by a horizontal translation.

We certainly did not list all possible combinations. These examples generalize, in an obvious way, to any other τ 's such that $G(q; \tau) = 0$ has a pair of non-trivial solutions, giving rise to non-periodic minimal surfaces that are asymptotic to unnamed TPMSs.

2.4. Historical remarks. The Hecke form $G(q; \tau)$ has been studied independently by the PDE and minimal surface communities. Hence we would like to point out some connections between their approaches.

Solutions to $G(q; \tau) = 0$ are particularly interesting as they are the critical points of the Green function on a flat torus T_τ [LW10, CKLW18]. This is no surprise in the context of node-opening construction of TPMSs. In [Tra08], the forces between nodes are compared to electrostatic forces between electric charges. The Green function is nothing but the potential function of the electric field generated by periodically arranged charges. The balancing condition asks that all charges are in equilibrium, hence at a critical point of the potential.

A 2-division point ω is degenerate if

$$\frac{\tau\wp(\omega; \tau) + \eta_2(\tau)}{\wp(\omega; \tau) + \eta_1(\tau)}$$

is real. This is the quotient of periods of the elliptic function $\wp(z; \tau) - \wp(\omega; \tau)$. So if ω is degenerate, the torus T_τ admits a meromorphic 1-form with a double pole, a double zero, and only real periods. Such tori are no stranger to the minimal surface theory. In particular,

the unique rhombic torus with period quotient -1 was used to construct helicoids with handles [Web02, WHW09], and its angle has an explicit expression as given in (4) (see [CW18b]). On the PDE side, existence of this torus was independently proved in [LW10].

Following [WHW09], we propose a simple construction for the torus and the 1-form: Slit the complex plane along the real segment $[-1, 1]$. Identify the top edge of $[-1, -x]$ (resp. $[-x, 1]$) with the bottom edge of $[x, 1]$ (resp. $[-1, x]$), where $x \in [0, 1)$ and $(x+1)/(x-1)$ is the quotient of periods. The result is a torus carrying a cone metric with two cone singularities, one of cone angle 6π at the point identified with ± 1 and $\pm x$, the other of cone angle -2π at ∞ . Its periods are obviously real. The same torus with flat metric is T_τ .

It follows easily from [Web02] that there exists a unique torus for each real period quotient. This essentially proves Theorem 6.1(1) in [CKLW18].

2.5. Solutions with $C \neq 0$. As said before, [BE16] proved again that the equation $G(z; \tau) = 0$ has either three or five solutions. Their elegant argument can be adapted to the case $C \neq 0$ and yields the following result:

Theorem 2.2. *For given τ and $C \in \mathbb{C}$, the equation $G(z; \tau) = C$ has at least 1 and at most 5 solutions.*

Proof. We adapt the argument of [BE16] to the case $C \neq 0$. First of all, following [BE16], we write

$$G(z; \tau) = \zeta(z; \tau) + az + b\bar{z} \quad \text{with } a = \frac{\pi}{\text{Im}(\tau)} - \eta_1 \quad \text{and} \quad b = -\frac{\pi}{\text{Im}(\tau)},$$

and define the anti-meromorphic function g by

$$g(z) = -\frac{1}{b} \left(\overline{\zeta(z)} + a\bar{z} - \bar{C} \right) = z - \frac{1}{b} \left(\overline{G(z; \tau)} - \bar{C} \right).$$

The only difference with [BE16] is that g is not odd anymore if $C \neq 0$.

It is proved in Lemma 4 of [BE16] using complex dynamics that g has at most two attracting fixed points modulo Γ . The proof carries over to the case $C \neq 0$ with no change. The function g satisfies $g(z + \omega) = g(z) + \omega$ for all $\omega \in \Gamma$. Hence we may define a map $\phi : \mathbb{C}/\Gamma \rightarrow \mathbb{C} \cup \{\infty\}$ by $\phi(z) = z - g(z)$. The equation $G(z; \tau) = C$ is equivalent to $\phi(z) = 0$. Since ϕ has a single simple pole, where the differential reverses orientation, its degree (as a map between compact manifolds of the same dimension) is -1 . Hence the equation $\phi(z) = 0$ always has at least one solution. In fact, $\phi(z) = 0$ has exactly one solution if $|C|$ is sufficiently large.

We have $\det(d\phi) = 1 - |\bar{\partial}g|^2$. If 0 is a regular value of ϕ , then writing N^+ and N^- for the number of zeros of ϕ with respectively positive and negative determinant of $d\phi$, we see that N^+ is the number of attracting fixed points of g , so $N^+ \leq 2$. Then since $\deg(\phi) = -1$, we have $N^- = N^+ + 1$ so the total number of zeros of ϕ is ≤ 5 . If 0 is a critical value of ϕ , the number of zeros of ϕ is still less than 5 by the same argument as in [BE16], Lemma 5.

Observe that if $C = 0$, then ϕ is odd so has the three half-lattice points as trivial zeros: this is the only place in this part of the argument of [BE16] where the parity of ϕ is really used. \square

Note that to apply Theorem 2.2 to minimal surfaces, we still need to study the non-degeneracy of the solutions.

3. CONSTRUCTION

3.1. Parameters. The parameters of the construction are a real number t in a neighborhood of 0 and four sequences of complex numbers

$$\mathbf{a} = (a_k)_{k \in \mathbb{Z}}, \quad \mathbf{b} = (b_k)_{k \in \mathbb{Z}}, \quad \mathbf{v} = (v_k)_{k \in \mathbb{Z}}, \quad \text{and} \quad \boldsymbol{\tau} = (\tau_k)_{k \in \mathbb{Z}}$$

in ℓ^∞ . Each parameter is in a small ℓ^∞ -neighborhood of a central value denoted with an underscore. We will calculate that the central value of the parameters are:

$$(5) \quad \underline{a}_k = -\frac{1}{2}, \quad \underline{b}_k = \frac{1}{2}\xi(\underline{v}_k; \underline{\tau}_k), \quad \underline{v}_k = (-\text{conj})^k q_k, \quad \underline{\tau}_k = (-\text{conj})^k \tau,$$

where conj denotes conjugation, τ and (q_k) prescribe the flat 2-torus and the configuration as in the introduction. We use $\mathbf{x} = (\mathbf{a}, \mathbf{b}, \mathbf{v}, \boldsymbol{\tau})$ to denote the vector of all parameters but t . When required, the dependence of objects on parameters will be denoted with a bracket as in $\Sigma[t, \mathbf{x}]$, but will be omitted most of the time.

3.2. Opening nodes and the Gauss map. We denote by $T_k = T_k[\mathbf{x}]$ the torus $\mathbb{C}/(\mathbb{Z} + \tau_k \mathbb{Z})$. The point $z = 0$ in T_k is denoted by 0_k . We define the elliptic function $g_k = g_k[\mathbf{x}]$ on T_k by

$$g_k(z) = a_k(\zeta(z; \tau_k) - \zeta(z - v_k; \tau_k)) + b_k.$$

It has two simple poles at 0_k and v_k , with residues a_k and $-a_k$, respectively. Observe that $1/g_k$ is a local complex coordinate in a neighborhood of 0_k and v_k . Hence for a sufficiently small $\varepsilon > 0$, $1/g_k$ gives a diffeomorphism z_k^+ from a neighborhood of v_k in T_k to the disk $D(0, 2\varepsilon) \subset \mathbb{C}$, and a diffeomorphism z_k^- from a neighborhood of 0_k in T_k to the disk $D(0, 2\varepsilon)$. Provided that \mathbf{x} is sufficiently close to $\underline{\mathbf{x}}$ and by Hypothesis 1.2, ε can be chosen independent of k and \mathbf{x} . Let D_k^\pm be the disk $|z_k^\pm| < \varepsilon$ in T_k .

Consider the disjoint union of all T_k for $k \in \mathbb{Z}$. If $t = 0$, identify $v_k \in T_k$ and $0_{k+1} \in T_{k+1}$ to create a node. The resulting Riemann surface with nodes is denoted $\Sigma[0, \mathbf{x}]$. If $t \neq 0$ and $|t| < \varepsilon$, then for each $k \in \mathbb{Z}$, remove the disks $|z_k^\pm| \leq t^2/\varepsilon$ from T_k , and let A_k^\pm be the annuli $t^2/\varepsilon < |z_k^\pm| < \varepsilon$. Identify A_k^+ and A_{k+1}^- by $z_k^+ z_{k+1}^- = t^2$. This opens nodes and creates a neck between T_k and T_{k+1} . The resulting Riemann surface is denoted $\Sigma = \Sigma[t, \mathbf{x}]$.

If $t \neq 0$, we define the Gauss map $g = g[t, \mathbf{x}]$ explicitly on $\Sigma[t, \mathbf{x}]$ by

$$g(z) = (tg_k(z))^{(-1)^{k+1}} \quad \text{in } T_k.$$

Then g takes the same value at the points that are identified when defining Σ . So g is a well-defined meromorphic function on Σ .

3.3. Height differential. We define

$$\Omega_k := T_k \setminus \left(\overline{D_k^+} \cup \overline{D_k^-} \right) \quad \text{and} \quad \Omega := \bigsqcup_{k \in \mathbb{Z}} \Omega_k \subset \Sigma.$$

All circles ∂D_k^- are homologous in Σ . This homology class is denoted γ . We denote by α_k and β_k the standard generators of the homology of T_k , namely the homology classes of $[0, 1]$ and $[0, \tau_k]$ modulo $\mathbb{Z} + \tau_k \mathbb{Z}$. We choose representatives of α_k and β_k within Ω_k , so they can be seen as curves on Σ .

By Proposition 5.1 in Section 5, for t small enough, there exists a holomorphic 1-form $\omega = \omega[t, \mathbf{x}]$ on $\Sigma[t, \mathbf{x}]$ with imaginary periods on α_k, β_k for all $k \in \mathbb{Z}$ and $\int_\gamma \omega = 2\pi i$. We define the height differential dh by

$$dh = t\omega.$$

If $t = 0$, ω is allowed to have simple poles at the nodes (a so-called *regular 1-form* on a Riemann surface with nodes). So ω has simple poles at 0_k and v_k , with residues 1 and -1 respectively, and imaginary periods on α_k and β_k . By Proposition 5.1, we have explicitly

$$(6) \quad \omega[0, \mathbf{x}] = (\zeta(z; \tau_k) - \zeta(z - v_k; \tau_k) - \xi(v_k; \tau_k)) dz \quad \text{in } T_k.$$

Finally, $\omega[t, \mathbf{x}]$ restricted to Ω depends smoothly on (t, \mathbf{x}) in a sense which we now explain.

Some care is required because the domain Ω depends on the parameters. To formulate the smooth dependence, we pullback ω to a fixed domain as follows. Let $\mathbb{T} = \mathbb{C}/(\mathbb{Z} + i\mathbb{Z})$ be the standard square torus. Let $\psi_k[\mathbf{x}]$ be the diffeomorphism defined by

$$\psi_k[\mathbf{x}] : \mathbb{T} \rightarrow T_k[\mathbf{x}], \quad \psi_k(x + iy) = x + \tau_k y.$$

Let $\tilde{v}_k = \psi_k^{-1}(v_k)$. Fix a small $\varepsilon' > 0$ and define

$$\tilde{\Omega}_k = \mathbb{T} \setminus (\overline{D(0, \varepsilon')} \cup \overline{D(\tilde{v}_k, \varepsilon')}) \quad \text{and} \quad \tilde{\Omega} = \bigsqcup_{k \in \mathbb{Z}} \tilde{\Omega}_k.$$

If ε' is small enough and \mathbf{x} is close enough to $\underline{\mathbf{x}}$, we have $\Omega_k \subset \psi_k(\tilde{\Omega}_k)$. Moreover, if t is small enough, the disks $|z_k^\pm| < t^2/\varepsilon$ which were removed when opening nodes are outside $\psi_k(\tilde{\Omega}_k)$, so we can see $\psi_k(\tilde{\Omega}_k)$ as a domain in Σ . We define $\psi : \tilde{\Omega} \rightarrow \Sigma$ by $\psi = \psi_k$ on $\tilde{\Omega}_k$. Then $\psi^*\omega$ is a smooth 1-form on $\tilde{\Omega}$. (Note that $\psi^*\omega$ is not holomorphic, because ψ_k is not conformal.)

We define the pointwise norm of a (not necessarily holomorphic) 1-form η on a domain U in \mathbb{C} or a torus \mathbb{C}/Γ by $|\eta(z)| = \sup_{X \in \mathbb{C}^*} \frac{|\eta(z)X|}{|X|}$. We denote $C^0(U)$ the Banach space of 1-forms $\eta = f_1 dx + f_2 dy$ with f_1, f_2 bounded continuous functions on U , with the sup norm. We can now state:

Proposition 3.1. *The map $(t, \mathbf{x}) \mapsto \psi^*\omega[t, \mathbf{x}]$ is smooth from a neighborhood of $(0, \underline{\mathbf{x}})$ to $C^0(\tilde{\Omega})$.*

This is the content of Proposition 5.1(c).

Remark 3.1. The point here is that $\tilde{\Omega}$ is a fixed domain, independent of the parameters. The domain $\psi(\tilde{\Omega}) \subset \Sigma$ depends on (τ_k) but not on t nor the other parameters. It contains the domain Ω which fully depends on \mathbf{x} . Since τ_k is in a neighborhood of $\underline{\tau}_k$, we have $c^{-1} \leq |\psi_k^* dz| \leq c$ for some uniform constant c . Hence for any holomorphic 1-form η on Σ ,

$$c^{-1} \|\psi_k^* \eta\|_{C^0(\tilde{\Omega})} \leq \|\eta\|_{C^0(\psi(\tilde{\Omega}))} \leq c \|\psi_k^* \eta\|_{C^0(\tilde{\Omega})}.$$

3.4. Zeros of the height differential. We use the Weierstrass parametrization

$$\Sigma[t, \mathbf{x}] \ni z \mapsto \operatorname{Re} \int_{z_0}^z (\Phi_1, \Phi_2, \Phi_3) \in \mathbb{R}^3,$$

where

$$(\Phi_1, \Phi_2, \Phi_3) := \left(\frac{1}{2}(g^{-1} - g), \frac{i}{2}(g^{-1} + g), 1 \right) dh$$

are holomorphic differentials, so that the Weierstrass parametrization is an immersion. So we need to solve the Regularity Problem, which asks that dh has a zero at each zero or pole of g , with the same multiplicity, and no other zeros.

The elliptic function $g_k[\mathbf{x}]$ has degree 2 so it has two zeros in T_k which we denote $Z_{k,1}[\mathbf{x}]$ and $Z_{k,2}[\mathbf{x}]$. Since $g_k[\mathbf{x}]$ has poles at 0_k and v_k , its zeros are in Ω_k provided that ε is small enough. Note that we cannot rule out the possibility of a double zero $Z_{k,1} = Z_{k,2}$ at $\underline{\mathbf{x}}$,

in which case $Z_{k,1}$ and $Z_{k,2}$ are not smooth functions of \mathbf{x} . Nevertheless, by Weierstrass Preparation Theorem, in a neighborhood of $\underline{\mathbf{x}}$, $Z_{k,1} + Z_{k,2}$ and $Z_{k,1}Z_{k,2}$ are smooth functions of \mathbf{x} . The gauss map g , by definition, has zeros (resp. poles) at $Z_{k,1}$ and $Z_{k,2}$ for k odd (resp. k even).

Proposition 3.2. *For (t, \mathbf{x}) close to $(0, \underline{\mathbf{x}})$, ω has two zeros in Ω_k for $k \in \mathbb{Z}$ (counting multiplicity) and no other zeros. The Regularity Problem is equivalent to*

$$(7) \quad \frac{\omega}{dz}(Z_{k,1}) + \frac{\omega}{dz}(Z_{k,2}) = 0$$

and

$$(8) \quad \int_{\partial\Omega_k} g_k^{-1} \omega = 0$$

for $k \in \mathbb{Z}$.

Proof. By (6), $\omega[0, \mathbf{x}]/dz$ is an elliptic function of degree 2 in T_k , with simple poles at 0_k and v_k . So it has two zeros in Ω_k as long as ε is small enough. Hence $\psi^*\omega[0, \mathbf{x}]$ has two zeros in $\tilde{\Omega}_k$, counting multiplicity. By Proposition 3.1 and the Argument Principle, for t small enough, $\psi^*\omega[t, \mathbf{x}]$ has two zeros in $\tilde{\Omega}_k$, so $\omega[t, \mathbf{x}]$ has two zeros in $\psi(\tilde{\Omega}_k)$. By the same proof of Corollary 2 in [Tra13], ω has no zero in the annuli A_k^\pm , so it has two zeros in Ω_k for each $k \in \mathbb{Z}$, and no further zero.

If $Z_{k,1} \neq Z_{k,2}$, then dz/g_k is a meromorphic 1-form on T_k with two simple poles at $Z_{k,1}$ and $Z_{k,2}$. Therefore, by the Residue Theorem,

$$\begin{aligned} \frac{1}{g'_k(Z_{k,1})} + \frac{1}{g'_k(Z_{k,2})} &= 0, \\ \int_{\partial\Omega_k} g_k^{-1} \omega &= 2\pi i \left(\frac{\omega}{g'_k dz}(Z_{k,1}) + \frac{\omega}{g'_k dz}(Z_{k,2}) \right) \\ &= \frac{2\pi i}{g'_k(Z_{k,1})} \left(\frac{\omega}{dz}(Z_{k,1}) - \frac{\omega}{dz}(Z_{k,2}) \right). \end{aligned}$$

Hence (7) and (8) are equivalent to $\frac{\omega}{dz}(Z_{k,1}) = \frac{\omega}{dz}(Z_{k,2}) = 0$.

If $Z_{k,1} = Z_{k,2}$, g_k has a double zero at $Z_{k,1}$. It is then easy to see, using the Residue Theorem, that (7) and (8) are equivalent to ω having a double zero at $Z_{k,1}$. \square

Proposition 3.3. *For t in a neighborhood of 0, there exists a unique value of $(b_k) \in \ell^\infty$, depending smoothly on t and the other parameters, such that (7) is solved for all $k \in \mathbb{Z}$. Moreover, at $t = 0$,*

$$b_k = -a_k \xi(v_k; \tau_k)$$

so

$$(9) \quad g_k dz = a_k \omega \quad \text{in } T_k.$$

Proof. Define

$$\mathcal{E}_k(t, \mathbf{x}) = \frac{\omega}{dz}(Z_{k,1}) + \frac{\omega}{dz}(Z_{k,2}).$$

Then by the Residue Theorem,

$$\mathcal{E}_k(t, \mathbf{x}) = \frac{1}{2\pi i} \int_{\partial\Omega_k} \frac{\omega}{z - Z_{k,1}} + \frac{\omega}{z - Z_{k,2}} = \frac{1}{2\pi i} \int_{\partial\Omega_k} \frac{(2z - (Z_{k,1} + Z_{k,2}))\omega}{z^2 - (Z_{k,1} + Z_{k,2})z + Z_{k,1}Z_{k,2}}.$$

Using Proposition 3.1, $(\mathcal{E}_k)_{k \in \mathbb{Z}}$ is a smooth map with value in ℓ^∞ . At $t = 0$, we have by (6)

$$\frac{\omega}{dz} = \frac{1}{a_k}(g_k(z) - b_k) - \xi(v_k; \tau_k)$$

Since $g_k(Z_{k,i}) = 0$,

$$\mathcal{E}_k(0, \mathbf{x}) = -2 \left(\frac{b_k}{a_k} + \xi(v_k; \tau_k) \right).$$

Since $\underline{a}_k = -1/2$, the partial differential of (\mathcal{E}_k) with respect to (b_k) is an automorphism of ℓ^∞ . Proposition 3.3 then follows from the Implicit Function Theorem. \square

If b_k is given by Proposition 3.3, then at $t = 0$, ω and g_k are proportional in T_k hence have the same zeros. Then (8) is satisfied at $t = 0$ disregard of the value of the other parameters. So we cannot easily solve (8) for $t \neq 0$ using the Implicit Function Theorem. We will solve (8) in Section 3.6.

3.5. The Period Problem. From now on, we assume that (b_k) is given by Proposition 3.3 and $\mathbf{x} = (a_k, v_k, \tau_k)_{k \in \mathbb{Z}}$ denotes the remaining parameters. The height differential has imaginary periods by definition. It remains to solve the following Period Problems for all $k \in \mathbb{Z}$:

$$(10) \quad \operatorname{Re} \int_{\alpha_k} \Phi_1 = (-1)^k, \quad \operatorname{Re} \int_{\alpha_k} \Phi_2 = 0,$$

$$(11) \quad \operatorname{Re} \int_{\beta_k} \Phi_1 = \operatorname{Re} \tau, \quad \operatorname{Re} \int_{\beta_k} \Phi_2 = \operatorname{Im} \tau,$$

$$(12) \quad \operatorname{Re} \int_{\gamma} \Phi_1 = 0, \quad \operatorname{Re} \int_{\gamma} \Phi_2 = 0.$$

Proposition 3.4. *For t small enough, there exists unique values for the parameters (a_k) and (τ_k) in ℓ^∞ , depending smoothly on t and (v_k) , such that (10) and (11) are satisfied for all $k \in \mathbb{Z}$. Moreover, at $t = 0$, $a_k = -1/2$ and $\tau_k = (-\operatorname{conj})^k(\tau)$, disregard of the value of (v_k) .*

Proof. we define

$$\begin{aligned} \mathcal{P}_{k,1}(t, \mathbf{x}) &= \operatorname{conj} \left(\int_{\alpha_k} g^{-1} dh \right) - \int_{\alpha_k} g dh \\ \mathcal{P}_{k,2}(t, \mathbf{x}) &= \operatorname{conj} \left(\int_{\beta_k} g^{-1} dh \right) - \int_{\beta_k} g dh \end{aligned}$$

Equations (10) and (11) are equivalent to

$$(13) \quad \begin{cases} \mathcal{P}_{k,1}(t, \mathbf{x}) = 2(-1)^k \\ \mathcal{P}_{k,2}(t, \mathbf{x}) = 2\tau. \end{cases}$$

We have in T_k :

$$g dh = \begin{cases} g_k^{-1} \omega & \text{if } k \text{ even} \\ t^2 g_k \omega & \text{if } k \text{ odd} \end{cases} \quad \text{and} \quad g^{-1} dh = \begin{cases} t^2 g_k \omega & \text{if } k \text{ even} \\ g_k^{-1} \omega & \text{if } k \text{ odd} \end{cases}$$

We can take $\alpha_k = \psi_k(\tilde{\alpha}_k)$ and $\beta_k = \psi_k(\tilde{\beta}_k)$ where $\tilde{\alpha}_k$ and $\tilde{\beta}_k$ are fixed curves in $\tilde{\Omega}_k$. By Proposition 3.1, $(\mathcal{P}_{k,1})_{k \in \mathbb{Z}}$ and $(\mathcal{P}_{k,2})_{k \in \mathbb{Z}}$ are smooth maps with value in ℓ^∞ . At $t = 0$, we have by (9) that: For k even,

$$\mathcal{P}_{k,1}(0, \mathbf{x}) = - \int_{\alpha_k} a_k^{-1} dz = \frac{-1}{a_k} \quad \text{and} \quad \mathcal{P}_{k,2}(0, \mathbf{x}) = - \int_{\beta_k} a_k^{-1} dz = \frac{-\tau_k}{a_k}.$$

The solution to (13) is then $a_k = -1/2$ and $\tau_k = \tau$. For k odd,

$$\mathcal{P}_{k,1}(0, \mathbf{x}) = \text{conj} \int_{\alpha_k} a_k^{-1} dz = \text{conj} \frac{1}{a_k} \quad \text{and} \quad \mathcal{P}_{k,2}(0, \mathbf{x}) = \text{conj} \int_{\beta_k} a_k^{-1} dz = \text{conj} \frac{\tau_k}{a_k}.$$

The solution to (13) is then $a_k = -1/2$ and $\tau_k = -\text{conj} \tau$. The partial differential of $((\mathcal{P}_{k,1}), (\mathcal{P}_{k,2}))$ with respect to $((a_k), (\tau_k))$ is clearly an automorphism of $\ell^\infty \times \ell^\infty$. Proposition 3.4 then follows from the Implicit Function Theorem. \square

3.6. Balancing. From now on, we assume that the parameters (a_k) and (τ_k) are given by Proposition 3.4. So the only remaining parameters are t and $\mathbf{v} = (v_k)$. It remains to solve (8) and (12). We define

$$\mathcal{G}_k(t, \mathbf{v}) = \text{conj}^k \int_{\partial D_k^-} g_k \omega.$$

Proposition 3.5. *For $t \neq 0$, (8) and (12) are equivalent to $\mathcal{G}_k(t, \mathbf{v}) = \mathcal{G}_0(t, \mathbf{v})$ for all $k \in \mathbb{Z}$.*

Proof. We have for $k \in \mathbb{Z}$:

$$\begin{aligned} \int_{\partial \Omega_k} g_k^{-1} \omega &= - \int_{\partial D_k^-} z_k^- \omega - \int_{\partial D_k^+} z_k^+ \omega \\ &= \int_{\partial D_{k-1}^+} \frac{t^2}{z_{k-1}^+} \omega + \int_{\partial D_{k+1}^-} \frac{t^2}{z_{k+1}^-} \omega \\ &= t^2 \int_{\partial D_{k-1}^+} g_{k-1} \omega + t^2 \int_{\partial D_{k+1}^-} g_{k+1} \omega \\ &= -t^2 \int_{\partial D_{k-1}^-} g_{k-1} \omega + t^2 \int_{\partial D_{k+1}^-} g_{k+1} \omega \quad (\text{because } g_{k-1} \omega \text{ is holomorphic in } \Omega_{k-1}) \\ &= t^2 \text{conj}^{k+1} (\mathcal{G}_{k+1} - \mathcal{G}_{k-1}). \end{aligned}$$

Hence (8) is equivalent to $\mathcal{G}_{k+1} = \mathcal{G}_{k-1}$ for $k \in \mathbb{Z}$.

We chose ∂D_1^- as a representative of γ . Equation (12) is equivalent to

$$\int_{\partial D_1^-} g^{-1} dh - \text{conj} \left(\int_{\partial D_1^-} g dh \right) = 0.$$

We have

$$\begin{aligned} \int_{\partial D_1^-} \overline{g dh} &= t^2 \int_{\partial D_1^-} \overline{g_1 \omega} = t^2 \mathcal{G}_1. \\ \int_{\partial D_1^-} g^{-1} dh &= \int_{\partial D_1^-} g_1^{-1} \omega = -t^2 \int_{\partial D_0^+} g_0 \omega = t^2 \int_{\partial D_0^-} g_0 \omega = t^2 \mathcal{G}_0. \end{aligned}$$

Hence (12) is equivalent to $\mathcal{G}_1 = \mathcal{G}_0$. \square

Proposition 3.6. *Assume that the configuration $\mathbf{q} = (q_k)$ is balanced and non-degenerate. For t in a neighborhood of 0, there exists a unique $\mathbf{v}(t)$ in ℓ^∞ , depending smoothly on t , such that $v_k(0) = (-\text{conj})^k q_k$ and*

$$(14) \quad \mathcal{G}_k(t, \mathbf{v}(t)) = -2\pi i G(q_0; \tau)$$

for all $k \in \mathbb{Z}$, so (8) and (12) are solved.

Proof. First of all, $(\mathcal{G}_k(t, \mathbf{v}))$ is a smooth function of (t, \mathbf{v}) with value in ℓ^∞ by Proposition 3.1. At $t = 0$, we have in T_k :

$$g_k \frac{\omega}{dz} = a_k \left(\frac{\omega}{dz} \right)^2 = \frac{-1}{2} (\zeta(z; \tau_k) - \zeta(z - v_k; \tau_k) - \xi(v_k; \tau_k))^2$$

$$\begin{aligned} \text{Res}_{0_k}(g_k \omega) &= \frac{-1}{2} \text{Res}_{0_k} [\zeta(z; \tau_k)^2 - 2\zeta(z; \tau_k)(\zeta(z - v_k; \tau_k) + \xi(v_k; \tau_k))] \\ &= -\zeta(v_k; \tau_k) + \xi(v_k; \tau_k) = -G(v_k; \tau_k). \end{aligned}$$

Here we used the fact that ζ is odd, hence ζ^2 is even and has no residue at 0. Then by the Residue Theorem,

$$\mathcal{G}_k(0, \mathbf{v}) = \text{conj}^k (-2\pi i G(v_k; \tau_k)) = -2\pi i (-\text{conj})^k G(v_k; \tau_k).$$

Recall that $\tau_k = (-\text{conj})^k(\tau)$ at $t = 0$. Now change to the variable $u_k = (-\text{conj})^k v_k$ with central value $\underline{u}_k = (-\text{conj})^k \underline{v}_k = q_k$. Using the definition of ζ , ξ and G , one easily checks that

$$G(-\bar{z}; -\bar{\tau}) = -\text{conj} G(z; \tau).$$

Hence

$$\mathcal{G}_k(0, \mathbf{v}) = -2\pi i G(u_k; \tau).$$

Then Proposition 3.6 follows from the balance and non-degeneracy of (q_k) and the Implicit Function Theorem. \square

Remark 3.2. The horizontal component of the flux of γ , identified with a complex number, is given by

$$-\text{i} \int_{\gamma} g \, dh = -\text{i} \int_{\partial D_1^-} t^2 g_1 \omega = -\text{i} t^2 \overline{\mathcal{G}_1}.$$

So (14) for $k = 1$ normalizes the horizontal part of the flux of γ (which can also be taken as a free parameter).

3.7. Embeddedness. We denote by $\mathbf{x}(t)$ the value of the parameters given by Proposition 3.3, 3.4 and 3.6, (Σ_t, g_t, dh_t) the corresponding Weierstrass data, $f_t : \Sigma_t \rightarrow \mathbb{R}^3/\Gamma$ the immersion given by Weierstrass Representation and $M_t = f_t(\Sigma_t)$. Recall that Γ is the 2-dimensional lattice generated by the horizontal vectors $(1, 0, 0)$ and $(\text{Re } \tau, \text{Im } \tau, 0)$. The goal of this section is to prove that M_t is embedded and has the geometry described in Section 1.2. The argument is very similar to Section 4.10 of [MT12], so we will only sketch it.

We write $f_t = (X_t, h_t)$ with

$$X_t(z) = \frac{1}{2} \text{conj} \left(\int_{z_0}^z g_t^{-1} dh_t \right) - \frac{1}{2} \int_{z_0}^z g_t \, dh_t \quad \text{and} \quad h_t(z) = \text{Re} \int_{z_0}^z dh_t.$$

We fix a base point \tilde{O}_k in $\tilde{\Omega}_k$, away from the zeros of $g_k \circ \psi_k$, and let $O_k = \psi_k(\tilde{O}_k) \in \Omega_k$. Let $w_k(t) \in \Sigma_t$ be the point $z_k^+ = t$ which is identified with the point $z_{k+1}^- = t$ (the “middle” of the k -th neck). For $r > 0$, we denote $\Omega_{k,r}$ the torus T_k minus the two disks $|z_k^\pm| \leq r$. By the computations in Section 3.5, we have in $\Omega_{k,r}$

$$(15) \quad \lim_{t \rightarrow 0} dX_t = (-\text{conj})^k dz$$

so the image of $\Omega_{k,r}$ is a graph for t small enough and

$$\lim_{t \rightarrow 0} X_t(w_k(t)) - X_t(w_{k-1}(t)) = (-\text{conj})^k \int_{0_k}^{\underline{v}_k} dz = (-\text{conj})^k(\underline{v}_k) = q_k.$$

Remark 3.3. This computation is not rigorous because the limit (15) only holds in $\Omega_{k,r}$. It can be made rigorous by expanding ω_t in Laurent series in the annuli A_k^\pm , see details in Appendix A of [MT12].

Recall that $q_k = p_k - p_{k-1}$. We may translate f_t horizontally so that $X_t(w_0(t)) = p_0$. Then

$$\lim_{t \rightarrow 0} X_t(w_k(t)) = p_k.$$

In other words, p_k is the limit position of the k -th neck. Note however that the convergence is not uniform with respect to k . By (6), we have for $z \in \Omega_{k,r}$,

$$\begin{aligned} \lim_{t \rightarrow 0} \frac{1}{t} (h_t(z) - h_t(O_k)) &= \text{Re} \lim_{t \rightarrow 0} \int_{O_k}^z \omega_t \\ &= \text{Re} \int_{O_k}^z (\zeta(z; \tau_k) - \zeta(z - \underline{v}_k; \tau_k) - \xi(\underline{v}_k; \tau_k)) dz =: \Upsilon_k(z). \end{aligned}$$

The function Υ_k is bounded in $\Omega_{k,r}$ by a uniform constant $C(r)$ depending only on r . By Lemma A.2 in [MT12],

$$\int_{O_{k-1}}^{O_k} \omega_t \simeq -2 \log t \text{Res}_{0_k}(\omega_0) = -2 \log t \quad \text{as } t \rightarrow 0.$$

Hence

$$h_t(O_k) - h_t(O_{k-1}) \sim -2t \log t.$$

This ensures that for t small enough, $f_t(\Omega_{k,r})$ lies strictly above $f_t(\Omega_{k-1,r})$ so the images $f_t(\Omega_{k,r})$ for $k \in \mathbb{Z}$ are disjoint.

Since the function Υ_k has two logarithmic singularities at 0_k and \underline{v}_k , for c large enough, the level lines $\Upsilon_k = \pm c$ are convex curves, which are included in $\Omega_{k,r}$ provided r is small enough. Define

$$h_k^\pm = h_t(O_k) \pm tc.$$

Then for t small enough, M_t intersects the planes $x_3 = h_k^+$ and $x_3 = h_k^-$ in two convex curves denoted γ_k^+ and γ_k^- , which are included in $f_t(\Omega_{k,r})$. Then $M_t \cap \{h_k^+ < x_3 < h_{k+1}^-\}$ is a minimal annulus bounded by two convex curves in parallel planes. Such an annulus is foliated by convex curves by a theorem of Shiffman [Shi56]. This proves that M_t is embedded.

4. CONVERGENCE TO TPMSS

In this section, we study the asymptotic behavior of the minimal surfaces that we just constructed. Readers who are not interested in the asymptotic behavior may skip this part and jump directly to the next section.

Assume that the configuration (q_k) is periodic. Then the corresponding minimal surface M_t is a TPMSS (as an easy consequence of uniqueness in the Implicit Function Theorem). Let (q'_k) be another balanced, non-degenerate configuration with the same horizontal lattice Γ , and assume that $q'_k = q_k$ for all $k \geq 0$. Let M'_t be the family of minimal surfaces corresponding to the configuration (q'_k) . In this section, we prove that M'_t is asymptotic to a translation of M_t as the vertical coordinate $x_3 \rightarrow +\infty$. This finally justify the term “TPMS twinning”.

We use primes for all objects associated to the configuration (q'_k) . So $\Sigma' = \Sigma[t, \mathbf{x}'(t)]$ and $f' : \Sigma' \rightarrow \mathbb{R}^3/\Gamma$ is the immersion given by the Weierstrass data $g' = g[t, \mathbf{x}'(t)]$ and $dh' = t\omega[t, \mathbf{x}'(t)]$. We will omit the dependence on t , hence will write, for instance, $\omega = \omega[t, \mathbf{x}(t)]$ and $\omega' = \omega[t, \mathbf{x}'(t)]$, and in the same way $\psi_k = \psi_k[t, \mathbf{x}(t)]$ and $\psi'_k = \psi_k[t, \mathbf{x}'(t)]$. Otherwise notations are as in Section 3.7.

We use the same letter C to denote any constant that is independent of $t > 0$ and $k \in \mathbb{Z}$.

Fix an arbitrary $\delta > 1$. We will prove in Proposition 6.5 that, for t sufficiently small, $\mathbf{x} - \mathbf{x}'$ decays like δ^{-k} . That is

$$\|x_k - x'_k\| \leq \frac{C}{\delta^k}.$$

Then Proposition 6.1 implies that, for t sufficiently small, the difference between $\psi_k^*\omega$ and $(\psi'_k)^*\omega'$ in $\tilde{\Omega}_k$ also decays like δ^{-k} ; see Equation (17) below.

It is convenient to scale the third coordinate of f and f' by t^{-1} . So let $S : \mathbb{R}^3 \rightarrow \mathbb{R}^3$ be the linear map defined by $S(x_1, x_2, x_3) = (x_1, x_2, t^{-1}x_3)$ and define $\hat{f} = S \circ f$ and $\hat{f}' = S \circ f'$.

Proposition 4.1. *For $k \in \mathbb{N}$,*

$$\|d(\hat{f} \circ \psi_k) - d(\hat{f}' \circ \psi'_k)\|_{C^0(\tilde{\Omega}_k)} \leq \frac{C}{\delta^k}$$

Proof. We have in Ω_k

$$(16) \quad d\hat{f} = \begin{cases} (\frac{1}{2}(t^2\bar{g}_k\omega - g_k^{-1}\omega), \operatorname{Re}\omega) & \text{if } k \text{ is even} \\ (\frac{1}{2}(g_k^{-1}\omega - t^2g_k\omega), \operatorname{Re}\omega) & \text{if } k \text{ is odd} \end{cases}$$

and similar formulas for $d\hat{f}'$. By Propositions 6.1 and 6.5, we have

$$(17) \quad \|\psi_k^*\omega - (\psi'_k)^*\omega'\|_{C^0(\tilde{\Omega}_k)} \leq \frac{C}{\delta^k}.$$

Using Proposition 6.5 and the definition of g_k , we obtain

$$(18) \quad \|\psi_k^*(g_k\omega) - (\psi'_k)^*(g'_k\omega')\|_{C^0(\tilde{\Omega}_k)} \leq \frac{C}{\delta^k}.$$

Let $\tilde{D}_{k,1}$ and $\tilde{D}_{k,2}$ be two disks containing the two zeros of $g_k \circ \psi_k$, so that $g_k^{-1} \circ \psi_k$ is uniformly bounded outside these disks. Then

$$(19) \quad \|\psi_k^*(g_k^{-1}\omega) - (\psi'_k)^*((g'_k)^{-1}\omega')\|_{C^0(\tilde{\Omega}_k \setminus \tilde{D}_{k,1} \cup \tilde{D}_{k,2})} \leq \frac{C}{\delta^k}.$$

Since the Regularity Problem is solved, $(g'_k)^{-1}\omega'$ extends holomorphically to the zeros of g'_k . Since $\psi_k(x + iy) - \psi'_k(x + iy) = (\tau_k - \tau'_k)y$, we have

$$(20) \quad \|\psi_k^*((g'_k)^{-1}\omega') - (\psi'_k)^*((g'_k)^{-1}\omega')\|_{C^0(\tilde{\Omega}_k)} \leq \frac{C}{\delta^k}.$$

From (19) and (20), we obtain by the Triangular Inequality

$$\|\psi_k^*[g_k^{-1}\omega - (g'_k)^{-1}\omega']\|_{C^0(\partial\tilde{D}_{k,i})} \leq \frac{C}{\delta^k}.$$

Since $g_k^{-1}\omega - (g'_k)^{-1}\omega'$ is holomorphic, we obtain by the Maximum Principle (for the holomorphic structure on \mathbb{T} induced by ψ_k)

$$\|\psi_k^*[g_k^{-1}\omega - (g'_k)^{-1}\omega']\|_{C^0(\tilde{D}_{k,i})} \leq \frac{C}{\delta^k}.$$

Using (20),

$$(21) \quad \|\psi_k^*(g_k^{-1}\omega) - (\psi'_k)^*((g'_k)^{-1}\omega')\|_{C^0(\tilde{D}_{k,i})} \leq \frac{C}{\delta^k}.$$

Proposition 4.1 follows from (17), (18), (19) and (21). \square

Recall that $O_k = \psi_k(\tilde{O}_k)$ and $O'_k = \psi'_k(\tilde{O}_k)$.

Proposition 4.2. *For $k \in \mathbb{N}$,*

$$\|\hat{f}(O_{k+1}) - \hat{f}(O_k) - \hat{f}'(O'_{k+1}) + \hat{f}'(O'_k)\| \leq \frac{C}{\delta^k}.$$

Hence the sequence $(\hat{f}(O_k) - \hat{f}'(O'_k))_{k \in \mathbb{N}}$ is Cauchy. By translation, we may assume that its limit is zero, so

$$\|\hat{f}(O_k) - \hat{f}'(O'_k)\| \leq \frac{C'}{\delta^k} \quad \text{with } C' = \frac{C\delta}{\delta - 1}.$$

Proof. Recall from Section 3.7 that $w_k \in \Sigma$ denotes the point $z_k^+ = t$, identified with $z_{k+1}^- = t$. Similarly, we introduce $w'_k \in \Sigma'$ to denote the point $z_k'^+ = t$, identified with $z_{k+1}^{'-} = t$. Moreover, let $m_k^\pm \in \Sigma$ denotes the point $z_k^\pm = \varepsilon$, and $m_k'^\pm \in \Sigma'$ denotes the point $z_k'^\pm = \varepsilon$.

Proposition 4.2 follows from the following three estimates: For $k \in \mathbb{N}$:

$$(22) \quad \|\hat{f}(O_k) - \hat{f}(m_k^\pm) - \hat{f}'(O'_k) + \hat{f}'(m_k'^\pm)\| \leq \frac{C}{\delta^k},$$

$$(23) \quad \|\hat{f}(m_k^+) - \hat{f}(w_k) - \hat{f}'(m_k'^+) + \hat{f}'(w'_k)\| \leq \frac{C}{\delta^k},$$

$$(24) \quad \|\hat{f}(m_{k+1}^-) - \hat{f}(w_k) - \hat{f}'(m_{k+1}^-) + \hat{f}'(w'_k)\| \leq \frac{C}{\delta^k}.$$

Inequality (22) follows from Proposition 4.1,

$$\psi_k^{-1}(O_k) = (\psi'_k)^{-1}(O'_k) = \tilde{O}_k \quad \text{and} \quad |\psi_k^{-1}(m_k^\pm) - (\psi'_k)^{-1}(m_k'^\pm)| \leq \frac{C}{\delta_k}.$$

To prove (23), we follow the proof of Lemma A.1 in [MT12]. We write the Laurent series of ω in the annulus A_k^+ in term of the complex coordinate $z = z_k^+$ as

$$\omega = \frac{-dz}{z} + \sum_{n \geq 1} c_{k,n}^+ z^{n-1} dz + \sum_{n \geq 1} t^{2n} c_{k,n}^- \frac{dz}{z^{n+1}}$$

where

$$\begin{aligned} c_{k,n}^+ &= \frac{1}{2\pi i} \int_{|z|=\varepsilon} \frac{\omega}{z^n} = \frac{1}{2\pi i} \int_{\partial D_k^+} \frac{\omega}{(z_k^+)^n} \\ c_{k,n}^- &= \frac{t^{-2n}}{2\pi i} \int_{|z|=\varepsilon} z^n \omega = \frac{1}{2\pi i} \int_{\partial D_k^+} (t^{-2} z_k^+)^n \omega = \frac{-1}{2\pi i} \int_{\partial D_{k+1}^-} \frac{\omega}{(z_{k+1}^-)^n}. \end{aligned}$$

We expand ω' in the annulus $A_k'^+$ in the same way, with coefficients $c'_{k,n}^\pm$ given by similar formulas. Using estimates (17) and (18), we obtain the following estimate

$$|c_{k,n}^\pm - c'_{k,n}^\pm| \leq \frac{Cn}{\delta^k (2\varepsilon)^n}.$$

By integration, we obtain the following estimates (see details in Appendix A of [MT12]):

$$\begin{aligned} \left| \int_{z=\varepsilon}^t \omega - \omega' \right| &\leq \frac{C}{\delta^k} \\ \left| \int_{z=\varepsilon}^t z(\omega - \omega') \right| &\leq \frac{C}{\delta^k} \\ \left| \int_{z=\varepsilon}^t t^2 z^{-1}(\omega - \omega') \right| &\leq \frac{C}{\delta^k} \end{aligned}$$

Then (23) follows from (16). (24) is proved in the same way, using $z = z_{k+1}^-$ as a local coordinate. \square

Assume that the configuration (q_k) is periodic with even period N , i.e. $q_{k+N} = q_k$. By uniqueness in the Implicit Function Theorem, the resulting immersion f is periodic. More precisely, if we define $\sigma : \Sigma \rightarrow \Sigma$ by $z \in T_k \mapsto z \in T_{k+N}$ then $f \circ \sigma = f + \mathcal{T}$ (where the period $\mathcal{T} \in \mathbb{R}^3$ depends on t).

Proposition 4.3. *Let $M = f(\Sigma)$ and $M' = f'(\Sigma')$. Define $M'_\ell = M' - \ell\mathcal{T}$ for $\ell \in \mathbb{N}$. Then*

$$\lim_{\ell \rightarrow \infty} M'_\ell = M.$$

Here the limit is for the smooth convergence on compact subsets of \mathbb{R}^3/Γ .

Proof. By periodicity we have

$$\tilde{\Omega}_{k+N} = \tilde{\Omega}_k \quad \text{and} \quad f \circ \psi_{k+N} = f \circ \psi_k + \mathcal{T} \quad \text{in } \tilde{\Omega}_k.$$

By Propositions 4.1 and 4.2, we have for $\ell \in \mathbb{N}$

$$\|f \circ \psi_{k+\ell N} - f' \circ \psi'_{k+\ell N}\|_{C^0(\tilde{\Omega}_k)} \leq \frac{C}{\delta^{k+\ell N}}.$$

Define $f'_\ell = f - \ell\mathcal{T}$. Then

$$\|f \circ \psi_k - f'_\ell \circ \psi'_{k+\ell N}\|_{C^0(\tilde{\Omega}_k)} \leq \frac{C}{\delta^{k+\ell N}}.$$

Hence

$$(25) \quad \lim_{\ell \rightarrow \infty} f'_\ell \circ \psi'_{k+\ell N}(\tilde{\Omega}_k) = f \circ \psi_k(\tilde{\Omega}_k).$$

Recall from Section 3.7 that we have defined heights h_k^\pm such that $M \cap \{h_k^- < x_3 < h_k^+\}$ is included in $f \circ \psi_k(\tilde{\Omega}_k)$ and is bounded by two convex curves denoted γ_k^+ and γ_k^- . Then for ℓ large enough, $M'_\ell \cap \{h_k^- < x_3 < h_k^+\}$ is included in $f'_\ell \circ \psi'_{k+\ell N}(\tilde{\Omega}_k)$ and is bounded by two convex curves denoted $\gamma'_{k,\ell}^+$ and $\gamma'_{k,\ell}^-$. By (25) we have

$$\lim_{\ell \rightarrow \infty} M'_\ell \cap \{h_k^- < x_3 < h_k^+\} = M \cap \{h_k^- < x_3 < h_k^+\}.$$

Let $A'_{k,\ell} = M'_\ell \cap \{h_k^+ < x_3 < h_{k+1}^-\}$. Then $A'_{k,\ell}$ is an unstable minimal annulus bounded by $\gamma'_{k,\ell}^+$ and $\gamma'_{k+1,\ell}^-$. By Theorem 2(a) in [Tra10], $A'_{k,\ell}$ converges subsequentially as $\ell \rightarrow \infty$ to an unstable annulus bounded by γ_k^+ and γ_{k+1}^- . By [MW91], this annulus is unique so the whole sequence converges and

$$\lim_{\ell \rightarrow \infty} A'_{k,\ell} = M \cap \{h_k^+ < x_3 < h_{k+1}^-\}.$$

Hence for any integers $k_1 < k_2$, we have

$$\lim_{\ell \rightarrow \infty} M'_\ell \cap \{h_{k_1}^+ < x_3 < h_{k_2}^+\} = M \cap \{h_{k_1}^+ < x_3 < h_{k_2}^+\}$$

which proves Proposition 4.3 since $\lim_{k \rightarrow \pm\infty} h_k^+ = \pm\infty$. \square

5. THE HOLOMORPHIC 1-FORMS ω

The goal of this section is to prove:

Proposition 5.1.

- (a) For (t, \mathbf{x}) in a neighborhood of $(0, \underline{\mathbf{x}})$, there exists a holomorphic (regular if $t = 0$) 1-form $\omega[t, \mathbf{x}]$ on $\Sigma[t, \mathbf{x}]$ with imaginary periods on α_k and β_k for all $k \in \mathbb{Z}$ and $\int_\gamma \omega = 2\pi i$.
- (b) At $t = 0$, we have for all $k \in \mathbb{Z}$:

$$\omega[0, \mathbf{x}] = (\zeta(z; \tau_k) - \zeta(z - v_k; \tau_k) - \xi(v_k; \tau_k)) dz \quad \text{in } T_k.$$

- (c) The pullback $\psi^* \omega$ is in $C^0(\tilde{\Omega})$ and depends smoothly on (t, \mathbf{x}) in a neighborhood of $(0, \underline{\mathbf{x}})$.

Remark 5.1. If the configuration is periodic with period $2N$ (namely, $q_{k+2N} = q_k$), the quotient of Σ by its period is a compact Riemann surface, obtained by opening $2N$ nodes between $2N$ tori. In this case, the existence of ω follows from the standard theory of Opening Nodes [Fay73]. To prove the existence of ω in the non-periodic case, we adapt the argument in [Tra13] which allows for infinitely many nodes. The difference is that Riemann spheres are replaced by tori.

In the following, we use the same letter C to designate all uniform constants.

5.1. Preliminaries.

Definition 5.2.

- (a) For $p, q \in T_k$, $p \neq q$, we denote by $\omega_{k,p,q}$ the unique meromorphic 1-form on T_k with simple poles at p, q with residues 1 and -1 , and imaginary periods on α_k and β_k . So $\omega_{k,p,q}$ is an abelian differential of the third kind with real normalisation.
- (b) For $n \geq 2$, we denote $\omega_{k,n}^+$ (resp. $\omega_{k,n}^-$) the unique meromorphic 1-form on T_k with a pole of multiplicity n at v_k (resp. 0_k) with principal part

$$\frac{dz_k^\pm}{(z_k^\pm)^n}$$

and imaginary periods on α_k and β_k . So $\omega_{k,n}^\pm$ are abelian differentials of the second kind with real normalisation. Recall that it depends on the choice of the local coordinate z_k^\pm used to define the principal part.

Lemma 5.3. *The abelian differential $\omega_{k,p,q}$ is explicitly given by*

$$(26) \quad \omega_{k,p,q} = (\zeta(z - p; \tau_k) - \zeta(z - q; \tau_k) - \xi(q - p; \tau_k)) dz.$$

Proof. Let $\omega'_{k,p,q}$ be the right-hand side of (26). Then $\omega'_{k,p,q}$ has simple poles at p, q with residues 1 and -1 . Using the quasi-periodicity of ζ , $\omega'_{k,p,q}$ is independent of the choice of the representatives of p and q modulo $\mathbb{Z} + \tau_k \mathbb{Z}$. We take these representatives in the fundamental parallelogram spanned by 1 and τ_k . We may represent α_k and β_k by curves which do not

intersect the segment $[p, q]$. Using the quasi-periodicity of ζ (and omitting the argument τ_k everywhere)

$$\frac{\partial}{\partial q} \int_{\alpha_k} (\zeta(z - p) - \zeta(z - q)) dz = \int_{\alpha_k} \frac{d\zeta}{dz} (z - q) dz = [\zeta(z - q)]_{\alpha_k(0)}^{\alpha_k(1)} = \eta_1.$$

Hence

$$\int_{\alpha_k} (\zeta(z - p) - \zeta(z - q)) dz = (q - p)\eta_1.$$

Write $q - p = x + y\tau_k$ and recall the definition of ξ and Legendre Relation $\eta_1\tau_k - \eta_2 = 2\pi i$, where we assumed that $\text{Im } \tau > 0$. Then

$$\int_{\alpha_k} \omega'_{k,p,q} = (x + y\tau_k)\eta_1 - (x\eta_1 + y\eta_2) = y(\eta_1\tau_k - \eta_2) = 2\pi iy.$$

In the same way,

$$\int_{\beta_k} \omega'_{k,p,q} = (x + y\tau_k)\eta_2 - (x\eta_1 + y\eta_2)\tau_k = x(\eta_2 - \eta_1\tau_k) = -2\pi ix.$$

Hence $\omega'_{k,p,q}$ has imaginary periods so is equal to $\omega_{k,p,q}$ by uniqueness. \square

Lemma 5.4. *There exists a uniform constant C such that for (t, \mathbf{x}) in a neighborhood of $(0, \underline{\mathbf{x}})$ and $k \in \mathbb{Z}$:*

$$\|\omega_{k,n}^\pm\|_{C^0(\Omega_k)} \leq C \left(\frac{2}{\varepsilon}\right)^{n-1}.$$

Proof. We only prove the + case. The - case follows similarly.

Let $\eta_{k,n}^+$ be the unique meromorphic 1-form on T_k with a pole at v_k with the same principal part as $\omega_{k,n}^+$ and normalized by $\int_{\alpha_k} \eta_{k,n}^+ = 0$. These two differentials are related by

$$(27) \quad \omega_{k,n}^+ = \eta_{k,n}^+ + \frac{i}{\text{Im}(\tau_k)} \left(\text{Re} \int_{\beta_k} \eta_{k,n}^+ \right) dz.$$

Indeed, the right-hand side has imaginary periods.

Write $\eta_{k,n}^+ = f_{k,n}^+ dz$. For p, q in $T_k \setminus D_k^+$, we have by the Residue Theorem in $T_k \setminus D_k^+$:

$$\int_{\partial D_k^+} f_{k,n}^+ \omega_{k,p,q} = -2\pi i (f_{k,n}^+(p) - f_{k,n}^+(q)).$$

On the other hand, since $\omega_{k,p,q}$ is holomorphic in D_k^+ and by definition of the principal part of $f_{k,n}^+$ at v_k :

$$\int_{\partial D_k^+} f_{k,n}^+ \omega_{k,p,q} = \int_{\partial D_k^+} \frac{dz_k^+}{dz} (z_k^+)^{-n} \omega_{k,p,q}.$$

Hence

$$f_{k,n}^+(p) - f_{k,n}^+(q) = -\chi_{k,n}^+(p, q) \quad \text{with} \quad \chi_{k,n}^+(p, q) = \frac{1}{2\pi i} \int_{\partial D_k^+} \frac{dz_k^+}{dz} (z_k^+)^{-n} \omega_{k,p,q}.$$

Integrating with respect to q on α_k , we obtain the following integral representation of $f_{k,n}^+(p)$ for $p \in T_k \setminus D_k^+$:

$$(28) \quad f_{k,n}^+(p) = \int_{\alpha_k} (f_{k,n}^+(p) - f_{k,n}^+(q)) dq = - \int_{\alpha_k} \chi_{k,n}^+(p, q) dq.$$

By Cauchy Theorem, we may replace the circle ∂D_k^+ by the circle $|z_k^+| = \frac{\varepsilon}{2}$ in the definition of $\chi_{k,n}^+$. Using Lemma 5.3, there exists a uniform constant C (independent of $k \in \mathbb{Z}$ and \mathbf{x} in a neighborhood of $\underline{\mathbf{x}}$) such that for all $p, q \in \Omega_k$ and z on the circle $|z_k^+| = \frac{\varepsilon}{2}$:

$$|\omega_{k,p,q}(z)| \leq C.$$

Then for $p, q \in \Omega_k$:

$$|\chi_{k,n}^+(p, q)| \leq \frac{C}{2\pi} \int_{|z_k^+|=\varepsilon/2} \frac{|dz_k^+|}{|z_k^+|^n} = \frac{C}{2\pi} \left(\frac{2}{\varepsilon}\right)^n 2\pi \frac{\varepsilon}{2} = C \left(\frac{2}{\varepsilon}\right)^{n-1}.$$

By (28),

$$(29) \quad \|\eta_{k,n}^+\|_{C^0(\Omega_k)} \leq C \left(\frac{2}{\varepsilon}\right)^{n-1}.$$

Lemma 5.4 then follows from (27). \square

5.2. Existence. Let Λ denotes the set $\mathbb{Z} \times \{n \in \mathbb{N} : n \geq 2\} \times \{+, -\}$. We look for ω in the form $\omega[t, \mathbf{x}] = \tilde{\omega}(\mathbf{x}, \boldsymbol{\lambda}(t, \mathbf{x}))$ where

$$(30) \quad \tilde{\omega}(\mathbf{x}, \boldsymbol{\lambda}) = \omega_{k,0_k,v_k} + \sum_{n=2}^{\infty} \rho^{n-1} (\lambda_{k,n}^+ \omega_{k,n}^+ + \lambda_{k,n}^- \omega_{k,n}^-) \quad \text{in } T_k,$$

where $\rho \leq \frac{\varepsilon}{4}$ is a fixed positive number, and $\boldsymbol{\lambda} = (\lambda_{k,n}^s)_{(k,n,s) \in \Lambda} \in \ell^\infty$ is a sequence of complex numbers to be determined as a function of (t, \mathbf{x}) . Observe that, formally, $\tilde{\omega}(\mathbf{x}, \boldsymbol{\lambda})$ has the desired periods. Regarding convergence, by Lemma 5.4, we have in Ω_k :

$$(31) \quad \sum_{n=2}^{\infty} \rho^{n-1} |(\lambda_{k,n}^+ \omega_{k,n}^+ + \lambda_{k,n}^- \omega_{k,n}^-)| \leq 2C \|\boldsymbol{\lambda}\|_\infty \sum_{n=2}^{\infty} \left(\frac{2\rho}{\varepsilon}\right)^{n-1} \leq 2C \|\boldsymbol{\lambda}\|_\infty.$$

so the series (30) converges absolutely in Ω_k and by Lemma 5.3,

$$(32) \quad \|\tilde{\omega}(\mathbf{x}, \boldsymbol{\lambda})\|_{C^0(\Omega_k)} \leq C(1 + \|\boldsymbol{\lambda}\|_\infty).$$

We assume for now the convergence outside Ω_k .

Lemma 5.5. *Assume that the series (30) converges in the annulus A_k^\pm for all $k \in \mathbb{Z}$. For $t \neq 0$, $\tilde{\omega}(\mathbf{x}, \boldsymbol{\lambda})$ is a well-defined 1-form on $\Sigma[t, \mathbf{x}]$ if and only if for all $k \in \mathbb{Z}$ and $n \geq 2$,*

$$\begin{aligned} \lambda_{k,n}^+ &= \frac{-1}{2\pi i} \int_{\partial D_{k+1}^-} \left(\frac{t^2}{\rho z_{k+1}^-} \right)^{n-1} \tilde{\omega}(\mathbf{x}, \boldsymbol{\lambda}) \quad \text{and} \\ \lambda_{k,n}^- &= \frac{-1}{2\pi i} \int_{\partial D_{k-1}^+} \left(\frac{t^2}{\rho z_{k-1}^+} \right)^{n-1} \tilde{\omega}(\mathbf{x}, \boldsymbol{\lambda}). \end{aligned}$$

Proof. Fix $t \neq 0$ and define a diffeomorphism

$$\varphi_k = (z_{k+1}^-)^{-1} \circ \frac{t^2}{z_k^+} : A_k^+ \rightarrow A_{k+1}^-$$

so $z \in A_k^+$ is identified with $\varphi_k(z) \in A_{k+1}^-$ when opening nodes. Then $\tilde{\omega}$ is well-defined on Σ if and only if $\varphi_k^* \tilde{\omega} = \tilde{\omega}$ in the annulus A_k^+ for all $k \in \mathbb{Z}$. Using the theorem on Laurent series,

this is equivalent to

$$(33) \quad \int_{\partial D_k^+} (z_k^+)^n (\varphi_k^* \tilde{\omega} - \tilde{\omega}) = 0 \quad \text{for all } k \in \mathbb{Z} \text{ and } n \in \mathbb{Z}.$$

We have

$$\begin{aligned} \int_{\partial D_k^+} (z_k^+)^n \varphi_k^* \tilde{\omega} &= \int_{\partial D_k^+} \varphi_k^* \left[\left(\frac{t^2}{z_{k+1}^-} \right)^n \tilde{\omega} \right] && \text{by definition of } \varphi_k \\ &= \int_{\varphi_k(\partial D_k^+)} \left(\frac{t^2}{z_{k+1}^-} \right)^n \tilde{\omega} && \text{by a change of variable} \\ &= - \int_{\partial D_{k+1}^-} \left(\frac{t^2}{z_{k+1}^-} \right)^n \tilde{\omega} && \text{because } \tilde{\omega} \text{ is holomorphic in } A_{k+1}^-. \end{aligned}$$

For $n = 0$, (33) is always satisfied, because

$$- \int_{\partial D_{k+1}^-} \tilde{\omega} - \int_{\partial D_k^+} \tilde{\omega} = -2\pi i \operatorname{Res}_{0_{k+1}}(\omega_{k+1,0_{k+1},v_{k+1}}) - 2\pi i \operatorname{Res}_{v_k}(\omega_{k,0_k,v_k}) = 0.$$

For $n \geq 1$, we have by the Residue Theorem and definition of $\tilde{\omega}(\mathbf{x}, \boldsymbol{\lambda})$

$$\int_{\partial D_k^+} (z_k^+)^n \tilde{\omega} = 2\pi i \rho^n \lambda_{k,n+1}^+,$$

so (33) is equivalent to

$$2\pi i \rho^n \lambda_{k,n+1}^+ = - \int_{\partial D_{k+1}^-} \left(\frac{t^2}{z_{k+1}^-} \right)^n \tilde{\omega}.$$

For $n \leq -1$, we have by the Residue Theorem

$$\int_{\partial D_{k+1}^-} \left(\frac{t^2}{z_{k+1}^-} \right)^n \tilde{\omega} = 2\pi i t^{2n} \rho^{-n} \lambda_{k+1,-n+1}^-$$

so (33) is equivalent to

$$2\pi i t^{2n} \rho^{-n} \lambda_{k+1,-n+1}^- = - \int_{\partial D_k^+} (z_k^+)^n \tilde{\omega}$$

which, after replacing n by $-n$ and k by $k-1$, becomes

$$2\pi i \rho^n \lambda_{k,n+1}^- = - \int_{\partial D_{k-1}^+} \left(\frac{t^2}{z_{k-1}^+} \right)^n \tilde{\omega}$$

for all $n \geq 1$. Collecting all results gives Lemma 5.5. \square

In view of Lemma 5.5, we define

$$L_{k,n}^\pm(t, \mathbf{x}, \boldsymbol{\lambda}) = \frac{-1}{2\pi i} \int_{\partial D_{k\pm 1}^\mp} \left(\frac{t^2}{\rho z_{k\pm 1}^\mp} \right)^{n-1} \tilde{\omega}(\mathbf{x}, \boldsymbol{\lambda})$$

and $\mathbf{L} = (L_{k,n}^s)_{(k,n,s) \in \Lambda}$, so $\tilde{\omega}(\mathbf{x}, \boldsymbol{\lambda})$ is well-defined on $\Sigma[t, \mathbf{x}]$ if and only if $\boldsymbol{\lambda} = \mathbf{L}(t, \mathbf{x}, \boldsymbol{\lambda})$. Observe that $\mathbf{L}(t, \mathbf{x}, \boldsymbol{\lambda})$ is defined for all $\boldsymbol{\lambda} \in \ell^\infty$. In particular, we do not need the convergence in A_k^\pm to define \mathbf{L} . Also, $\tilde{\omega}$ and \mathbf{L} are affine with respect to $\boldsymbol{\lambda}$.

Lemma 5.6. *For (t, \mathbf{x}) in a neighborhood of $(0, \underline{\mathbf{x}})$, $\lambda \mapsto \mathbf{L}(t, \mathbf{x}, \lambda)$ is contracting from ℓ^∞ to itself, hence has a fixed point $\lambda(t, \mathbf{x})$ by the Fixed Point Theorem.*

Proof. We can bound the length of ∂D_k^\pm by a uniform constant ℓ . By Estimate (31):

$$|L_{k,n}^\pm(t, \mathbf{x}, \lambda) - L_{k,n}^\pm(t, \mathbf{x}, \mathbf{0})| \leq \frac{\ell}{2\pi} \left(\frac{t^2}{\rho\varepsilon} \right)^{n-1} 2C\|\lambda\|_\infty.$$

Hence if $t^2 \leq \rho\varepsilon$,

$$\|\mathbf{L}(t, \mathbf{x}, \lambda) - \mathbf{L}(t, \mathbf{x}, \mathbf{0})\|_\infty \leq \frac{C\ell t^2}{\pi\rho\varepsilon} \|\lambda\|_\infty.$$

so \mathbf{L} is contracting for t sufficiently small. \square

Now we verify the convergence of (30) outside Ω_k .

Lemma 5.7. *If $\lambda = \mathbf{L}(t, \mathbf{x}, \lambda)$ and $t \neq 0$ is sufficiently small, the series (30) converges absolutely in the annulus A_k^\pm for all $k \in \mathbb{Z}$.*

Proof. We only deal with the convergence of $\sum_{n \geq 2} \rho^{n-1} \lambda_{k,n}^+ \omega_{k,n}^+$. Its convergence in A_k^- is straightforward because $\omega_{k,n}^+$ is holomorphic in D_k^- and we already know the convergence on ∂D_k^- . It remains to prove the convergence in A_k^+ .

By Cauchy Theorem, we can replace the circle ∂D_{k+1}^- by the circle $|z_{k+1}^-| = 2\varepsilon$ in the definition of $L_{k,n}^+(t, \mathbf{x}, \lambda)$. Using Estimate (32), this gives

$$(34) \quad |\lambda_{k,n}^+| = |L_{k,n}^+(t, \mathbf{x}, \lambda)| \leq C(1 + \|\lambda\|_\infty) \left(\frac{t^2}{2\rho\varepsilon} \right)^{n-1}.$$

By definition, the function

$$\frac{\omega_{k,n}^+}{dz} - \frac{(z_k^+)'}{(z_k^+)^n}$$

extends holomorphically to the disk D_k^+ . By the maximum principle and Lemma 5.4

$$\sup_{D_k^+} \left| \frac{\omega_{k,n}^+}{dz} - \frac{(z_k^+)'}{(z_k^+)^n} \right| = \max_{\partial D_k^+} \left| \frac{\omega_{k,n}^+}{dz} - \frac{(z_k^+)'}{(z_k^+)^n} \right| \leq C \left(\frac{2}{\varepsilon} \right)^{n-1} + \frac{C}{\varepsilon^n} \leq C \left(\frac{2}{\varepsilon} \right)^n.$$

Hence recalling the definition of A_k^+ , and provided $2t^2 \leq \varepsilon^2$:

$$\sup_{A_k^+} |\omega_{k,n}^+| \leq C \left(\frac{2}{\varepsilon} \right)^n + C \left(\frac{\varepsilon}{t^2} \right)^n \leq C \left(\frac{\varepsilon}{t^2} \right)^n.$$

Using Estimate (34), we obtain

$$\sup_{A_k^+} \rho^{n-1} |\lambda_{k,n}^+ \omega_{k,n}^+| \leq \frac{C\varepsilon}{t^2 2^n} (1 + \|\lambda\|_\infty).$$

Hence the series $\sum_{n \geq 2} \rho^{n-1} \lambda_{k,n}^+ \omega_{k,n}^+$ converges absolutely in A_k^+ .

Convergence of $\sum_{n \geq 2} \rho^{n-1} \lambda_{k,n}^- \omega_{k,n}^-$ follows similarly. \square

We define $\omega[t, \mathbf{x}] = \tilde{\omega}(t, \boldsymbol{\lambda}(t, \mathbf{x}))$. By Lemmas 5.5 and 5.7, $\omega[t, \mathbf{x}]$ is a well-defined holomorphic 1-form on $\Sigma[t, \mathbf{x}]$ and has the desired periods by definition. This proves Proposition 5.1(a). At $t = 0$, $\mathbf{L} = \mathbf{0}$ so $\boldsymbol{\lambda} = \mathbf{0}$ and $\omega = \omega_{k,0_k,v_k}$ in T_k . Proposition 5.1(b) follows from Lemma 5.3.

5.3. Smooth dependence on parameters. We denote $\tilde{\gamma}_k^-$ the circle $|z| = 2\varepsilon'$ in $\mathbb{T} = \mathbb{C}/(\mathbb{Z} + i\mathbb{Z})$ and $\tilde{\gamma}_k^+$ the circle $|z - \tilde{v}_k| = 2\varepsilon'$. These two circles are fixed and included in the domain $\tilde{\Omega}_k$. Define for $\eta \in C^0(\tilde{\Omega})$

$$\tilde{L}_{k,n}^\pm(t, \mathbf{x}, \eta) = \frac{-1}{2\pi i} \int_{\tilde{\gamma}_{k\pm 1}^\mp} \left(\frac{t^2}{\rho z_{k\pm 1}^\mp \circ \psi_{k\pm 1}} \right)^{n-1} \eta$$

and let $\tilde{\mathbf{L}} = (\tilde{L}_{k,n}^s)_{(k,n,s) \in \Lambda}$. Using a change of variable

$$\tilde{L}_{k,n}^\pm(t, \mathbf{x}, (\psi^*\tilde{\omega})(\mathbf{x}, \boldsymbol{\lambda})) = \frac{-1}{2\pi i} \int_{\psi_{k\pm 1}(\tilde{\gamma}_{k\pm 1}^\mp)} \left(\frac{t^2}{\rho z_{k\pm 1}^\mp} \right)^{n-1} \tilde{\omega}(\mathbf{x}, \boldsymbol{\lambda}) = L_{k,n}^\pm(t, \mathbf{x}, \boldsymbol{\lambda}).$$

Hence

$$(35) \quad \mathbf{L}(t, \mathbf{x}, \boldsymbol{\lambda}) = \tilde{\mathbf{L}}(t, \mathbf{x}, (\psi^*\tilde{\omega})(\mathbf{x}, \boldsymbol{\lambda})).$$

By Lemma 5.8 below and composition, \mathbf{L} is smooth so its fixed point $\boldsymbol{\lambda}(t, \mathbf{x})$ depends smoothly on (t, \mathbf{x}) . By the first point of Lemma 5.8, $(\psi^*\omega)[t, \mathbf{x}] = (\psi^*\tilde{\omega})(\mathbf{x}, \boldsymbol{\lambda}(t, \mathbf{x}))$ depends smoothly on (t, \mathbf{x}) . This proves Proposition 5.1(c).

Lemma 5.8.

- (a) $\psi^*\tilde{\omega}$ is a smooth function of \mathbf{x} in an ℓ^∞ -neighborhood of $\underline{\mathbf{x}}$ and $\boldsymbol{\lambda} \in \ell^\infty$, with value in $C^0(\tilde{\Omega})$.
- (b) $\tilde{\mathbf{L}}$ is a smooth function of t in a neighborhood of 0, \mathbf{x} in an ℓ^∞ -neighborhood of $\underline{\mathbf{x}}$ and $\eta \in C^0(\tilde{\Omega})$, with value in ℓ^∞ .

For any infinite set K , if $(V_k)_{k \in K}$ is a sequence of normed spaces, we denote

$$\left(\bigoplus_{k \in K} V_k \right)_\infty = \{x \in \prod_{k \in K} V_k : \|x\|_\infty = \sup_{k \in K} \|x_k\| < \infty\}.$$

To prove Lemma 5.8, we use the following elementary fact.

Proposition 5.9. For $k \in K$, let $f_k : B(0, r) \subset U_k \rightarrow V_k$ be a smooth function between normed spaces. Assume that there exists uniform constants $C(m)$ such that

$$\forall m \in \mathbb{N}, \quad \forall k \in K, \quad \forall x_k \in B(0, r), \quad \|d^m f_k(x_k)\| \leq C(m)$$

where $d^m f_k$ denotes the m -th order differential of f_k . Let $U^\infty = (\bigoplus_{k \in K} U_k)_\infty$ and $V^\infty = (\bigoplus_{k \in K} V_k)_\infty$. Define $\mathbf{f} : B(0, r) \subset U^\infty \rightarrow V^\infty$ by $\mathbf{f}(\mathbf{x}) = (f_k(x_k))_{k \in K}$. Then \mathbf{f} is smooth and $d\mathbf{f}(\mathbf{x})\mathbf{h} = (df_k(x_k)h_k)_{k \in K}$.

We summarize the hypothesis of Proposition 5.9 by saying that the functions f_k have uniformly bounded derivatives.

Proof. It is straightforward to prove that f is differentiable (with the indicated differential) using Taylor Formula with integral remainder. Smoothness follows by induction. \square

Recall that $\Omega_{k,r}$ denotes the torus T_k minus the disks $|z_k^\pm| \leq r$. We fix a uniform positive $\varepsilon'' < \varepsilon$ so that for all \underline{x} in a neighborhood of \underline{x} and $k \in \mathbb{Z}$, $\psi_k(\tilde{\Omega}_k) \subset \Omega_{k,\varepsilon''}$. We choose ρ such that $\rho \leq \varepsilon''/4$.

Claim 5.10.

- (a) For $k \in \mathbb{Z}$, $\psi_k^* \omega_{k,0_k, v_k}$ is a smooth function of (τ_k, v_k) in a neighborhood of $(\underline{\tau}_k, \underline{v}_k)$, with value in $C^0(\tilde{\Omega}_k)$ and has uniformly bounded derivatives.
- (b) For $k \in \mathbb{Z}$ and $n \geq 2$, $(\frac{\varepsilon''}{2})^{n-1} \psi_k^* \omega_{k,n}^\pm$ is a smooth function of $x_k = (a_k, b_k, v_k, \tau_k)$ in a neighborhood of \underline{x}_k , with value in $C^0(\tilde{\Omega}_k)$, and has uniformly (with respect to k and n) bounded derivatives.
- (c) If $t^2 < \rho \varepsilon''$, then for $k \in \mathbb{Z}$ and $n \geq 2$, $\left(\frac{t^2}{\rho z_k^\pm \circ \psi_k} \right)^{n-1}$ restricted to $\tilde{\gamma}_k^\pm$ is a smooth function of t in a neighborhood of 0 and x_k in a neighborhood of \underline{x}_k , with value in $C^0(\tilde{\gamma}_k^\pm)$, and has uniformly bounded derivatives.

Proof.

- (a) follows from the explicit formula in Lemma 5.3 and Hypothesis 1.2.
- (b) By (29), we have, for some uniform constant C

$$\|\eta_{k,n}^\pm\|_{C^0(\Omega_{k,\varepsilon''})} \leq C \left(\frac{2}{\varepsilon''} \right)^{n-1}.$$

Hence

$$\|\psi_k^* \eta_{k,n}^\pm\|_{C^0(\tilde{\Omega}_k)} \leq 2C \left(\frac{2}{\varepsilon''} \right)^{n-1}.$$

Observe that ψ_k depends holomorphically on τ_k . Also, $\eta_{k,n}^\pm$ depends holomorphically on x_k ($\omega_{k,n}^\pm$ does not). Hence for $z \in \tilde{\Omega}_k$, $\psi_k^* \eta_{k,n}^\pm(z)$ depends holomorphically on x_k . By Cauchy Estimate, restricting the parameter \underline{x} to a smaller neighborhood of \underline{x} , we have

$$\|d^m \psi_k^* \eta_{k,n}^\pm\|_{C^0(\tilde{\Omega}_k)} \leq C(m) \left(\frac{2}{\varepsilon''} \right)^{n-1}$$

for some uniform constants $C(m)$, where d^m denotes the m -th order differential with respect to x_k . (b) follows from (27).

- (c) Since $\psi_k(\tilde{\gamma}_k^\pm) \subset \psi_k(\tilde{\Omega}_k) \subset \Omega_{k,\varepsilon''}$, we have $|z_k^\pm \circ \psi_k| \geq \varepsilon''$ on $\tilde{\gamma}_k^\pm$. Hence

$$\left\| \left(\frac{t^2}{\rho z_k^\pm \circ \psi_k} \right)^{n-1} \right\|_{C^0(\tilde{\gamma}_k^\pm)} \leq 1.$$

Since $z_k^\pm \circ \psi_k(z)$ depends holomorphically on x_k , we obtain uniform estimates of the derivatives by Cauchy Estimate.

□

Proof of Lemma 5.8. We write $\tilde{\omega}_1$ for the first term in the definition of $\tilde{\omega}$ and $\tilde{\omega}_2$ for the second term (the sum for $n \geq 2$).

- (a) $(\psi^*\tilde{\omega}_1)(\mathbf{x}) \in C^0(\tilde{\Omega})$ and is a smooth function of \mathbf{x} . This follows from Claim 5.10(a) and Proposition 5.9. $(\psi^*\tilde{\omega}_2)(\mathbf{x}, \boldsymbol{\lambda}) \in C^0(\tilde{\Omega})$ and is a smooth function of \mathbf{x} and $\boldsymbol{\lambda}$. This follows from Claim 5.10(b), Proposition 5.9 and the fact that the bilinear operator

$$(36) \quad (\eta, \boldsymbol{\lambda}) \mapsto \left(\sum_{n=2}^{\infty} \left(\frac{2\rho}{\varepsilon''} \right)^{n-1} (\lambda_{k,n}^+ \eta_{k,n}^+ + \lambda_{k,n}^- \eta_{k,n}^-) \right)_{k \in \mathbb{Z}}$$

is bounded from $(\bigoplus_{(k,n,s) \in \Lambda} C^0(\tilde{\Omega}_k))_\infty \times \ell^\infty$ to $C^0(\tilde{\Omega})$. (Since $\rho \leq \varepsilon''/4$, it has norm at most 2). This proves Lemma 5.8(a).

- (b) Lemma 5.8(b) follows from Claim 5.10(c), Proposition 5.9 and the fact that the bilinear operator

$$(37) \quad (\mathbf{f}, \eta) \mapsto \left(\frac{-1}{2\pi i} \int_{\gamma_{k+s}^-} f_{k+s,n}^- \eta \right)_{(k,n,s) \in \Lambda}$$

is bounded from $(\bigoplus_{(k,n,s) \in \Lambda} C^0(\tilde{\gamma}_k^s))_\infty \times C^0(\tilde{\Omega})$ to ℓ^∞ .

□

6. ASYMPTOTIC BEHAVIOR

Assume that we are given two configurations (q_k) and (q'_k) such that $q_k = q'_k$ for all $k \geq 0$. In this section we prove that the holomorphic 1-form ω' and the parameters \mathbf{x}' are asymptotic to ω and \mathbf{x} . These results were used in Section 4 to prove the asymptotic behaviors of the minimal surfaces.

6.1. Asymptotic behavior of ω . For any infinite set K equipped with a weight function $\sigma : K \rightarrow [1, \infty)$, if $(V_k)_{k \in K}$ is a sequence of normed spaces, we define

$$\left(\bigoplus_{k \in K} V_k \right)_{\infty, \sigma} = \{ \mathbf{x} \in \prod_{k \in K} V_k : \| \mathbf{x} \|_{\infty, \sigma} = \sup_{k \in K} \sigma(k) \| x_k \| < \infty \}.$$

If $V_k = \mathbb{C}^n$ for all $k \in K$, then we simply use the notation $\ell^{\infty, \sigma}(K)$. The argument K will be omitted if it is clear in the context.

Let $\underline{\mathbf{x}}$ and $\underline{\mathbf{x}'}$ be the central values corresponding to the configurations (q_k) and (q'_k) , as given by (5). Our goal is to compare $\omega[t, \mathbf{x}]$ to $\omega[t, \mathbf{x}']$ for \mathbf{x}, \mathbf{x}' in a neighborhood of $\underline{\mathbf{x}}, \underline{\mathbf{x}'}$. For this purpose, we replace the definition of $\tilde{\Omega}_k$ and $\tilde{\Omega}$ in Section 3.3 by

$$\tilde{\Omega}_k = \mathbb{T} \setminus (\overline{D}(0, \varepsilon') \cup \overline{D}(\tilde{v}_k, \varepsilon') \cup \overline{D}(\tilde{v}'_k, \varepsilon')) \quad \text{and} \quad \tilde{\Omega} = \bigsqcup_{k \in \mathbb{Z}} \tilde{\Omega}_k.$$

Now $(\psi^*\omega)[t, \mathbf{x}]$ and $(\psi^*\omega)[t, \mathbf{x}']$ are both defined on the same fixed domain $\tilde{\Omega}$ so we can compare them.

Fix $\delta > 1$ and define the weight $\sigma : \mathbb{Z} \rightarrow [1, \infty)$ by $\sigma(k) = 1$ if $k \leq 0$ and $\sigma(k) = \delta^k$ if $k \geq 0$. We extend this weight to Λ by $\sigma(k, n, s) = \sigma(k)$ for all $(k, n, s) \in \Lambda$. We have $\underline{x}_k = \underline{x}'_k$ for all $k \geq 0$ so $\underline{\mathbf{x}}' - \underline{\mathbf{x}} \in \ell^{\infty, \sigma}$. It will be convenient to write

$$\Delta \mathbf{x} = \mathbf{x}' - \mathbf{x}.$$

We define the weighted space $C^{0, \sigma}(\tilde{\Omega})$ (not to be confused with a Hölder space) by

$$C^{0, \sigma}(\tilde{\Omega}) = \left(\bigoplus_{k \in \mathbb{Z}} C^0(\tilde{\Omega}_k) \right)_{\infty, \sigma}$$

So functions in $C^{0,\sigma}(\tilde{\Omega})$ decay like δ^{-k} in $\tilde{\Omega}_k$ as $k \rightarrow +\infty$.

Proposition 6.1. *For t small enough, \mathbf{x} in an ℓ^∞ -neighborhood of $\underline{\mathbf{x}}$ and $\Delta\mathbf{x}$ in an $\ell^{\infty,\sigma}$ neighborhood of $\Delta\underline{\mathbf{x}} = \underline{\mathbf{x}}' - \underline{\mathbf{x}}$,*

$$(\psi^*\omega)[t, \mathbf{x} + \Delta\mathbf{x}] - (\psi^*\omega)[t, \mathbf{x}] \in C^{0,\sigma}(\tilde{\Omega})$$

and depends smoothly on t , $\mathbf{x} \in \ell^\infty$ and $\Delta\mathbf{x} \in \ell^{\infty,\sigma}$.

Proof. Recall that $\boldsymbol{\lambda}(t, \mathbf{x})$ is given by Lemma 5.6 and define

$$\boldsymbol{\mu}(t, \mathbf{x}, \Delta\mathbf{x}) = \boldsymbol{\lambda}(t, \mathbf{x} + \Delta\mathbf{x}) - \boldsymbol{\lambda}(t, \mathbf{x}) \in \ell^\infty(\Lambda).$$

Our goal is to prove that $\boldsymbol{\mu}(t, \mathbf{x}, \Delta\mathbf{x}) \in \ell^{\infty,\sigma}(\Lambda)$.

Let

$$\Delta\mathbf{L}(t, \mathbf{x}, \Delta\mathbf{x}, \boldsymbol{\lambda}, \Delta\boldsymbol{\lambda}) = \mathbf{L}(t, \mathbf{x} + \Delta\mathbf{x}, \boldsymbol{\lambda} + \Delta\boldsymbol{\lambda}) - \mathbf{L}(t, \mathbf{x}, \boldsymbol{\lambda}).$$

Then

$$\Delta\mathbf{L}(t, \mathbf{x}, \Delta\mathbf{x}, \boldsymbol{\lambda}(t, \mathbf{x}), \boldsymbol{\mu}(t, \mathbf{x}, \Delta\mathbf{x})) = \mathbf{L}(t, \mathbf{x} + \Delta\mathbf{x}, \boldsymbol{\lambda}(t, \mathbf{x} + \Delta\mathbf{x})) - \mathbf{L}(t, \mathbf{x}, \boldsymbol{\lambda}(t, \mathbf{x})) = \boldsymbol{\mu}(t, \mathbf{x}, \Delta\mathbf{x}).$$

In other words, $\boldsymbol{\mu}(t, \mathbf{x}, \Delta\mathbf{x})$ is a fixed point of $\Delta\mathbf{L}$ with respect to the $\Delta\boldsymbol{\lambda}$ variable.

Define

$$\Delta\tilde{\mathbf{L}}(t, \mathbf{x}, \Delta\mathbf{x}, \eta, \Delta\eta) = \tilde{\mathbf{L}}(t, \mathbf{x} + \Delta\mathbf{x}, \eta + \Delta\eta) - \tilde{\mathbf{L}}(t, \mathbf{x}, \eta)$$

and

$$\mathbf{H}(\mathbf{x}, \Delta\mathbf{x}, \boldsymbol{\lambda}, \Delta\boldsymbol{\lambda}) = (\psi^*\tilde{\omega})(\mathbf{x} + \Delta\mathbf{x}, \boldsymbol{\lambda} + \Delta\boldsymbol{\lambda}) - (\psi^*\tilde{\omega})(\mathbf{x}, \boldsymbol{\lambda}).$$

Recalling (35), we have

$$\Delta\mathbf{L}(t, \mathbf{x}, \Delta\mathbf{x}, \boldsymbol{\lambda}, \Delta\boldsymbol{\lambda}) = \Delta\tilde{\mathbf{L}}(t, \mathbf{x}, \Delta\mathbf{x}, (\psi^*\tilde{\omega})(\mathbf{x}, \boldsymbol{\lambda}), \mathbf{H}(\mathbf{x}, \Delta\mathbf{x}, \boldsymbol{\lambda}, \Delta\boldsymbol{\lambda})).$$

By Lemma 6.2 below, $\Delta\mathbf{L} \in \ell^{\infty,\sigma}$ is smooth with respect to $\mathbf{x}, \boldsymbol{\lambda} \in \ell^\infty$ and $\Delta\mathbf{x}, \Delta\boldsymbol{\lambda} \in \ell^{\infty,\sigma}$, and is contracting with respect to $\Delta\boldsymbol{\lambda}$, so its unique fixed point $\boldsymbol{\mu}(t, \mathbf{x}, \Delta\mathbf{x})$ is in $\ell^{\infty,\sigma}$ and depends smoothly on $t, \mathbf{x}, \Delta\mathbf{x}$ in their respective spaces. Finally, we have by definition

$$\begin{aligned} (\psi^*\omega)[t, \mathbf{x} + \Delta\mathbf{x}] - (\psi^*\omega)[t, \mathbf{x}] &= (\psi^*\tilde{\omega})(\mathbf{x} + \Delta\mathbf{x}, \boldsymbol{\lambda}(t, \mathbf{x} + \Delta\mathbf{x})) - (\psi^*\tilde{\omega})(\mathbf{x}, \boldsymbol{\lambda}(t, \mathbf{x})) \\ &= \mathbf{H}(\mathbf{x}, \Delta\mathbf{x}, \boldsymbol{\lambda}(t, \mathbf{x}), \boldsymbol{\mu}(t, \mathbf{x}, \Delta\mathbf{x})) \end{aligned}$$

so Proposition 6.1 follows from Lemma 6.2(a). \square

Lemma 6.2.

- (a) *For \mathbf{x} in an ℓ^∞ -neighborhood of $\underline{\mathbf{x}}$, $\Delta\mathbf{x}$ in an $\ell^{\infty,\sigma}$ -neighborhood of $\Delta\underline{\mathbf{x}}$, $\boldsymbol{\lambda} \in \ell^\infty$ and $\Delta\boldsymbol{\lambda} \in \ell^{\infty,\sigma}$,*

$$\mathbf{H}(\mathbf{x}, \Delta\mathbf{x}, \boldsymbol{\lambda}, \Delta\boldsymbol{\lambda}) \in C^{0,\sigma}(\tilde{\Omega})$$

and depends smoothly on $\mathbf{x}, \Delta\mathbf{x}, \boldsymbol{\lambda}, \Delta\boldsymbol{\lambda}$.

- (b) *For t in a neighborhood of 0, \mathbf{x} in an ℓ^∞ -neighborhood of $\underline{\mathbf{x}}$, $\Delta\mathbf{x}$ in an $\ell^{\infty,\sigma}$ -neighborhood of $\Delta\underline{\mathbf{x}}$, $\eta \in C^0(\tilde{\Omega})$ and $\Delta\eta \in C^{0,\sigma}(\tilde{\Omega})$,*

$$\Delta\tilde{\mathbf{L}}(t, \mathbf{x}, \Delta\mathbf{x}, \eta, \Delta\eta) \in \ell^{\infty,\sigma}$$

and depends smoothly on $t, \mathbf{x}, \Delta\mathbf{x}, \eta, \Delta\eta$.

- (c) *For t small enough, $\Delta\mathbf{L}$ is contracting with respect to $\Delta\boldsymbol{\lambda}$, as a map from $\ell^{\infty,\sigma}$ to itself.*

We need the following

Proposition 6.3. *Under the same notations and hypothesis as in Proposition 5.9, let $\sigma : K \rightarrow [1, \infty)$ be an arbitrary weight. Let $U^{\infty, \sigma} = (\bigoplus_{k \in K} U_k)_{\infty, \sigma}$ and $V^{\infty, \sigma} = (\bigoplus_{k \in K} V_k)_{\infty, \sigma}$. Define for $\mathbf{x} \in B(\mathbf{0}, r/2) \subset U^\infty$ and $\Delta\mathbf{x} \in B(\mathbf{0}, r/2) \subset U^{\infty, \sigma}$*

$$\Delta\mathbf{f}(\mathbf{x}, \Delta\mathbf{x}) = (f_k(x_k + \Delta x_k) - f_k(x_k))_{k \in K}.$$

Then $\Delta\mathbf{f}(\mathbf{x}, \Delta\mathbf{x}) \in V^{\infty, \sigma}$, $\Delta\mathbf{f}$ is smooth and

$$d(\Delta\mathbf{f})(\mathbf{x}, \Delta\mathbf{x})(\mathbf{h}, \Delta\mathbf{h}) = (df_k(x_k + \Delta x_k)(h_k + \Delta h_k) - df_k(x_k)h_k)_{k \in K}.$$

Proof. By the Mean Value Inequality

$$\sigma(k)\|f_k(x_k + \Delta x_k) - f_k(x_k)\| \leq C\sigma(k)\|\Delta x_k\|$$

Hence $\Delta\mathbf{f}(\mathbf{x}, \Delta\mathbf{x}) \in V^{\infty, \sigma}$. Define

$$l_k(h_k, \Delta h_k) = df_k(x_k + \Delta x_k)(h_k + \Delta h_k) - df_k(x_k)h_k \quad \text{and} \quad \mathbf{l}(\mathbf{h}, \Delta\mathbf{h}) = (l_k(h_k, \Delta h_k))_{k \in K}.$$

Using the Mean Value Inequality, one easily obtains

$$\sigma(k)\|l_k(h_k, \Delta h_k)\| \leq C\sigma(k)(\|\Delta h_k\| + \|\Delta x_k\| \|h_k\|).$$

Hence \mathbf{l} is a bounded operator from $U^\infty \times U^{\infty, \sigma}$ to $V^{\infty, \sigma}$. Using Taylor Formula with integral remainder, we have

$$\begin{aligned} & \Delta f_k(x_k + h_k, \Delta x_k + \Delta h_k) - \Delta f_k(x_k, \Delta x_k) - l_k(h_k, \Delta h_k) \\ &= f_k(x_k + \Delta x_k + h_k + \Delta h_k) - f_k(x_k + \Delta x_k) \\ &\quad - df_k(x_k + \Delta x_k)(h_k + \Delta h_k) - [f_k(x_k + h_k) - f_k(x_k) - df_k(x_k)h_k] \\ &= \int_0^1 (1-t) [d^2 f_k(x_k + \Delta x_k + t(h_k + \Delta h_k))(h_k + \Delta h_k)^2 - d^2 f_k(x_k + th_k)h_k^2] dt \end{aligned}$$

By the Mean Value Inequality

$$\begin{aligned} & \sigma(k)\|\Delta f_k(x_k + h_k, \Delta x_k + \Delta h_k) - \Delta f_k(x_k, \Delta x_k) - l_k(h_k, \Delta h_k)\| \\ & \leq C\sigma(k)[2\|h_k\|\|\Delta h_k\| + \|\Delta h_k\|^2 + (\|\Delta x_k\| + \|\Delta h_k\|)\|h_k\|^2]. \end{aligned}$$

Hence

$$\|\Delta\mathbf{f}(\mathbf{x} + \mathbf{h}, \Delta\mathbf{x} + \Delta\mathbf{h}) - \Delta\mathbf{f}(\mathbf{x}, \Delta\mathbf{x}) - \mathbf{l}(\mathbf{h}, \Delta\mathbf{h})\|_{\infty, \sigma} = O((\|\mathbf{h}\|_\infty + \|\Delta\mathbf{h}\|_{\infty, \sigma})^2)$$

so $\Delta\mathbf{f}$ is differentiable with $d(\Delta\mathbf{f})(\mathbf{x}, \Delta\mathbf{x}) = \mathbf{l}$. Smoothness follows by induction. \square

We shall use the following corollary with $K = \mathbb{Z}$, $K^+ = \mathbb{N}$ and $K^- = \mathbb{Z} \setminus \mathbb{N}$:

Corollary 6.4. *With the same notation as in Proposition 6.3, assume that for $k \in K$, f_k is defined in $B(\underline{x}_k, r) \cup B(\underline{x}'_k, r)$ in U_k and has uniformly bounded derivatives. Assume that K admits a partition (K^+, K^-) such that for all $k \in K^+$, $\underline{x}_k = \underline{x}'_k$, and for all $k \in K^-$, $\sigma(k) = 1$. Then for $\mathbf{x} \in B(\underline{\mathbf{x}}, r/2) \subset U^\infty$ and $\Delta\mathbf{x} \in B(\underline{\mathbf{x}}' - \underline{\mathbf{x}}, r/2) \subset U^{\infty, \sigma}$, $\Delta\mathbf{f}(\mathbf{x}, \Delta\mathbf{x}) \in V^{\infty, \sigma}$ and depends smoothly on \mathbf{x} and $\Delta\mathbf{x}$.*

Proof. We decompose a sequence $\mathbf{x} = (x_k)_{k \in K}$ as $\mathbf{x} = \mathbf{x}^+ + \mathbf{x}^-$ with \mathbf{x}^+ supported on K^+ and \mathbf{x}^- supported on K^- . By Proposition 5.9, $\mathbf{f}^-(\mathbf{x}^-) \in V^\infty$ and $\mathbf{f}^-(\mathbf{x}^- + \Delta\mathbf{x}^-) \in V^\infty$ so $\Delta\mathbf{f}^-(\mathbf{x}^-, \Delta\mathbf{x}^-) \in V^\infty$. Since $\sigma = 1$ on K^- , $\Delta\mathbf{f}^-(\mathbf{x}^-, \Delta\mathbf{x}^-) \in V^{\infty, \sigma}$. Since $\underline{\mathbf{x}}^+ = (\underline{\mathbf{x}}')^+$, we may use the change of variable $\mathbf{x}^+ = \underline{\mathbf{x}}^+ + \mathbf{y}^+$ and conclude that $\Delta\mathbf{f}^+(\mathbf{x}^+, \Delta\mathbf{x}^+) \in V^{\infty, \sigma}$ by Proposition 6.3. \square

Proof of Lemma 6.2. Lemma 6.2(a) follows from the following.

- $(\psi^*\tilde{\omega}_1)(\mathbf{x} + \Delta\mathbf{x}) - (\psi^*\tilde{\omega}_1)(\mathbf{x}) \in C^{0,\sigma}(\tilde{\Omega})$ and is a smooth function of \mathbf{x} , $\Delta\mathbf{x}$. This follows from Claim 5.10(a) and Corollary 6.4.
- $(\psi^*\tilde{\omega}_2)(\mathbf{x} + \Delta\mathbf{x}, \boldsymbol{\lambda}) - (\psi^*\tilde{\omega}_2)(\mathbf{x}, \boldsymbol{\lambda}) \in C^{0,\sigma}(\tilde{\Omega})$ and is a smooth function of \mathbf{x} , $\Delta\mathbf{x}$ and $\boldsymbol{\lambda}$. This follows from Claim 5.10(b), Corollary 6.4 and the fact that the bilinear operator (36) is bounded from $(\bigoplus_{(k,n,s) \in \Lambda} C^0(\tilde{\Omega}_k))_{\infty,\sigma} \times \ell^\infty(\Lambda)$ to $C^{0,\sigma}(\tilde{\Omega})$.
- $(\psi^*\tilde{\omega}_2)(\mathbf{x} + \Delta\mathbf{x}, \Delta\boldsymbol{\lambda}) \in C^{0,\sigma}(\tilde{\Omega})$ and is a smooth function of \mathbf{x} , $\Delta\mathbf{x}$ and $\Delta\boldsymbol{\lambda}$. This follows from Claim 5.10(b), Proposition 5.9 and the fact that the bilinear operator (36) is bounded from $(\bigoplus_{(k,n,s) \in \Lambda} C^0(\tilde{\Omega}_k))_\infty \times \ell^{\infty,\sigma}(\Lambda)$ to $C^{0,\sigma}(\tilde{\Omega})$.

Lemma 6.2(b) follows from the following.

- $\tilde{\mathbf{L}}(t, \mathbf{x} + \Delta\mathbf{x}, \eta) - \tilde{\mathbf{L}}(t, \mathbf{x}, \eta) \in \ell^{\infty,\sigma}(\Lambda)$ and depends smoothly on $t, \mathbf{x}, \Delta\mathbf{x}$ and η . This follows from Claim 5.10(c), Corollary 6.4 and the fact that the bilinear operator (37) is bounded from $(\bigoplus_{(k,n,s) \in \Lambda} C^0(\tilde{\gamma}_k^s))_{\infty,\sigma} \times C^0(\tilde{\Omega})$ to $\ell^{\infty,\sigma}(\Lambda)$. This uses that $\frac{\sigma(k)}{\sigma(k \pm 1)} \leq \delta$ and explains our choice of the weight σ .
- $\tilde{\mathbf{L}}(t, \mathbf{x} + \Delta\mathbf{x}, \Delta\eta) \in \ell^{\infty,\sigma}(\Lambda)$ and depends smoothly on $t, \mathbf{x}, \Delta\mathbf{x}$ and $\Delta\eta$. This follows from Claim 5.10(c), Proposition 5.9 and the fact that the bilinear operator (37) is bounded from $(\bigoplus_{(k,n,s) \in \Lambda} C^0(\tilde{\gamma}_k^s))_\infty \times C^{0,\sigma}(\tilde{\Omega})$ to $\ell^{\infty,\sigma}(\Lambda)$.

Finally, we have

$$\Delta\mathbf{L}(t, \mathbf{x}, \Delta\mathbf{x}, \boldsymbol{\lambda}, \Delta\boldsymbol{\lambda}) - \Delta\mathbf{L}(t, \mathbf{x}, \Delta\mathbf{x}, \boldsymbol{\lambda}, 0) = \mathbf{L}(t, \mathbf{x} + \Delta\mathbf{x}, \boldsymbol{\lambda} + \Delta\boldsymbol{\lambda}) - \mathbf{L}(t, \mathbf{x} + \Delta\mathbf{x}, \boldsymbol{\lambda}).$$

Using Estimate (31) as in the proof of Lemma 5.6,

$$\|\mathbf{L}(t, \mathbf{x} + \Delta\mathbf{x}, \boldsymbol{\lambda} + \Delta\boldsymbol{\lambda}) - \mathbf{L}(t, \mathbf{x} + \Delta\mathbf{x}, \boldsymbol{\lambda})\|_{\infty,\sigma} \leq \frac{C\ell\delta t^2}{\pi\rho\varepsilon} \|\Delta\boldsymbol{\lambda}\|_{\infty,\sigma}$$

so $\Delta\mathbf{L}$ is contracting with respect to $\Delta\boldsymbol{\lambda}$ for t small enough. \square

6.2. Asymptotic behavior of the parameters. Let $\mathbf{x}(t)$ and $\mathbf{x}'(t)$ be the solutions obtained in Section 3 from the configurations (q_k) and (q'_k) , respectively.

Proposition 6.5. *For t small enough, $\mathbf{x}'(t) - \mathbf{x}(t) \in \ell^{\infty,\sigma}$.*

Proof. Recall the definition of \mathcal{E}_k in Section 3.4, $\mathcal{P}_{k,1}$ and $\mathcal{P}_{k,2}$ in Section 3.5 and \mathcal{G}_k in Section 3.6. We have solved equations by three consecutive applications of the Implicit Function Theorem. But we could have solved all of them by one single application. Indeed, consider the change of parameter

$$b_k = -a_k\xi(v_k, \tau_k) + \hat{b}_k.$$

By the computations in Sections 3.4, 3.5 and 3.6, the jacobian of $(\mathcal{E}_k, \mathcal{P}_{k,1}, \mathcal{P}_{k,2}, \mathcal{G}_k)$ with respect to $(\hat{b}_k, a_k, \tau_k, v_k)$ has upper-triangular form with \mathbb{R} -linear automorphisms of \mathbb{C} on the diagonal, whose inverses are uniformly bounded with respect to k . Define

$$\mathcal{F}_k(t, \mathbf{x}) = (\mathcal{E}_k(t, \mathbf{x}), \mathcal{P}_{k,1}(t, \mathbf{x}), \mathcal{P}_{k,2}(t, \mathbf{x}), \mathcal{G}_k(t, \mathbf{x}) + 2\pi i G(q_0; T)) \quad \text{and} \quad \mathcal{F} = (\mathcal{F}_k)_{k \in \mathbb{Z}}.$$

Then $d_{\mathbf{x}}\mathcal{F}(0, \mathbf{x}')$ is an automorphism of ℓ^∞ , and restricts to an automorphism of $\ell^{\infty,\sigma}$. Define, for \mathbf{x} in an ℓ^∞ -neighborhood of $\underline{\mathbf{x}}$ and $\Delta\mathbf{x}$ in an $\ell^{\infty,\sigma}$ -neighborhood of $\Delta\underline{\mathbf{x}} = \mathbf{x}' - \underline{\mathbf{x}}$

$$\Delta\mathcal{F}(t, \mathbf{x}, \Delta\mathbf{x}) = \mathcal{F}(t, \mathbf{x} + \Delta\mathbf{x}) - \mathcal{F}(t, \mathbf{x}).$$

By Lemma 6.6 below, $\Delta\mathcal{F}(t, \mathbf{x}, \Delta\mathbf{x}) \in \ell^{\infty, \sigma}$. We have

$$\Delta\mathcal{F}(0, \underline{\mathbf{x}}, \Delta\underline{\mathbf{x}}) = \mathcal{F}(t, \mathbf{x}') - \mathcal{F}(t, \underline{\mathbf{x}}) = 0 \quad \text{and} \quad d_{\Delta\mathbf{x}}(\Delta\mathcal{F})(0, \underline{\mathbf{x}}, \Delta\underline{\mathbf{x}}) = d_{\mathbf{x}}\mathcal{F}(0, \underline{\mathbf{x}}').$$

By the Implicit Function Theorem, for t small enough and \mathbf{x} in a neighborhood of $\underline{\mathbf{x}}$, there exists $\Delta\mathbf{x}(t, \mathbf{x}) \in \ell^{\infty, \sigma}$ such that $\Delta\mathcal{F}(t, \mathbf{x}, \Delta\mathbf{x}(t, \mathbf{x})) = 0$. We substitute $\mathbf{x} = \mathbf{x}(t)$ and obtain $\mathcal{F}(t, \mathbf{x}(t) + \Delta\mathbf{x}(t, \mathbf{x}(t))) = \mathcal{F}(t, \mathbf{x}'(t)) = 0$. By uniqueness, $\mathbf{x}'(t) = \mathbf{x}(t) + \Delta\mathbf{x}(t, \mathbf{x}(t))$, which proves Proposition 6.5. \square

Lemma 6.6. *For t in a neighborhood of 0, \mathbf{x} in an ℓ^∞ -neighborhood of $\underline{\mathbf{x}}$ and $\Delta\mathbf{x}$ in an $\ell^{\infty, \sigma}$ -neighborhood of $\Delta\underline{\mathbf{x}}$, $\Delta\mathcal{F}(t, \mathbf{x}, \Delta\mathbf{x}) \in \ell^{\infty, \sigma}$ and depends smoothly on t , \mathbf{x} and $\Delta\mathbf{x}$.*

Proof. Define for $z \in \mathbb{T}$:

$$f_k[\mathbf{x}](z) = \frac{\psi_k(z) - (Z_{k,1} + Z_{k,2})}{\psi_k(z)^2 - (Z_{k,1} + Z_{k,2})\psi_k(z) + Z_{k,1}Z_{k,2}} \quad \text{and} \quad \mathbf{f}[\mathbf{x}] = (f_k[\mathbf{x}])_{k \in \mathbb{Z}}.$$

By Cauchy Theorem and a change of variable,

$$\mathcal{E}_k(t, \mathbf{x}) = \frac{1}{2\pi i} \int_{\partial\tilde{\Omega}_{k, 2\varepsilon'}} f_k \psi_k^* \omega[t, \mathbf{x}].$$

Hence we can write

$$\mathcal{E}(t, \mathbf{x}) = \mathbf{B}(\mathbf{f}[\mathbf{x}], (\psi^* \omega)[t, \mathbf{x}]) \quad \text{where} \quad \mathbf{B}(\mathbf{f}, \eta) = \left(\frac{1}{2\pi i} \int_{\partial\tilde{\Omega}_{k, 2\varepsilon'}} f_k \eta_k \right)_{k \in \mathbb{Z}}.$$

Using Weierstrass Preparation Theorem, the symmetric functions of $Z_{k,1}$ and $Z_{k,2}$ are holomorphic functions of x_k . Hence f_k is a smooth function of x_k with value in $C^0(\partial\tilde{\Omega}_{k, 2\varepsilon'})$. Using Corollary 6.4 and that the bilinear operator

$$\mathbf{B} : \left(\bigoplus_{k \in \mathbb{Z}} C^0(\partial\tilde{\Omega}_{k, 2\varepsilon'}) \right)_{\infty, \sigma} \times C^0(\tilde{\Omega}) \rightarrow \ell^{\infty, \sigma}$$

is bounded, we conclude that

$$(38) \quad \mathbf{B}(\mathbf{f}[\mathbf{x} + \Delta\mathbf{x}] - \mathbf{f}[\mathbf{x}], (\psi^* \omega)[t, \mathbf{x}]) \in \ell^{\infty, \sigma}$$

and depends smoothly on t , \mathbf{x} and $\Delta\mathbf{x}$. Using Proposition 6.1 and that the bilinear operator

$$\mathbf{B} : \left(\bigoplus_{k \in \mathbb{Z}} C^0(\partial\tilde{\Omega}_{k, 2\varepsilon'}) \right)_\infty \times C^{0, \sigma}(\tilde{\Omega}) \rightarrow \ell^{\infty, \sigma}$$

is bounded, we obtain

$$(39) \quad \mathbf{B}(\mathbf{f}[\mathbf{x} + \Delta\mathbf{x}], (\psi^* \omega)[t, \mathbf{x} + \Delta\mathbf{x}] - (\psi^* \omega)[t, \mathbf{x}]) \in \ell^{\infty, \sigma}$$

and depends smoothly on t , \mathbf{x} and $\Delta\mathbf{x}$. Adding (38) and (39), we conclude that

$$\mathcal{E}(t, \mathbf{x} + \Delta\mathbf{x}) - \mathcal{E}(t, \mathbf{x}) \in \ell^{\infty, \sigma}$$

and depends smoothly on t , \mathbf{x} and $\Delta\mathbf{x}$.

Finally, $\mathcal{P}_{k,1}$, $\mathcal{P}_{k,2}$ and \mathcal{G}_k are defined as integrals of ω times powers of g_k on certain curves in T_k , so we can deal with them in the same way as \mathcal{E}_k . \square

REFERENCES

- [BE16] Walter Bergweiler and Alexandre Eremenko. Green's function and anti-holomorphic dynamics on a torus. *Proc. Amer. Math. Soc.*, 144(7):2911–2922, 2016.
- [BMMS17] Konstantin Bogdanov, Khudoyor Mamayusupov, Sabyasachi Mukherjee, and Dierk Schleicher. Antiholomorphic perturbations of Weierstrass Zeta functions and Green's function on tori. *Nonlinearity*, 30(8):3241–3254, 2017.
- [Bra92] Kenneth A. Brakke. The Surface Evolver. *Experiment. Math.*, 1(2):141–165, 1992.
- [CCM⁺06] Charlotte E. Conn, Oscar Ces, Xavier Mulet, Stephanie Finet, Roland Winter, John M. Seddon, and Richard H. Templer. Dynamics of structural transformations between lamellar and inverse bicontinuous cubic lyotropic phases. *Physical review letters*, 96(10):108102, 2006.
- [CF97] Thierry Charitat and Bertrand Fourcade. Lattice of passages connecting membranes. *Journal de Physique II*, 7(1):15–35, 1997.
- [Che19a] Hao Chen. Existence of the rhombohedral and tetragonal deformation families of the gyroid. page 21 pp., 2019. preprint, [arXiv:1901.04006](https://arxiv.org/abs/1901.04006).
- [Che19b] Hao Chen. Minimal twin surfaces. *Exp. Math.*, 28(4):404–419, 2019.
- [CKLW18] Zhijie Chen, Ting-Jung Kuo, Chang-Shou Lin, and Chin-Lung Wang. Green function, Painlevé VI equation, and Eisenstein series of weight one. *J. Differential Geom.*, 108(2):185–241, 2018.
- [CW18a] Hao Chen and Matthias Weber. A new deformation family of Schwarz' D surface. page 15 pp., 2018. to appear in Trans. Amer. Math. Soc., [arXiv:1804.01442](https://arxiv.org/abs/1804.01442).
- [CW18b] Hao Chen and Matthias Weber. An orthorhombic deformation family of Schwarz' H surfaces. page 17 pp., 2018. to appear in Trans. Amer. Math. Soc., [arXiv:1807.10631](https://arxiv.org/abs/1807.10631).
- [Fay73] John D. Fay. *Theta Functions on Riemann Surfaces*, volume 352 of *Lecture Notes in Mathematics*. 1973.
- [FH92] Andrew Fogden and Stephen T Hyde. Parametrization of triply periodic minimal surfaces. ii. regular class solutions. *Acta Crystallographica Section A: Foundations of Crystallography*, 48(4):575–591, 1992.
- [FH99] Andrew Fogden and Stephen T. Hyde. Continuous transformations of cubic minimal surfaces. *The European Physical Journal B-Condensed Matter and Complex Systems*, 7(1):91–104, 1999.
- [FHL93] Andrew Fogden, Markus Haeberlein, and Sven Lidin. Generalizations of the gyroid surface. *J. Phys. I*, 3(12):2371–2385, 1993.
- [GBW96] Karsten Groß-Brauckmann and Meinhard Wohlgemuth. The gyroid is embedded and has constant mean curvature companions. *Calc. Var. Partial Differential Equations*, 4(6):499–523, 1996.
- [HBL⁺96] Stephen T. Hyde, Zoltan Blum, Tomas Landh, Sven Lidin, Barry W. Ninham, Sten Andersson, and Kåre Larsson. *The Language of Shape: The Role of Curvature in Condensed Matter: Physics, Chemistry and Biology*. Elsevier Science, 1996.
- [Hec27] Erich Hecke. Zur Theorie der elliptischen Modulfunktionen. *Math. Ann.*, 97(1):210–242, 1927.
- [HXBC11] Lu Han, Ping Xiong, Jingfeng Bai, and Shunai Che. Spontaneous formation and characterization of silica mesoporous crystal spheres with reverse multiply twinned polyhedral hollows. *Journal of the American Chemical Society*, 133(16):6106–6109, 2011.
- [Lan95] Serge Lang. *Introduction to modular forms*, volume 222 of *Grundlehren der Mathematischen Wissenschaften*. Springer-Verlag, Berlin, 1995. With appendixes by D. Zagier and Walter Feit, Corrected reprint of the 1976 original.
- [Lin16] Chang-Shou Lin. Green function, mean field equation and Painlevé VI equation. In *Current developments in mathematics 2015*, pages 137–188. Int. Press, Somerville, MA, 2016.
- [LW10] Chang-Shou Lin and Chin-Lung Wang. Elliptic functions, Green functions and the mean field equations on tori. *Ann. of Math. (2)*, 172(2):911–954, 2010.
- [LW17] Chang-Shou Lin and Chin-Lung Wang. On the minimality of extra critical points of Green functions on flat tori. *Int. Math. Res. Not. IMRN*, (18):5591–5608, 2017.
- [MBF94] Xavier Michalet, David Bensimon, and Bertrand Fourcade. Fluctuating vesicles of nonspherical topology. *Physical review letters*, 72(1):168, 1994.
- [MT12] Filippo Morabito and Martin Traizet. Non-periodic Riemann examples with handles. *Adv. Math.*, 229(1):26–53, 2012.
- [MW91] William H. Meeks and Brian White. Minimal surfaces bounded by convex curves in parallel planes. *Comment. Math. Helvetici*, 66:263–278, 1991.

- [Sch70] Alan H. Schoen. Infinite periodic minimal surfaces without self-intersections. Technical Note D-5541, NASA, Cambridge, Mass., May 1970.
- [Shi56] Max Shiffman. On surfaces of stationary area bounded by two circles, or convex curves, in parallel planes. *Ann. of Math. (2)*, 63:77–90, 1956.
- [TBC⁺15] T.-Y. Dora Tang, Nicholas J. Brooks, Oscar Ces, John M. Seddon, and Richard H. Templer. Structural studies of the lamellar to bicontinuous gyroid cubic (Q GII) phase transitions under limited hydration conditions. *Soft matter*, 11(10):1991–1997, 2015.
- [Tra02] Martin Traizet. An embedded minimal surface with no symmetries. *J. Diff. Geom.*, 60:103–153, 2002.
- [Tra08] Martin Traizet. On the genus of triply periodic minimal surfaces. *J. Diff. Geom.*, 79(2):243–275, 2008.
- [Tra10] Martin Traizet. On minimal surfaces bounded by two convex curves in parallel planes. *Comment. Math. Helv.*, 85:39–71, 2010.
- [Tra13] Martin Traizet. Opening infinitely many nodes. *J. Reine Angew. Math.*, 684:165–186, 2013.
- [Web02] Matthias Weber. Period quotient maps of meromorphic 1-forms and minimal surfaces on tori. *J. Geom. Anal.*, 12(2):325–354, 2002.
- [WHW09] Matthias Weber, David Hoffman, and Michael Wolf. An embedded genus-one helicoid. *Ann. of Math. (2)*, 169(2):347–448, 2009.

(Chen) GEORG-AUGUST-UNIVERSITÄT GÖTTINGEN, INSTITUT FÜR NUMERISCHE UND ANGEWANDTE MATHEMATIK

Email address: h.chen@math.uni-goettingen.de

(Traizet) INSTITUT DENIS POISSON, CNRS UMR 7350, FACULTÉ DES SCIENCES ET TECHNIQUES, UNIVERSITÉ DE TOURS

Email address: martin.traizet@lmpt.univ-tours.fr

A NEW DEFORMATION FAMILY OF SCHWARZ' D SURFACE

HAO CHEN AND MATTHIAS WEBER

ABSTRACT. We prove the existence of a new 2-parameter family Δ of embedded triply periodic minimal surfaces of genus 3. The new surfaces share many properties with classical orthorhombic deformations of Schwarz' D surface, but also exotic in many ways. In particular, they do not belong to Meeks' 5-dimensional family. Nevertheless, Δ meets classical deformations in a 1-parameter family on its boundary.

1. INTRODUCTION

This is the first of two papers dealing with new 2-dimensional families of embedded triply periodic minimal surfaces (TPMS) of genus three whose 1-dimensional “intersections” with the well-known Meeks family exhibit singularities in the moduli space of TPMS.

In the past three decades, the classification of complete, embedded minimal surfaces of finite topology in Euclidean space forms has largely been accomplished for the smallest reasonable genus ([MPR98, LHM01, PRT05, MR05, PT07]). In all these cases, the moduli space of these surfaces has been found to be a smooth manifold.

In the case of triply periodic minimal surfaces, no such classification has been found. For the lowest possible genus 3, there is an explicit 5-dimensional smooth family described by Meeks [Mee90] that contains most of the then known examples, with the notable exception of Schwarz' H surfaces and Schoen's Gyroid. Work of Traizet [Tra08] implies that the H-surfaces belong to a second 5-dimensional family for which no explicit description is known. Our other paper will explore that family.

In this paper, we construct a new 2-dimensional family of embedded triply periodic minimal surfaces of genus 3 that does not belong to the Meeks family but whose closure meets the Meeks family in a 1-dimensional subset. More specifically, the surfaces in this subset are *bifurcation instances* in the sense that, with the same deformation of their lattices, they may deform either within a classical 2-parameter Meeks family, or into a new 2-parameter non-Meeks family. Existence of the latter is the focus of this paper.

In fact, all these surfaces can be seen as orthorhombic deformations of Schwarz' D surface. Hence we begin with a description of the classical orthorhombic deformations of D, which all belong to the Meeks family.

Consider an embedded minimal surface S inside an axis parallel box $[-A, A] \times [-B, B] \times [0, 1]$ that solves the following partially free boundary problem: S satisfies free boundary condition on the vertical planes $x = \pm A$ and $y = \pm B$, and fixed (Plateau) boundary condition on the horizontal segments $\{(x, 0, 0) \mid -A \leq x \leq A\}$ and $\{(0, y, 1) \mid -B \leq y \leq B\}$, and the intersection of ∂S with each face of the

Date: July 27, 2020.

2010 *Mathematics Subject Classification.* Primary 53A10.

Key words and phrases. Triply periodic minimal surfaces.

H. Chen is supported by Individual Research Grant from Deutsche Forschungsgemeinschaft within the project “Defects in Triply Periodic Minimal Surfaces”, Projektnummer 398759432.

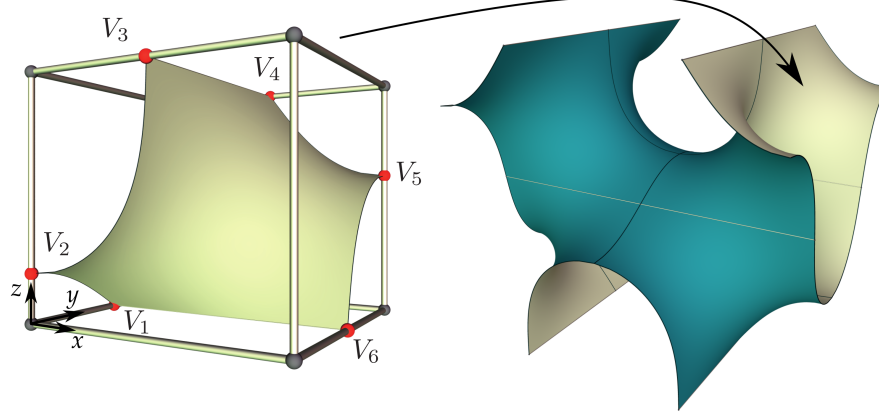


FIGURE 1.1. Fundamental Piece and Translational Fundamental Piece

box has at most one component. S is therefore a right-angled embedded minimal hexagon. See Figure 1.1 (left) for an example.

Because the two horizontal segments are in the middle of the top and bottom faces of the box, rotations about them and reflections in the lateral faces of the box extend S to an embedded TPMS $\tilde{\Sigma}$. More specifically, $\tilde{\Sigma}$ is invariant under the lattice Λ spanned by $(4A, 0, 0)$, $(0, 4B, 0)$ and $(2A, 2B, 2)$. In the 3-torus \mathbb{R}^3/Λ , $\Sigma = \tilde{\Sigma}/\Lambda$ is a compact surface of genus 3. In Figure 1.1 (right) we show a translational fundamental domain of $\tilde{\Sigma}$ nicely presented in a box. It consists of eight copies of S .

Remark 1.1. For crystallographers, the orthorhombic lattice spanned by $(4A, 0, 0)$, $(0, 4B, 0)$ and $(0, 0, 4)$ is probably more convenient. This is responsible for the letter “o” in our naming. The quotient of $\tilde{\Sigma}$ by this lattice is a double cover of Σ , hence of genus 5.

We use \mathcal{D} to denote the set of all TPMS obtained in this way.

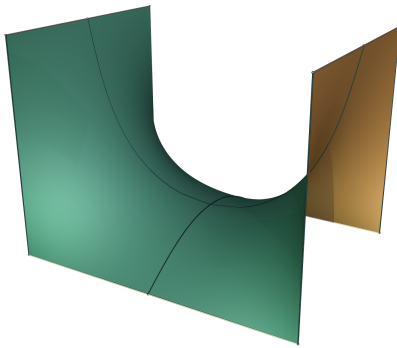


FIGURE 1.2. Plateau construction of oD surfaces

A well-known family of surfaces in \mathcal{D} is the tD family of H. A. Schwarz, which is a tetragonal deformation family of his famous D surface. They are obtained as described above with $A = B$ and S containing the vertical segment $\{(0, 0, z) \mid 0 \leq z \leq 1\}$. The same construction also applies when $A \neq B$, yielding an orthorhombic deformation of Schwarz’ D surface, known as oDb in the literature to distinguish

from another orthorhombic deformation family oDa; see [FK89, FH92]. In this paper, we simply use oD in place of oDb.

An alternative (better known) construction of an oD surface starts with a box of the same dimensions and then solves the Plateau problem for a polygonal contour running along edges of the box, as shown in Figure 1.2. The Plateau solution is unique and therefore shares the symmetries of the contour. In particular, it has reflectional symmetries by vertical planes. To relate with the previous construction, just divide the minimal surface into quarts by cutting along these planes, then extend one of the quarts by rotating it about its vertical edge.

The main result of this paper is to confirm the existence of another 2-parameter family in \mathcal{D} .

Theorem 1.2. *There exists a second 2-parameter continuous family o Δ in \mathcal{D} , lacking the vertical straight line of the oD surfaces.*

The o Δ family, well hidden in the radiance of the famous oD family, is understandably unexpected. The second author confesses his complete bafflement and initial disbelief when the first author provided him with evidence of o Δ . In Figure 1.3 we compare oD and o Δ surfaces with the same lattice (the surfaces in this figure actually have tetragonal lattices, hence belong to tD and t Δ subfamilies that we will discuss in Section 6.)

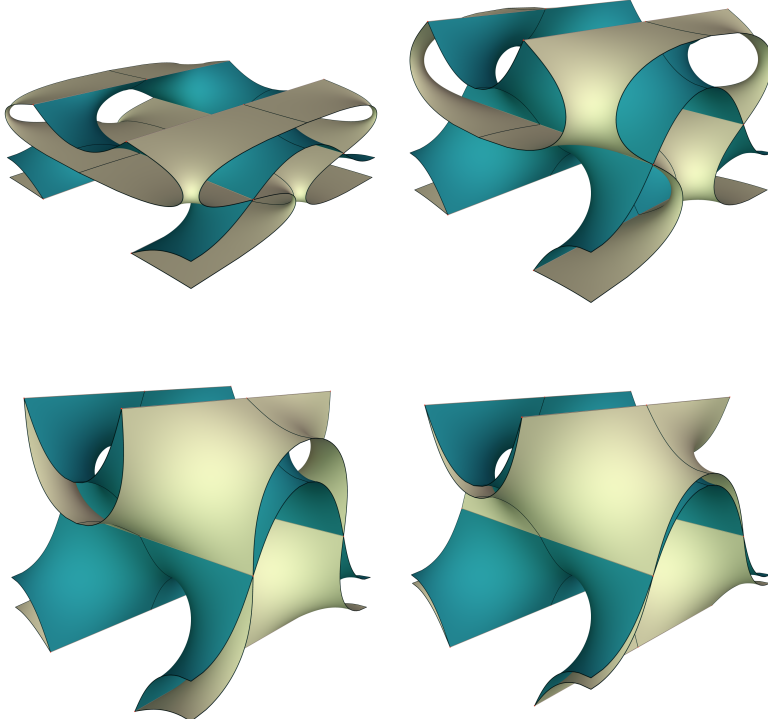


FIGURE 1.3. Comparison of oD (dark) and o Δ (bright) surfaces with the same lattice. These surfaces actually belong to the tD and t Δ subfamily.

The $o\Delta$ family is not merely a surprise. Its significance is revealed in the following proposition.

Proposition 1.3. *The surfaces in $o\Delta$ do not belong to the Meeks family. That is, the branched values of the Gauss map of an $o\Delta$ surface do not form four antipodal pairs. In fact, the only Meeks surfaces in \mathcal{D} are the oD surface. However, the closure $\overline{o\Delta}$ intersects oD in a 1-parameter family of TPMS.*

We now provide some context for the proposition.

For the purpose of this paper, a TPMS is a complete, embedded minimal surface $\tilde{\Sigma}$ in Euclidean space \mathbb{R}^3 invariant under a lattice Λ of Euclidean translations. The quotient $\Sigma = \tilde{\Sigma}/\Lambda$ then is a compact Riemann surface in the 3-torus \mathbb{R}^3/Λ . The lowest possible genus for a non-trivial TPMS is 3. In this case, the Gauss map of Σ has degree 2, and the surface is therefore necessarily hyperelliptic.

The first examples of TMPS were given by H. A. Schwarz [Sch90] around 1867, with explicit Weierstrass data for very symmetric cases. Schwarz understood that the eight branched values of the Gauss map play a crucial role. More generally, W. Meeks III [Mee90] explicitly constructed a family \mathcal{M} of TPMS of genus 3. He showed that if eight points on the sphere come in four antipodal pairs, then they are the branched values of the Gauss map for two conjugate TPMS of genus 3. The Meeks family \mathcal{M} , considered up to congruence and dilation, is a connected, smooth, (real) 5-dimensional manifold, and includes almost all previously known examples.

Famous exceptions are the H surfaces of Schwarz, for which the branched values are placed at the north pole, the south pole, and the vertices of a prism over an equilateral triangle inside the sphere; and the Gyroid of A. Schoen [Sch70], whose Gauss map has the same branched values as those of Schwarz' P and D surfaces, but does not belong to the Meeks family. We use \mathcal{N} to denote the complement of \mathcal{M} in the set of all TPMS of genus 3. Since then, more examples in \mathcal{N} have been found, either as isolated examples or as 1-parameter families, and some of them only numerically [FHL93, FH99, Wey06, Wey08]. Our 2-parameter family $o\Delta$ is therefore an important step towards the understanding of non-Meeks TPMS of genus 3.

Meeks' result is extended into the following rigidity statement: In the neighborhood of a non-degenerate TPMS, there is a bijection between TPMS and lattices in \mathbb{R}^3 ; see [KPS14] for instance. Hence up to congruence and dilation, a non-degenerate TPMS belongs (locally) to a 5-parameter family. Besides that, very little is known about the structure of \mathcal{N} . We would like to conjecture that \mathcal{N} is, like \mathcal{M} , connected and smooth, but none of these is known.

There is evidence [FHL93, FH99, Wey06, Wey08] that \mathcal{M} and the closure $\overline{\mathcal{N}}$ have non-empty intersection. Proposition 1.3 provides the first concrete example of such intersection in the form of a 1-dimensional family of TPMS. This is of considerable importance for stability questions of TPMS.

A TPMS of genus 3 is called a *bifurcation instance* if there are non-congruent deformations (bifurcation branches) of the TPMS with the same deformation of the lattice. Koiso, Piccione and Shoda [KPS14] identified isolated *bifurcation instances* among classical deformations of TPMS; see also [ES14, ES18]. They found bifurcation branches for most of these bifurcation instances. But for three “exotic” bifurcation instances, they only suggested that a bifurcation branch from them would not be a “classical” TPMS.

The intersection $o\Delta \cap oD$ is a 1-parameter family of bifurcation instances. In particular, a 1-parameter subfamily of $o\Delta$, which we call $t\Delta$, has the same tetragonal lattices as the tD family. The intersection $\overline{t\Delta} \cap tD$ contains a single TPMS, denoted by tD^* , which turns out to be one of the exotic bifurcation instances in [KPS14].

We also find a bifurcation branch $t\Pi$ from the conjugate of tD^* , another exotic bifurcation instance in Schwarz' tP family. But $t\Pi$ is not the focus of this paper, since it is nothing but a classical oPa deformation [FK89, FH92].

For sufficiently large A and B , the existence of $o\Delta$ surfaces is implied by results of Traizet [Tra08], who constructed TPMS by opening catenoidal nodes among 2-tori. The positions of the nodes have to satisfy a balance condition, formulated in terms of elliptic functions, and a non-degeneracy condition. The Traizet limit of $o\Delta$ was noted by the first author in an earlier experimental work [Che18]. He used Brakke's Surface Evolver [Bra92] to numerically deform the TPMS from near the Traizet limit up to Schwarz' tD family, and obtained the first images of $t\Delta$. In particular, he observed that $t\Delta$ eventually intersects tD , but Surface Evolver fails to converge near the intersection. This failure can now be explained by numeric bifurcation.

Our paper is organized as follows:

In Section 2, we describe the Weierstrass data for surfaces in \mathcal{D} , prove their embeddedness, and formulate the period problem, depending on three real positive parameters a, b and t . The case $a = b$ corresponds to the oD surfaces, where the period problem is automatically solved. In the case $a \neq b$, the period problem becomes 1-dimensional but is rather complicated.

In Section 3 we show that, if $a \neq b$, the branched values of the Gauss map can *not* be antipodal. This proves that $\mathcal{D} \cap \mathcal{M} = oD$, and that any solution with $a \neq b$ (namely $o\Delta$) lies in \mathcal{N} .

Section 4 is dedicated to the existence proof of $o\Delta$. We show that for any choice of $a \neq b$, there is a value of t that solves the period problem. This is accomplished through a careful asymptotic analysis of the period integrals. We also conjecture the uniqueness of t based on numerical experiments.

To prove that $oD \subset \mathcal{M}$ and the closure of $o\Delta \subset \mathcal{N}$ have a non-empty intersection, we consider in Section 5 a modified period problem that eliminates the trivial solutions coming from oD . It turns out that this period problem can be solved explicitly in terms of elliptic integrals.

In section 6 we consider the surfaces with tetragonal lattices. They are \mathcal{D} surfaces whose parameters satisfy $ab = t$. In this case, we obtain two 1-parameter families of surfaces: $tD \subset oD$ containing Schwarz' D surface, and $t\Delta \subset o\Delta$. The intersection $t\Delta \cap tD$ contains a single TPMS tD^* . As the existence of $t\Delta$ does not follow from Section 4, we give an independent proof for this case using an extremal length argument.

Acknowledgements. The first author thanks his newborn daughter for keeping him awake through the nights, which helped noticing the $t\Delta$ family.

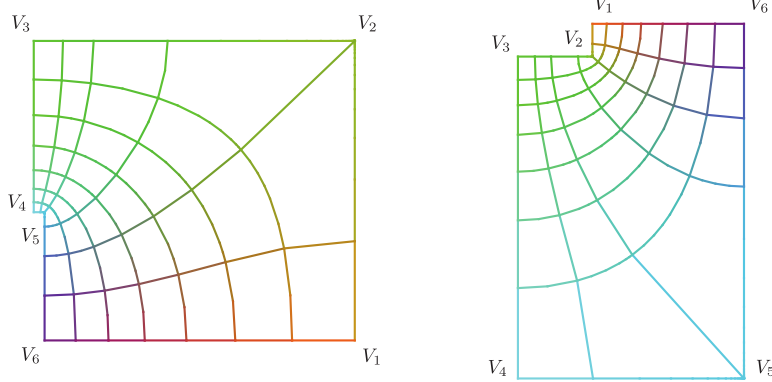
The second author thanks his teenage daughter for keeping him sleepless as well, thus providing time to work on this paper.

We are grateful to the anonymous referee for suggestions and corrections after carefully reading a previous version of the manuscript.

2. WEIERSTRASS DATA AND PERIOD PROBLEM

We parameterise a surface in \mathcal{D} with a Weierstrass representation defined on the upper half plane such that the real axis is mapped to the boundary of the hexagon S . Let the vertices of S be labeled by V_1, V_2, \dots, V_6 as in Figure 1.1 (left). Denote the preimage of V_k by $v_k \in \mathbb{R}$, and assume that $v_1 < v_2 < \dots < v_6$.

Given a \mathcal{D} surface, denote by dh its height differential and by G its Gauss map. Let $\phi_1 := dh \cdot G$ and $\phi_2 := dh/G$. The assumed boundary symmetries of the surface imply that $\Phi_j : z \mapsto \int^z \phi_j$ ($j = 1$ or 2) map the upper half plane to “right angled”

FIGURE 2.1. Images of a fundamental piece under Φ_1 and Φ_2 .

Euclidean hexagons. The interior angle is 270° at $\Phi_1(v_5)$ and $\Phi_2(v_2)$. Indeed, the Gauss map is vertical at V_2 and V_5 , hence v_2 and v_5 are respectively the pole and the zero of G . Interior angles at all other vertices are 90° ; see Figure 2.1.

Such maps are given by Schwarz-Christoffel maps. More specifically, we have

$$\begin{aligned}\phi_1 &:= \rho(z - v_1)^{-1/2}(z - v_2)^{-1/2}(z - v_3)^{-1/2}(z - v_4)^{-1/2}(z - v_5)^{+1/2}(z - v_6)^{-1/2} dz, \\ \phi_2 &:= -\frac{1}{\rho}(z - v_1)^{-1/2}(z - v_2)^{+1/2}(z - v_3)^{-1/2}(z - v_4)^{-1/2}(z - v_5)^{-1/2}(z - v_6)^{-1/2} dz, \\ dh &:= -i(z - v_1)^{-1/2} \times (z - v_3)^{-1/2}(z - v_4)^{-1/2} \times (z - v_6)^{-1/2} dz.\end{aligned}$$

Here, the real positive Lopéz-Ros factor ρ determines scaling of the image domains. The Gauss map is $G := i\rho(z - v_2)^{-1/2}(z - v_5)^{+1/2}$.

Proposition 2.1. *Up to congruence and dilation, the image of the upper half plane under the map*

$$(2.1) \quad z \mapsto \operatorname{Re} \int^z (\omega_1, \omega_2, \omega_3) = \operatorname{Re} \int^z \left(\frac{1}{2}(\phi_2 - \phi_1), \frac{i}{2}(\phi_2 + \phi_1), dh \right)$$

is almost the fundamental hexagon of a \mathcal{D} surface in the following sense: The intervals v_1v_2 , v_2v_3 , v_4v_5 and v_5v_6 are mapped to planar symmetry curves in the lateral faces of an axis parallel box. The intervals v_6v_1 and v_3v_4 are mapped, respectively, to straight segments parallel to the x and y axis, but not necessarily in the middle, in the bottom and top faces of the box.

Proof. Note that the integrand in ϕ_1 (resp. ϕ_2) is real positive (resp. negative) for $z > v_6$. This implies that the image of the segment v_6v_1 under the Schwarz-Christoffel map Φ_1 (resp. Φ_2) is horizontal rightward (resp. leftward), as in Figure 2.1.

The Schwarz-Christoffel maps Φ_j and $z \mapsto \int^z dh$ can be continued by reflection across any edge to the lower half plane, inducing symmetries of the minimal surface. We now determine what kind of symmetry is induced on each edge.

For that, we only carry out a detailed analysis on the edge v_6v_1 . The integrands in both ϕ_j are real on v_6v_1 , hence their continuations across this edge are given by $\overline{\phi_j(\bar{z})}$. Meanwhile, the integrand in dh is imaginary on v_6v_1 , so its continuation is given by $-dh(\bar{z})$. Therefore, after crossing v_6v_1 , $\operatorname{Re} \omega_1$ remains unchanged while $\operatorname{Re} \omega_2$ and $\operatorname{Re} \omega_3$ change sign. This means that the surface is extended by a rotation about a straight line parallel to the x -axis.

Similar analysis on the other edges then prove that the image of the upper half plane under (2.1) has the claimed boundary curves. Note that the surface obtained

is free of singularities. Indeed, the metric is regular away from v_k , and the exponents at v_k guarantee a smooth extension. \square

We now study the condition for the two horizontal segments to lie in the middle of the top and the bottom faces of the box. To this end, we introduce notations for the edge lengths of the Euclidean hexagons

$$I_k := \left| \int_{v_k}^{v_{k+1}} \phi_1 \right|, \quad J_k := \left| \int_{v_k}^{v_{k+1}} \phi_2 \right|$$

for $1 \leq k \leq 5$. These are positive real numbers that depend analytically on the parameters v_1, \dots, v_6 and ρ .

Proposition 2.2. *The image of the upper half plane under the Weierstrass representation (2.1) is the fundamental hexagon of a surface in \mathcal{D} if and only if the following period conditions are satisfied:*

$$(2.2) \quad \begin{aligned} I_1 + I_5 &= J_1 + J_5 \\ I_2 + I_4 &= J_2 + J_4 \end{aligned}$$

Proof. The bottom segment V_6V_1 lies in the middle of the bottom face if and only if

$$\operatorname{Re} \int_{v_1}^{v_2} \omega_2 = \operatorname{Re} \int_{v_5}^{v_6} \omega_2 .$$

This is equivalent to

$$\operatorname{Im} \int_{v_1}^{v_2} (\phi_2 + \phi_1) = \operatorname{Im} \int_{v_5}^{v_6} (\phi_2 + \phi_1) .$$

Observe on v_1v_2 that the integrand in ϕ_1 (resp. ϕ_2) is positive (resp. negative) imaginary, and on v_5v_6 that the integrand in ϕ_1 (resp. ϕ_2) is negative (resp. positive) imaginary. So the equation above can be written as

$$I_1 - J_1 = J_5 - I_5,$$

which proves the first period condition. The second follows analogously. \square

We can eliminate ρ by taking the quotient of the two equations, therefore:

Corollary 2.3. *If*

$$Q_I := \frac{I_1 + I_5}{I_2 + I_4} = \frac{J_1 + J_5}{J_2 + J_4} =: Q_J$$

or, equivalently, if

$$(2.3) \quad Q := Q_I - Q_J = \frac{I_1 + I_5}{I_2 + I_4} - \frac{J_1 + J_5}{J_2 + J_4} = 0$$

for some choice of v_1, \dots, v_6 , then $\rho \in \mathbb{R}_{>0}$ can be uniquely adjusted so that the period conditions (2.2) are satisfied.

Thus we have expressed the period condition as a single equation $Q = 0$, where Q depends on six parameters v_1, \dots, v_6 . The number of parameters can be reduced to three after a normalization by Möbius transformations. More specifically, we can assume

$$v_1 = -t, v_2 = -a, v_3 = -1, v_4 = 1, v_5 = b, v_6 = t$$

with $-t < -a < -1 < 1 < b < t$. We also assume that $a \leq b$. If it is not the case, we may simply switch a and b ; this only exchanges I_k and J_{6-k} , $1 \leq k \leq 5$, up to the scaling ρ , hence leaves Q invariant.

We note two special cases.

If $a = b$, the period conditions (2.2) are satisfied automatically with $\rho = 1$. In this case, the involution $z \mapsto -\bar{z}$ induces an order-2 rotation of the surface about a

vertical axis. This can be seen by noting that ω_1 and ω_2 change sign but ω_3 keeps sign under this involution. Indeed, on the imaginary axis (fixed by the involution), ϕ_1 and ϕ_2 are conjugate and dh is real. Hence the positive imaginary axis is mapped by the Weierstrass representation (2.1) to the vertical straight segment between the middle points of V_3V_4 and of V_6V_1 , which serves as the axis of the order-2 rotation. This shows that the surface is in oD.

If $ab = t$, we will see in Section 6 that the period conditions are satisfied with $Q_I = Q_J = 1$ and $\rho^4 = a/b$. In this case, the involution $\iota : z \mapsto -t/z$ induces an order-2 orientation-preserving rotation of the surface around a horizontal axis, because

$$\iota^* dh = -dh \quad \text{and} \quad G(\iota(z))G(z) = i.$$

This rotation exchanges V_k with V_{k+3} , $1 \leq k \leq 3$. In particular, the segments V_6V_1 and V_3V_4 must have the same length, implying that the bounding box has a square base. The unique fixed point of the involution, namely $i\sqrt{t}$, is mapped to the fixed point of the rotation. We will consider this case in detail in Section 6.

Proposition 2.4. *The minimal hexagons S in \mathcal{D} are embedded. Consequently, the triply periodic minimal surfaces generated by extending across symmetry lines are embedded as well.*

Proof. Denote the projection onto the xz -plane by ϖ , and let $V'_i = \varpi(V_i)$. We will prove (refering to Figure 1.1 (left)):

- (1) The boundary of S is a graph over a simple curve γ in the xz -plane, except for the straight segment V_3V_4 which is parallel to the y -axis. Thus γ bounds a simply connected (open) domain Ω .

To see this, note that the Gauss map $G := i\rho(z - v_2)^{-1/2}(z - v_5)^{+1/2}$ is horizontal (i.e. perpendicular to the y -direction) along the segments $V_2V_3V_4V_5$ and strictly monotone. This implies that the arcs $V'_2V'_3$ and $V'_4V'_5$ of γ are simple, disjoint, and lie in the rectangle $[-A, A] \times [0, 1]$. The remaining segments $V'_5V'_6$, $V'_6V'_1$ and $V'_1V'_2$ are straight segments on the boundary of that rectangle.

- (2) The projection $\varpi(S)$ lies within $\bar{\Omega}$.

To see this, assume the opposite. Take a boundary point of $\varpi(S)$ that does not lie in $\bar{\Omega}$. By (the contraposition of) the Implicit Function Theorem, its preimage on the S has a horizontal normal (parallel to the xz -plane). By the formula for the Gauss map, the only points with horizontal normal occur on the boundary of S , a contradiction.

- (3) The projection ϖ restricted to the interior of S has the unique path and homotopy lifting properties.

To see this, we again use that the interior of S has no point with horizontal normal. The claim follows from the Implicit Function Theorem, applied in the compact region where the curve (or homotopy) resides.

Then it follows that the interior of S is a graph over Ω : Otherwise, take a curve on S that connects two distinct points in $\varpi^{-1}(p)$, $p \in \Omega$. Its projection onto Ω is closed in Ω and can be retracted onto p within a compact subset of Ω . By the unique homotopy lifting property, the endpoints of the lifted curves stay the same, contradicting the assumption that they are two distinct points in $\varpi^{-1}(p)$. \square

3. BRANCHED VALUES OF THE GAUSS MAP

To locate the branched points of the Gauss map, we use the following simple observation:

Lemma 3.1. *At every orthogonal intersection of a planar symmetry curve and a straight line on a minimal surface, the Gauss map has a branched point.*

Proof. At points on the straight line that are symmetric with respect to the symmetry plane, the Gauss map takes the same value. Hence it cannot be single valued in a neighborhood of the intersection point. \square

We now show

Theorem 3.2. *The branched values of the Gauss map of a surface in \mathcal{D} are antipodal if and only if $a = b$.*

Proof. By the Lemma, the Gauss map has branched points at V_1 , V_3 , V_4 and V_6 . On a translational fundamental domain, each of these points occurs twice, giving eight branched points as expected.

Recall that the stereographically projected Gauss map is given by

$$G(z) = i\rho(z+a)^{-1/2}(z-b)^{+1/2}.$$

We then compute the branched values explicitly as

$$\begin{aligned}\pm G(+1) &= \mp\rho\sqrt{\frac{b-1}{a+1}}, & \pm G(-1) &= \mp\rho\sqrt{\frac{b+1}{a-1}}, \\ \pm G(+t) &= \pm i\rho\sqrt{\frac{t-b}{t+a}}, & \pm G(-t) &= \pm i\rho\sqrt{\frac{t+b}{t-a}}.\end{aligned}$$

Recall that $-t < -a < -1 < 1 < b < t$, so the expressions under the square roots are all positive real. We then see that they lie on the real and imaginary axis, respectively, which helps matching them in possible antipodal pairs. Recall that, after stereographic projection, the antipodal point of z is $-1/\bar{z}$.

Assume that the branched values do occur in antipodal pairs and, for the sake of contradiction, that $a \neq b$. First note that $G(+1)$ and $-G(+1)$ cannot be antipodal. Otherwise, $G(-1)$ and $-G(-1)$ must also be antipodal. Then they must have the same norm, i.e. $\frac{b-1}{a+1} = \frac{b+1}{a-1}$, forcing $a+b=0$ which violates our assumption. Thus the only possibility is that $\pm G(-1)$ and $\pm G(+1)$ are antipodal, with two possible choices of signs. Either choice implies that

$$\rho^4 = \frac{a^2 - 1}{b^2 - 1}.$$

The same analysis on $\pm G(\pm t)$ leads to

$$\rho^4 = \frac{t^2 - a^2}{t^2 - b^2}.$$

Combining the two equations for ρ^4 shows, after a brief computation, that either $t = 1$ or $a = b$. The contradiction with our assumptions proves the “only if”.

For the “if” part, assume that $a = b$. Then we find the branched points become antipodal (only) with $\rho = 1$. More specifically, we have

$$\begin{aligned}\pm G(+1) &= \mp\sqrt{\frac{a-1}{a+1}}, & \pm G(-1) &= \mp\sqrt{\frac{a+1}{a-1}}, \\ \pm G(+t) &= \pm i\sqrt{\frac{t-a}{t+a}}, & \pm G(-t) &= \pm i\sqrt{\frac{t+a}{t-a}}.\end{aligned}$$

Geometrically, these points on the unit sphere are vertices of two axis parallel rectangles in the planes $x = 0$ and $y = 0$, respectively. Remarkably, an image of two such rectangles already appears in Figure 44 of the *Nachtrag* of Schwarz’ paper “Bestimmung einer speciellen Minimalfläche” from 1867. \square

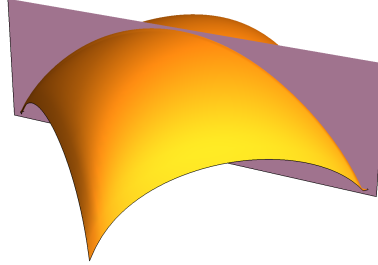


FIGURE 4.1. Numerical plot of the solution set of $Q(a, b; t) = 0$. The vertical plane in gray is the set of trivial solutions with $a = b$ corresponding to the $\text{o}D$ surfaces. The other surface is the set of non-trivial solutions corresponding to the $\text{o}\Delta$ surfaces.

We note that in the case $a = b$ the branched values lie at the vertices of a cube if and only if $a^2 = b^2 = t = 3$. This is the case of the classical D surface of Schwarz.

4. EXISTENCE OF NON-TRIVIAL SOLUTIONS

Recall that $1 < a \leq b < t$, and the periodic condition (2.3) as we copy below

$$Q(a, b; t) = \frac{I_1 + I_5}{I_2 + I_4} - \frac{J_1 + J_5}{J_2 + J_4} = 0.$$

The quantity Q is our focus in the remaining of this paper. From now on, we will ignore the Lopéz-Ros factor ρ in our calculations, since Q is independent of this factor.

We now prove the main theorem of this paper.

Theorem 4.1. *If $a = b$, the period condition (2.3) is solved for any choice of t . If $a < b$, then there exists a value of t that solves the period condition (2.3).*

The solution set of $Q(a, b; t) = 0$ is numerically plotted in Figure 4.1. The case $a = b$, shown here as a vertical plane in gray, has been discussed in Section 2. The case $a < b$, as well as our main theorem, follows from the continuity of Q in t , and the following proposition.

Proposition 4.2. *If $1 < a < b < t$ then*

$$(4.1) \quad \lim_{t \rightarrow b+} Q(a, b; t) > 0,$$

$$(4.2) \quad \lim_{t \rightarrow +\infty} Q(a, b; t) = -\infty.$$

The remainder of this section is devoted to the proof of this proposition.

We begin by analyzing the limit $t \rightarrow b+$.

Proof of (4.1). We can evaluate the period integrals explicitly. Recall that, if $p < q$, we have

$$\int_p^q \sqrt{\frac{1}{(q-z)(z-p)}} dz = \pi, \quad \int_p^q \sqrt{\frac{z-p}{q-z}} dz = \frac{q-p}{2}\pi.$$

By the Mean Value Theorem for integrals, we have

$$\lim_{t \rightarrow b+} I_1(a, b; t) = \lim_{t \rightarrow b+} \int_{-t}^{-a} \frac{1}{\sqrt{(t^2 - z^2)(z^2 - 1)}} \sqrt{\frac{b-z}{-a-z}} dz = C \int_a^b \sqrt{\frac{1}{(b-z)(z-a)}} dz,$$

where $C = 1/\sqrt{c^2 - 1}$ for some $c \in [a, t]$. So this limit is finite and non-zero. Similarly,

$$\begin{aligned} \lim_{t \rightarrow b+} I_2(a, b; t) &= C \int_1^a \sqrt{\frac{1}{(a-z)(z-1)}} dz, \\ \lim_{t \rightarrow b+} J_1(a, b; t) &= C \int_a^b \sqrt{\frac{z-a}{b-z}} dz, \quad \lim_{t \rightarrow b+} J_2(a, b; t) = C \int_1^a \sqrt{\frac{z-1}{a-z}} dz, \\ \lim_{t \rightarrow b+} I_4(a, b; t) &= C \int_1^b \sqrt{\frac{1}{z-1}} dz, \quad \lim_{t \rightarrow b+} J_5(a, b; t) = C \lim_{t \rightarrow b+} \int_b^t \sqrt{\frac{1}{(t-z)(z-b)}} dz \end{aligned}$$

are all finite and non-zero. Here C denote any finite positive number. On the other hand,

$$\lim_{t \rightarrow b+} I_5(a, b; t) = C \lim_{t \rightarrow b+} \int_b^t \sqrt{\frac{z-b}{t-z}} dz = 0$$

and

$$\lim_{t \rightarrow b+} J_4(a, b; t) \geq C \lim_{t \rightarrow b+} \int_1^b \sqrt{\frac{1}{(t-z)(b-z)}} dz$$

diverges to infinity. Consequently, as $t \rightarrow b+$, $Q_I = (I_1 + I_5)/(I_2 + I_4)$ has a finite and non-zero limit, while $Q_J = (J_1 + J_5)/(J_2 + J_4) \rightarrow 0$, hence $\lim_{t \rightarrow b+} Q > 0$. \square

Now we turn to the limit $t \rightarrow \infty$, which is more amusing.

Proof of (4.2). For the periods in the denominators, we note that

$$\begin{aligned} \lim_{t \rightarrow \infty} t \cdot I_2(a, b; t) &= \int_{-a}^{-1} \sqrt{\frac{1}{z^2 - 1}} \sqrt{\frac{b-z}{a+z}} dz, \\ \lim_{t \rightarrow \infty} t \cdot J_2(a, b; t) &= \int_{-a}^{-1} \sqrt{\frac{1}{z^2 - 1}} \sqrt{\frac{a+z}{b-z}} dz, \\ \lim_{t \rightarrow \infty} t \cdot I_4(a, b; t) &= \int_1^b \sqrt{\frac{1}{z^2 - 1}} \sqrt{\frac{b-z}{a+z}} dz, \\ \lim_{t \rightarrow \infty} t \cdot J_4(a, b; t) &= \int_1^b \sqrt{\frac{1}{z^2 - 1}} \sqrt{\frac{a+z}{b-z}} dz \end{aligned}$$

are all finite. We now show that

$$(4.3) \quad \lim_{t \rightarrow \infty} t \cdot (I_2 + I_4) > \lim_{t \rightarrow \infty} t \cdot (J_2 + J_4),$$

or equivalently,

$$\lim_{t \rightarrow \infty} t \cdot (I_2 - J_2) > \lim_{t \rightarrow \infty} t \cdot (J_4 - I_4).$$

We prove this by considering the functions

$$\begin{aligned} f(a, b) &= \lim_{t \rightarrow \infty} t \cdot (I_2 - J_2) = \int_1^a \frac{2z-a+b}{\sqrt{(z^2-1)(a-z)(b+z)}} dz, \\ g(a, b) &= \lim_{t \rightarrow \infty} t \cdot (J_4 - I_4) = \int_1^b \frac{2z+a-b}{\sqrt{(z^2-1)(a+z)(b-z)}} dz, \end{aligned}$$

and show that $f(a, b) > g(a, b)$ for all $1 < a < b$. Note that $f(a, b) = g(b, a)$. Since

$$\frac{\partial}{\partial b} f(a, b) = \int_1^a \frac{a+b}{\sqrt{(z^2-1)(a-z)(b+z)^3}} dz > 0,$$

f is monotone increasing in its second argument for $1 < a < b$. Then g is monotone increasing in its first argument. Note also that $f(a, a) = \pi$ is a constant. Hence

$$f(a, b) > f(a, a) = f(b, b) = g(b, b) > g(a, b),$$

which finishes the proof of (4.3).

The periods in the numerators are more delicate to deal with, as they have logarithmic asymptotics. For instance,

$$\begin{aligned}
 t \cdot J_5(a, b; t) &= \int_b^t \frac{t}{\sqrt{t^2 - z^2}} \sqrt{\frac{z+a}{z-b}} \sqrt{\frac{1}{z^2-1}} dz \\
 &> \int_b^t \frac{t}{\sqrt{t^2 - z^2}} \frac{1}{z} dz \\
 (4.4) \quad &= \log \frac{\sqrt{t^2 - b^2} + t}{b},
 \end{aligned}$$

hence $t \cdot J_5(a, b; t)$ diverges to $+\infty$ as $t \rightarrow \infty$.

Fortunately, the integrals I_1 and J_1 (and I_5 and J_5) have the same logarithmic singularities. By the dominated convergence theorem, we obtain the following estimates:

$$\begin{aligned}
 \lim_{t \rightarrow \infty} t \cdot (I_1 - J_1) &= \lim_{t \rightarrow \infty} \int_{-t}^{-a} \frac{t(a+b)}{\sqrt{(t^2-z^2)(z^2-1)(b-z)(-a-z)}} dz \\
 &= \int_{-\infty}^{-a} \frac{a+b}{\sqrt{z^2-1}\sqrt{b-z}\sqrt{-a-z}} dz, \\
 (4.5) \quad \lim_{t \rightarrow \infty} t \cdot (I_5 - J_5) &= \lim_{t \rightarrow \infty} \int_b^t \frac{-t(a+b)}{\sqrt{t^2-z^2}\sqrt{z^2-1}\sqrt{z-b}\sqrt{z+a}} dz \\
 &= \int_b^{\infty} \frac{-a-b}{\sqrt{z^2-1}\sqrt{z-b}\sqrt{z+a}} dz.
 \end{aligned}$$

Note that they are finite and non-zero.

Finally, we write

$$Q(a, b; t) = \frac{t(I_1 - J_1) + t(I_5 - J_5)}{tI_2 + tI_4} + t(J_1 + J_5) \left[\frac{1}{tI_2 + tI_4} - \frac{1}{tJ_2 + tJ_4} \right].$$

The part in the square bracket is negative by (4.3). As $t \rightarrow \infty$, the first fraction is bounded by (4.5), and $J_5 \rightarrow +\infty$. This then concludes the proof of the proposition. \square

Before ending this section, we propose the following uniqueness conjecture based on numeric experiments:

Conjecture 4.3. *If $a < b$, then there exists a unique t that solves the period condition (2.3).*

5. INTERSECTION WITH THE MEEKS-LOCUS

By definition, the two families $\text{oD} \subset \mathcal{M}$ and $\text{o}\bar{\Delta} \subset \mathcal{N}$ are disjoint in \mathcal{D} . However, we will show in this section that the closure $\text{o}\bar{\Delta}$ intersects oD , and give an explicit description of the intersection in terms of elliptic integrals. This result is not strictly needed for this paper, but gives insight into the nature of the bifurcation locus.

To make this precise, we use on \mathcal{D} the topology induced by the space of possible Weierstrass data, which are determined by the four real parameters a, b, t and ρ . Clearly, the convergence of Weierstrass data implies the locally uniform convergence of the minimal surfaces.

The goal is to determine the intersection of the Meeks locus

$$\text{oD} = \{(a, b, t) : Q(a, b; t) = 0, a = b, -t < -a < -1 < 1 < b < t\}$$

with the closure of the non-Meeks locus

$$\text{o}\bar{\Delta} = \{(a, b, t) : Q(a, b; t) = 0, a \neq b, -t < -a < -1 < 1 < b < t\}.$$

The idea is to divide the function $Q(a, b; t)$ by $b - a$ and take the limit for $a \rightarrow b$ to eliminate solutions in the Meeks locus. We claim:

Theorem 5.1. *The intersection $\overline{o\Delta} \cap oD$ is described by the equation*

$$(5.1) \quad \bar{K}(m_1)E(m_2) + \bar{E}(m_1)K(m_2) = \bar{K}(m_1)K(m_2),$$

where

$$\begin{aligned} K(m) &= \int_0^{\pi/2} \frac{1}{\sqrt{1 - m \sin^2(\theta)}} d\theta, \\ E(m) &= \int_0^{\pi/2} \sqrt{1 - m \sin^2(\theta)} d\theta \end{aligned}$$

are complete elliptic integrals of the first and the second kind, $\bar{K}(m) = K(1 - m)$ and $\bar{E}(m) = E(1 - m)$ are the associated elliptic integrals, and the moduli

$$m_1 = \frac{a^2 - 1}{t^2 - 1}, \quad m_2 = \frac{t^2}{a^2} \frac{a^2 - 1}{t^2 - 1}.$$

Note that $0 < m_1 < m_2 < 1$.

Remark 5.2. It is interesting to notice the similarity of (5.1) with the Legendre relation $\bar{K}(m)E(m) + \bar{E}(m)K(m) - \bar{K}(m)K(m) = \pi/2$.

Before we sketch the technical proof, we note that the function Q can be extended to a holomorphic function of its arguments a, b and t for a near b . To see this, note that the integrand of each of the integrals I_k and J_k used in the definition of Q can be adjusted by multiplication with a constant factor e^{it} so that the absolute values are not necessary. The square roots of the integrands cause a potential multivaluedness when the roots $-t, -a, b$ and t are close to each other, which is not the case for a near b . As $Q(a, a, t) = 0$, this implies that also \tilde{Q} extends to a holomorphic function of its arguments. In particular, the extension of \tilde{Q} for real arguments is real analytic.

The theorem follows from the following proposition:

Proposition 5.3. *The function*

$$\tilde{Q}(a, b; t) = \frac{1}{b - a} Q(a, b; t)$$

extends analytically to $a = b$ by

$$\tilde{Q}(a, a; t) = \frac{a(t^2 - 1)}{(a^2 - 1)(t^2 - a^2)} \frac{\bar{K}(m_1)K(m_2) - \bar{K}(m_1)E(m_2) - \bar{E}(m_1)K(m_2)}{K(m_2)^2}.$$

Remark 5.4. Technical details in the following proof are omitted. The integrals we need can all be evaluated in terms of the complete elliptic integrals of the first and the second kind. Integral tables in [BF71] have been very helpful for this purpose, especially after a well-known computer algebra system failed us here.

Proof. With the help of the integral tables in [BF71], we obtain the following explicit evaluation of the periods.

$$\begin{aligned} (I_1 + I_5)(a, a; t) &= (J_1 + J_5)(a, a; t) = \frac{2\bar{K}(m_1)}{\sqrt{t^2 - 1}}, \\ (I_2 + I_4)(a, a; t) &= (J_2 + J_4)(a, a; t) = \frac{2K(m_2)}{\sqrt{t^2 - 1}}. \end{aligned}$$

Then we evaluate the derivatives

$$I'_k(a, a; t) = \frac{\partial}{\partial b} \Big|_{a=b} I_k(a, b, t), \quad J'_k(a, a; t) = \frac{\partial}{\partial b} \Big|_{a=b} J_k(a, b, t),$$

and obtain

$$\begin{aligned} (I'_2 + I'_4)(a, a; t) &= \frac{K(m_2)}{a\sqrt{t^2 - 1}}, & (I'_1 + I'_5)(a, a; t) &= 0, \\ (J'_1 + J'_5)(a, a; t) &= \frac{2a\bar{K}(m_1)}{\sqrt{t^2 - 1}(t^2 - a^2)} - \frac{2a\bar{E}(m_1)\sqrt{t^2 - 1}}{(a^2 - 1)(t^2 - a^2)}, \\ (J'_2 + J'_4)(a, a; t) &= \frac{K(m_2)}{a\sqrt{t^2 - 1}} - \frac{2aK(m_2)}{\sqrt{t^2 - 1}(a^2 - 1)} + \frac{2aE(m_2)\sqrt{t^2 - 1}}{(a^2 - 1)(t^2 - a^2)}. \end{aligned}$$

Finally, by L'Hôpital,

$$\begin{aligned} (5.2) \quad \lim_{a \rightarrow b} \frac{1}{b - a} Q(a, b; t) &= \frac{\partial Q}{\partial b} \Big|_{a=b} \\ &= \frac{a(t^2 - 1)}{(a^2 - 1)(t^2 - a^2)} \frac{\bar{K}(m_1)K(m_2) - \bar{K}(m_1)E(m_2) - \bar{E}(m_1)K(m_2)}{K(m_2)^2}. \end{aligned}$$

□

6. THE TETRAGONAL CASE

We denote by \mathcal{T} surfaces in \mathcal{D} with tetragonal lattice. That is, their unit cells are prisms over squares. We have seen that this occurs when $ab = t$. Again, we have the classical family $tD = oD \cap \mathcal{T}$ when $a = b = \sqrt{t}$. The final specialization arises when $t = 3$. In this case, all diagonals and midpoint bisectors of the embedded minimal hexagon are straight lines, and we have the classical D surface.

In this section we will show that $t\Delta = o\Delta \cap \mathcal{T}$ is non-empty and, in fact, contains a 1-parameter family of surfaces meeting tD on its boundary. More specifically, these surfaces are characterized by $ab = t$, hence they all admit a conformal involution, that exchanges V_k with V_{k+3} , $1 \leq k \leq 3$.

Lemma 6.1. *When $ab = t$, the period condition is solved if and only if $I_1 + I_5 = I_2 + I_4$, in which case $\rho^4 = a/b$.*

Proof. The assumption $t = ab$ implies that

$$I_k = \rho^2 \sqrt{\frac{b}{a}} J_{k+3}, \quad \text{and} \quad J_k = \frac{1}{\rho^2} \sqrt{\frac{a}{b}} I_{k+3}$$

for $k = 1, 2, 3$. Therefore

$$Q_I = \frac{I_1 + I_5}{I_2 + I_4} = \frac{J_2 + J_4}{J_1 + J_5} = Q_J^{-1}.$$

Hence $Q = Q_I - Q_J = 0$ implies that $Q_I = 1$. □

We use this lemma to construct right angled hexagons that solve the period problem.

Begin with an axis parallel rectangle R of size $1 \times A$, where $1 < A < 2$ is the height; see Figure 6.1. Draw a line from the top left vertex of R in the 45° south-east direction. Choose a point p on this line in the lower half of R (possible because $A < 2$), and use it as the bottom right vertex of a smaller rectangle R' with the same symmetries. Cut the rectangular annulus between R and R' into four along the symmetry lines. The top right component is a right angled hexagon that solves the period problem.

Its conformal type, however, is still too general. It needs to have a holomorphic involution permuting the edges.

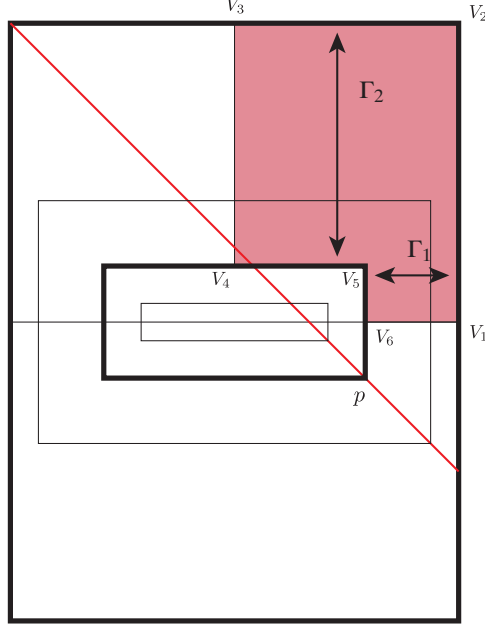


FIGURE 6.1. Existence Proof for $t\Delta$

Theorem 6.2. *For any choice of $1 < A < 2$, there is a choice of p so that the hexagon has a conformal involution.*

Proof. The proof uses an extremal length argument.

Consider the curve families Γ_1 and Γ_2 connecting edges as in Figure 6.1. These families are obtained from each other by the topological order 2 rotation. So in a conformally correct hexagon, they need to have the same extremal length.

Vice versa, we claim that if $\text{ext}\Gamma_1 = \text{ext}\Gamma_2$ then the hexagon has a conformal involution. To see this, we map the hexagon to the upper half plane by the inverse of the Schwarz-Christoffel map $z \mapsto \int^z \phi_1$. The hexagon vertices V_i are mapped to real numbers v_i , and the curve family Γ_1 is mapped to the curves family connecting the edge v_1v_2 with the edge v_5v_6 . Therefore its extremal length is that of the conformal rectangle $v_1v_2v_5v_6$, and thus determines the cross ratio of these four points. Similarly, the extremal length of Γ_2 determines the cross ratio of the four points $v_2v_3v_4v_5$. If we normalize the v_i as before, the equality of these cross ratios

$$\frac{(a+t)(b+t)}{2t(a+b)} = \frac{(a+1)(b+1)}{2(a+b)}$$

implies that $ab = t$, so the hexagon has indeed a conformal involution.

Thus we have to show that we can adjust the position of p so that the two extremal lengths are equal. Note that moving p to the left will pinch the vertical edge V_5V_6 , while moving p to the right will pinch the horizontal edge V_6V_1 . This shows that the extremal length of Γ_1 will vary between infinity and 0. On the other hand, during this variation, the extremal length of Γ_2 stays bounded away from 0 and infinity. Hence there must be a p for which $\text{ext}\Gamma_1 = \text{ext}\Gamma_2$. \square

Note that the tD family corresponds to the case when both rectangles degenerate to squares.

Remark 6.3. In the tetratonical case $ab = t$, the substitution $\zeta = z - t/z$ allows us to express the I_k 's in terms of the complete elliptic integral $K(\mu)$ with complex modulus

$$\mu = \frac{(1+a)(1-b)}{2} \frac{(\sqrt{t}-i)^2}{(t-1)} \frac{1}{(\sqrt{a}+i\sqrt{b})^2}.$$

Then the period condition in Lemma 6.1 is equivalent to

$$\cot \left(\arg \frac{K(\mu) + iK'(\mu)}{\sqrt{b} - i\sqrt{a}} \right) = \frac{\sqrt{b} - \sqrt{a}}{\sqrt{b} + \sqrt{a}}.$$

The intersection with tD can be determined explicitly using the equation from Section 5. Note that for $a = b = \sqrt{t}$, we have

$$m = m_2 = 1 - m_1 = \frac{a^2}{1 + a^2}.$$

Simplifying (5.1) shows that the intersection occurs when

$$2E(m) = K(m).$$

This is solved numerically with $a = a^* \approx 2.17966$. We use tD^* to denote the surface with parameters $a = b = \sqrt{t} = a^*$. In Figure 6.2 we compare Schwarz' D surface, the most symmetric surface in the tD family, with the surface tD^* at the junction of tD and $t\Delta$.

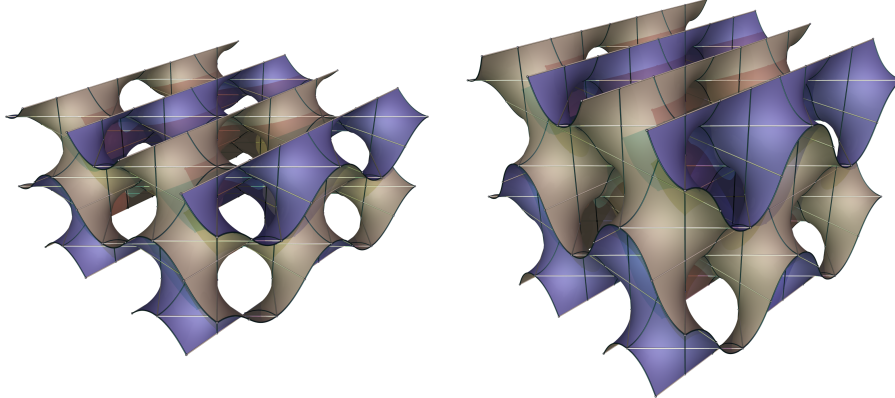


FIGURE 6.2. Schwarz' D and the unstable tD^* surface

The Gauss map of the tD^* surface has eight branched values at $\pm\alpha^{\pm 1}$ and $\pm\alpha^{\pm 1}i$, where $\alpha = \sqrt{(a^* - 1)/(a^* + 1)}$. They are the eight roots of $z^8 + kz^4 + 1 = 0$, where

$$k = \alpha^{-4} + \alpha^4 = \frac{(a^* - 1)^2}{(a^* + 1)^2} + \frac{(a^* + 1)^2}{(a^* - 1)^2} \approx 7.40284$$

This is precisely the value calculated by Koiso, Piccione and Shoda [KPS14] for a bifurcation instance in the tD family. An explicit bifurcation branch from tD^* was then missing, but now provided by the $t\Delta$ family.

Remark 6.4. Surprisingly, numerical computations show that, near the bifurcation point, $t\Delta$ surfaces have actually *smaller* area than the corresponding tD surfaces with the same lattice.

The conjugate of tD^* , denoted by tP^* , was identified in [KPS14] as a bifurcation instance in the tP family. We also find a bifurcation branch from tP^* , denoted by $t\Pi$. As one deforms the tetragonal lattice, the horizontal handles deform uniformly along the tP branch. But along the $t\Pi$ branch, the handles in the x direction shrink while the handles in the y direction expand. The $t\Pi$ family turns out to be a subfamily of oPa , a 2-parameter orthorhombic deformation family of Schwarz P surface. Since $oPa \subset \mathcal{M}$, $t\Pi$ is less interesting for understanding non-Meeks surfaces, hence not a focus of the current paper.

REFERENCES

- [BF71] Paul F. Byrd and Morris D. Friedman. *Handbook of elliptic integrals for engineers and scientists*. Die Grundlehren der mathematischen Wissenschaften, Band 67. Springer-Verlag, New York-Heidelberg, 1971. Second edition, revised.
- [Bra92] Kenneth A. Brakke. The surface evolver. *Experiment. Math.*, 1(2):141–165, 1992.
- [Che18] Hao Chen. Minimal twin surfaces. *Exp. Math.*, 2018. online first.
- [ES14] Norio Ejiri and Toshihiro Shoda. On a moduli theory of minimal surfaces. In *Prospects of differential geometry and its related fields*, pages 155–172. World Sci. Publ., Hackensack, NJ, 2014.
- [ES18] Norio Ejiri and Toshihiro Shoda. The Morse index of a triply periodic minimal surface. *Differential Geom. Appl.*, 58:177–201, 2018.
- [FH92] Andrew Fogden and Stephen T. Hyde. Parametrization of triply periodic minimal surfaces. II. regular class solutions. *Acta Cryst. Sect. A*, 48(4):575–591, 1992.
- [FH99] Andrew Fogden and Stephan T. Hyde. Continuous transformations of cubic minimal surfaces. *The European Physical Journal B-Condensed Matter and Complex Systems*, 7(1):91–104, 1999.
- [FHL93] Andrew Fogden, M. Haeberlein, and Sven Lidin. Generalizations of the gyroid surface. *J. Phys. I*, 3(12):2371–2385, 1993.
- [FK89] Werner Fischer and Elke Koch. Genera of minimal balance surfaces. *Acta Cryst. Sect. A*, 45(10):726–732, 1989.
- [KPS14] Miyuki Koiso, Paolo Piccione, and Toshihiro Shoda. On bifurcation and local rigidity of triply periodic minimal surfaces in \mathbb{R}^3 , 2014. preprint, [arXiv:1408.0953](https://arxiv.org/abs/1408.0953).
- [LHM01] Hippolyte Lazard-Holly and William H. Meeks, III. Classification of doubly-periodic minimal surfaces of genus zero. *Invent. Math.*, 143(1):1–27, 2001.
- [Mee90] William H. Meeks, III. The theory of triply periodic minimal surfaces. *Indiana Univ. Math. J.*, 39(3):877–936, 1990.
- [MPR98] William H. Meeks, III, Joaquín Pérez, and Antonio Ros. Uniqueness of the Riemann minimal examples. *Invent. Math.*, 133(1):107–132, 1998.
- [MR05] William H. Meeks, III and Harold Rosenberg. The uniqueness of the helicoid. *Ann. of Math.* (2), 161(2):727–758, 2005.
- [PRT05] Joaquín Pérez, M. Magdalena Rodríguez, and Martin Traizet. The classification of doubly periodic minimal tori with parallel ends. *J. Differential Geom.*, 69(3):523–577, 2005.
- [PT07] Joaquín Pérez and Martin Traizet. The classification of singly periodic minimal surfaces with genus zero and Scherk-type ends. *Trans. Amer. Math. Soc.*, 359(3):965–990, 2007.
- [Sch90] Hermann A. Schwarz. *Gesammelte Mathematische Abhandlungen*, volume 1. Springer, Berlin, 1890.
- [Sch70] Alan H. Schoen. Infinite periodic minimal surfaces without self-intersections. Technical Note D-5541, NASA, Cambridge, Mass., May 1970.
- [Tra08] Martin Traizet. On the genus of triply periodic minimal surfaces. *J. Differential Geom.*, 79(2):243–275, 2008.
- [Wey06] Adam G. Weyhaupt. *New families of embedded triply periodic minimal surfaces of genus three in euclidean space*. ProQuest LLC, Ann Arbor, MI, 2006. Thesis (Ph.D.)–Indiana University.
- [Wey08] Adam G. Weyhaupt. Deformations of the gyroid and Lidinoid minimal surfaces. *Pacific J. Math.*, 235(1):137–171, 2008.

(Chen) GEORG-AUGUST-UNIVERSITÄT GÖTTINGEN, INSTITUT FÜR NUMERISCHE UND ANGEWANDTE MATHEMATIK

Email address: h.chen@math.uni-goettingen.de

(Weber) INDIANA UNIVERSITY, DEPARTMENT OF MATHEMATICS

Email address: matweber@indiana.edu

SCRIBABILITY PROBLEMS FOR POLYTOPES

HAO CHEN AND ARNAU PADROL

ABSTRACT. In this paper we study various scribability problems for polytopes. We begin with the classical k -scribability problem proposed by Steiner and generalized by Schulte, which asks about the existence of d -polytopes that can not be realized with all k -faces tangent to a sphere. We answer this problem for stacked and cyclic polytopes for all values of d and k . We then continue with the weak scribability problem proposed by Grünbaum and Shephard, for which we are able to complete the work by Schulte by presenting non weakly circumscribable 3-polytopes. Finally, we propose new (i, j) -scribability problems, in a strong and a weak version, which generalize the classical ones. They ask about the existence of d -polytopes that can not be realized with all their i -faces “avoiding” the sphere and all their j -faces “cutting” the sphere. We are able to provide such examples for all the cases where $j - i \leq d - 3$.

CONTENTS

Introduction	2
Acknowledgements	3
1. Lorentzian view of polytopes	4
1.1. Convex polyhedral cones in Lorentzian space	4
1.2. Spherical, Euclidean and hyperbolic polytopes	5
2. Definitions and properties	6
2.1. Strong k -scribability	6
2.2. Weak k -scribability	7
2.3. Strong and weak (i, j) -scribability	7
2.4. Properties of (i, j) -scribability	8
3. Weak scribability	9
3.1. Weak k -scribability	10
3.2. Weak (i, j) -scribability	12
4. Stacked polytopes	12
4.1. Circumscribability	13
4.2. Ridge-scribability	14
4.3. The $(i, i + 1)$ scribability	16
5. Cyclic polytopes	17
5.1. k -ply systems and k -sets	17
5.2. Even dimensional cyclic polytopes	18
5.3. Odd dimensional cyclic polytopes	19
5.4. Neighborly polytopes	20
6. Stamps	21
7. Open problems	22
References	22

Key words and phrases. Scribability; Stacked polytopes; Cyclic polytopes; Ball packing.

H. Chen is supported by the ERC Advanced Grant number 247029 “SDModels”.

A. Padrol’s research is supported by the DFG Collaborative Research Center SFB/TR 109 “Discretization in Geometry and Dynamics”.

INTRODUCTION

In this paper we consider various *scribability problems*, which include the classical k -scribability considered by Schulte [Sch87], the weak version introduced by Grünbaum and Shephard [GS87], and new concepts of strong and weak (i, j) -scribability that generalize the previous. We present a collection of techniques for either (i) showing that certain polytopes are non-scribable or (ii) constructing scribed realizations for prescribed families of combinatorial types. Scribability problems show the interplay between polytope theory, sphere configurations, and hyperbolic geometry, and the techniques used in our paper draw from all these topics.

The first scribability problem was asked by Steiner in 1832 [Ste81], when he proposed the inscribability problem for 3-dimensional polytopes. It can be formulated as follows: Does there exist a 3-dimensional polytope that is not *inscribable*? In other words, is there any 3-polytope that can not be realized with all its vertices on a sphere?

A counterexample was discovered nearly 100 years later, when Steinitz [Ste28] presented a technique to construct infinitely many non-inscribable 3-polytopes. For instance, the so-called *triakis tetrahedron*, obtained by gluing a tetrahedron on top of each facet of a tetrahedron, is not inscribable. By polarity, the polytope obtained by truncating all the vertices of a tetrahedron is not *circumscribable*, i.e. has no realization with all the facets tangent to the sphere. Inscribable 3-polytopes were characterized by Rivin [Riv96] (see also [HRS92, Riv93, Riv94, Riv03]) in terms of the hyperbolic dihedral angles, although a fully combinatorial description is still missing (cf. [DS96]).

Schulte [Sch87] considered *k -scribability problems*, higher-dimensional analogues of Steiner's problem: For $0 \leq k \leq d - 1$, is there a d -polytope that can not be realized with all its k -faces tangent to a sphere? Leaving aside the trivial cases of $d \leq 2$, he constructed non- k -scribable examples for all the cases except for $d = 3$ and $k = 1$, i.e. 3-polytopes that are not *edge-scribable*. Surprisingly, it turns out that, as a consequence of the remarkable Koebe–Andreev–Thurston disk packing theorem, every 3-polytope does have a realization with all the edges tangent to the sphere (see [Zie07, Section 1.3] and references therein).

Our investigation on k -scribability problems, which we call *strong* to differentiate from the upcoming *weak* version, focuses on two important families of polytopes: *stacked polytopes* and *cyclic polytopes*.

By Barnette's Lower Bound Theorem [Bar71, Bar73], stacked polytopes have the minimum number of faces among all simplicial polytopes with the same number of vertices. Some stacked polytopes are among the first examples of non-inscribable 3-polytopes in Steinitz's work [Ste28]. Gonska and Ziegler [GZ13] fully characterized inscribable stacked polytopes, while Eppstein, Kuperberg and Ziegler [EKZ03] showed that stacked 4-polytopes are essentially not edge-scribable. In Section 4, we look at the other side of the story and prove the following result, which completely answers the strong k -scribability problems for stacked polytopes.

Theorem 1. *For any $0 \leq k \leq d - 3$, there are stacked d -polytopes that are not k -scribable. However, every stacked polytope is $(d - 1)$ -scribable (i.e. circumscribable) and $(d - 2)$ -scribable (i.e. ridge-scribable).*

The proof of Theorem 1 is divided into three parts: Proposition 4.1 for $0 \leq k \leq d - 3$, Proposition 4.3 for $k = d - 1$ and Proposition 4.5 for $k = d - 2$.

On the other hand, McMullen's Upper Bound Theorem [McM70] states that cyclic polytopes have the maximum number of faces among all polytopes with the same number of vertices. All cyclic polytopes are inscribable; see [Car11], [GS87, p. 67] [Sei91, p. 521] and [GZ13, Proposition 17]. The following theorem completely answers the strong k -scribability problems for cyclic polytopes.

Theorem 2. *For any $1 \leq k \leq d - 1$, a cyclic d -polytope with sufficiently many vertices is not k -scribable.*

Theorem 2 is derived from more general results on (i, j) -scribability problems, namely Corollary 5.8 and Proposition 5.12.

The *weak k -scribability problems* were originally proposed by Grünbaum and Shephard [GS87] for 3-dimensional polytopes. It asks for realizations of polytopes with the affine hull of every k -face tangent to the sphere. Schulte [Sch87] considered, again, the analogues of this problem in higher dimensions. However, because the definition does not behave well under polarity, Schulte was not able to construct counterexamples for weak k -scribability of d -polytopes when $k \geq d - 2$. In the current paper, we identify convex polytopes with pointed polyhedral cones in Lorentzian space; see Section 1 for details. By adopting this new point of view, we slightly modify the definition of weak k -scribability, and avoid the problem of polarity. This allows us to tie up the loose ends left by Schulte, and prove the following:

Theorem 3. *For $d \geq 3$ and $0 \leq k \leq d - 1$ with the exception of $(d, k) = (3, 1)$, there is a d -polytope that is not weakly k -scribable.*

We also propose new *(i, j) -scribability* problems, which ask about realizations of polytopes with all their i -faces “avoiding” the sphere and all their j -faces “cutting” the sphere. The definitions of cutting and avoiding, which come in a *strong* and a *weak* form, imply that (i, j) -scribability is well-behaved under polarity, and that (k, k) -scribability is nothing but classical k -scribability. This makes (i, j) -scribability, an interesting topic in its own right, also into a useful tool for classical k -scribability problems, as we will see with cyclic polytopes. In dimension 3, $(0, 1)$ -scribed polytopes have been studied as “hyperideal polyhedra” in hyperbolic space [BB02, Sch05].

The weak (i, j) -scribability turns out to be indeed quite weak, as we can see in the following theorem.

Theorem 4. *Every d -polytope is weakly (i, j) -scribable for $0 \leq i < j \leq d - 1$.*

As for the strong (i, j) -scribability, we are able to construct examples that prove:

Theorem 5. *For $d > 3$ and $0 \leq i \leq j \leq d - 1$, there are d -polytopes that are not strongly (i, j) -scribable for $j - i \leq d - 2$ when d is even, or $j - i \leq d - 3$ when d is odd.*

Theorem 5 follows from Proposition 5.6, which asserts that even dimensional cyclic polytopes with sufficiently many vertices are not strongly $(1, d - 1)$ -scribable. The proof of Proposition 5.6 uses the sphere separator theorem [MTTV97]. Similar techniques also prove that j -neighborly d -polytopes with many vertices are not $(1, j)$ -scribable; see Proposition 5.12. This implies that:

Theorem 6. *For $d \geq 4$ and any $1 \leq k \leq d - 2$, there are f -vectors such that no d -polytope with those f -vectors are k -scribable.*

For $k = d - 3$, examples of such f -vectors are already given by stacked d -polytopes with more than $d + 2$ vertices. See [EKZ03] for $d = 4$ and Proposition 4.1 for higher dimensions.

As for the (i, j) -scribability of stacked polytopes, we prove that

Theorem 7. *For any $d > 3$ and $0 \leq i \leq d - 4$, there is a stacked d -polytope that is not $(i, i + 1)$ -scribable.*

An alternative construction for polytopes that are not strongly $(0, d - 3)$ -scribable is given in Proposition 6.3, which uses the Stamp Theorem of Below [Bel02] and Dobbins [Dob11].

The paper is organized as follows: Section 1 is dedicated to introduce the set-up for our scribability problems: polyhedral cones in Lorentz space and spherical polytopes. The different scribability problems that we work with are presented in Section 2. Section 4 contains our results about stacked and truncated polytopes, and Section 5 contains those about cyclic and neighborly polytopes. An alternative technique for constructing polytopes that are not (i, j) -scribable is given in Section 6. Finally, in Section 7, we present some problems that we leave open.

Acknowledgements. We want to thank Karim Adiprasito, Ivan Izmestiev and Günter M. Ziegler for sharing their useful suggestions and insights during many interesting conversations on this topic.

1. LORENTZIAN VIEW OF POLYTOPES

The classical scribability problems only consider bounded convex polytopes in Euclidean space. To define polarity properly in this set-up, one must assume that the polytope contains the origin in its interior. This presents the major difficulty in Schulte's work on weak k -scribability, and also leads to a minor flaw in his proof regarding strong k -scribability (see Remark 2.3).

We find it more natural and convenient to work with spherical polytopes, which arise from pointed polyhedral cones in Lorentzian space. The current section is dedicated to the introduction of this set-up. The main advantage is that, for spherical polytopes, polarity is always well-defined and well-behaved. This facilitates the study of weak scribability, which enables us to obtain Theorem 3. At the same time, as we will see in Lemma 2.2, strong scribability in spherical space and in Euclidean space are equivalent, so the new setting is compatible with previous studies. In fact, the presence of spherical geometry is necessary only in few occasions (e.g. Example 2.5).

1.1. Convex polyhedral cones in Lorentzian space. A (closed) non-empty subset of \mathbb{R}^{d+1} is a *convex cone* if it is closed under positive linear combinations. A convex cone is *pointed* if it does not contain any subspace of \mathbb{R}^{d+1} . A convex cone is *polyhedral* if it is the conical hull of finitely many vectors in \mathbb{R}^{d+1} , i.e. a set \mathcal{K} of the form

$$\mathcal{K} = \text{cone}(V) := \left\{ \sum \lambda_i v_i \mid \lambda_i \geq 0, v_i \in V \right\}.$$

for some finite set $V \subset \mathbb{R}^{d+1}$.

Let \mathcal{K} be a convex cone and let $H \subset \mathbb{R}^{d+1}$ be a linear hyperplane disjoint from the interior of \mathcal{K} . We say that H is *supporting* for \mathcal{K} if $H \cap \mathcal{K}$ contains non-zero vectors. In this case, the closed half-space H^- that contains \mathcal{K} is called a *supporting half-space*.

If \mathcal{K} is polyhedral, the intersections of \mathcal{K} with its supporting hyperplanes are its *faces*. The set of faces ordered by inclusion forms the *face lattice* of \mathcal{K} . A polyhedral cone \mathcal{K}' is *combinatorially equivalent* to \mathcal{K} if their face lattices are isomorphic. In this case, we also say \mathcal{K} and \mathcal{K}' have the same *combinatorial type*, or that \mathcal{K}' is a *realization* of \mathcal{K} .

The *Lorentzian space* $\mathbb{L}^{1,d}$ is \mathbb{R}^{d+1} endowed with the Lorentzian scalar product:

$$\langle \mathbf{x}, \mathbf{y} \rangle := -x_0 y_0 + x_1 y_1 + \cdots + x_d y_d, \quad \mathbf{x}, \mathbf{y} \in \mathbb{R}^{d+1}.$$

The *light cone* of $\mathbb{L}^{1,d}$ is the pointed convex cone

$$\mathcal{L} := \left\{ \mathbf{x} \in \mathbb{L}^{1,d} \mid \langle \mathbf{x}, \mathbf{x} \rangle \leq 0, x_0 \geq 0 \right\}.$$

Remark 1.1. In the literature, the term “*light cone*” usually denotes the set of vectors \mathbf{x} such that $\langle \mathbf{x}, \mathbf{x} \rangle = 0$, i.e. the boundary of $\mathcal{L} \cup -\mathcal{L}$, which is not a convex cone.

We work with the polarity induced by the Lorentzian scalar product. Hence, the *polar* of a set $X \subseteq \mathbb{L}^{1,d}$ is the convex cone

$$X^* := \left\{ \mathbf{x} \in \mathbb{L}^{1,d} \mid \langle \mathbf{x}, \mathbf{y} \rangle \leq 0 \text{ for all } \mathbf{y} \in X \right\}.$$

We also define the *orthogonal companion* X^\perp as the polar of its linear span

$$X^\perp := \text{span}(X)^* = \left\{ \mathbf{x} \mid \langle \mathbf{x}, \mathbf{y} \rangle = 0 \text{ for all } \mathbf{y} \in X \right\}.$$

The light cone is self-polar, i.e. $\mathcal{L}^* = \mathcal{L}$. If $\mathcal{V} \subset \mathbb{L}^{1,d}$ is a linear subspace, then $\mathcal{V}^* = \mathcal{V}^\perp$.

If \mathcal{K} is a pointed polyhedral cone, then \mathcal{K}^* is *combinatorially dual* to \mathcal{K} . That is, the face lattice of \mathcal{K}^* is obtained from that of \mathcal{K} by reversing the inclusion relations. Indeed, to each face F of \mathcal{K} is associated a face F^\diamond of \mathcal{K}^* , which we call the *associated face* of F , given by

$$F^\diamond := F^\perp \cap \mathcal{K}^*.$$

We recall some standard properties of polarity.

Lemma 1.2. *A subspace \mathcal{V} is disjoint from \mathcal{L} if and only if \mathcal{V}^\perp intersects the interior of \mathcal{L} , and \mathcal{V} is tangent to \mathcal{L} (that is, $\mathcal{V} \cap \mathcal{L}$ consists of a single ray) if and only if \mathcal{V}^\perp is tangent to \mathcal{L} .*

Lemma 1.3. *If \mathbf{x} is a non-zero vector on the boundary of pointed polyhedral cone \mathcal{K} and belongs to a face F , then \mathbf{x}^\perp is a supporting hyperplane for \mathcal{K}^* that contains the associate face F^\diamond , and \mathbf{x}^* is the corresponding supporting half-space.*

Let F be a k -dimensional face of a pointed polyhedral cone \mathcal{K} . The *face figure* of F , denoted by \mathcal{K}/F , is the projection of \mathcal{K} onto the quotient space $\mathcal{K}/\text{span } F$. The combinatorial type of \mathcal{K}/F is induced by the faces of \mathcal{K} that contain F as a proper face. So \mathcal{K}/F is combinatorially dual to the associated face F^\diamond .

1.2. Spherical, Euclidean and hyperbolic polytopes. Let \mathbb{S}^d be the d -dimensional spherical space, identified with the set

$$\mathbb{S}^d = \{\mathbf{x} \in \mathbb{R}^{d+1} \mid \|\mathbf{x}\|_2 = 1\}.$$

A *spherical polytope* in \mathbb{S}^d is an intersection of finitely many hemispheres that does not contain any antipodal points. Every pointed polyhedral cone $\mathcal{K} \subset \mathbb{R}^{d+1}$ corresponds to a *spherical polytope* \mathcal{P} in \mathbb{S}^d given by $\mathcal{P} = \mathcal{K} \cap \mathbb{S}^d$, and every spherical polytope arises this way. The face lattice of \mathcal{P} is inherited from \mathcal{K} , and the polar of \mathcal{K} induces the polar of \mathcal{P} given by $\mathcal{P}^* := \mathcal{K}^* \cap \mathbb{S}^d$. Note that a hyperplane in \mathbb{S}^d is the intersection $H \cap \mathbb{S}^d$ where H is a linear hyperplane in \mathbb{R}^{d+1} , and a half-space in \mathbb{S}^d is a hemisphere. The light cone appears as a spherical cap $\mathcal{B} := \mathcal{L} \cap \mathbb{S}^d$, whose boundary is a $(d-1)$ -sphere “at latitude 45°N ”, which we denote by $\mathcal{S} := \partial\mathcal{B}$ to avoid confusion with the ambient d -sphere \mathbb{S}^d .

Every pointed polyhedral cone $\mathcal{K} \subset \mathbb{R}^{d+1}$ admits a *transversal hyperplane*, i.e. an affine hyperplane H intersecting every ray of \mathcal{K} . If we identify H with the Euclidean space \mathbb{E}^d , then the intersection $\mathcal{P} = \mathcal{K} \cap H$ is a bounded convex d -polytope in \mathbb{E}^d . Conversely, every d -dimensional Euclidean polytope can be *homogenized* to the $(d+1)$ -dimensional pointed polyhedral cone $\text{hom}(\mathcal{P}) := \{(\lambda, \lambda\mathbf{x}) \mid \mathbf{x} \in \mathcal{P}, \lambda \geq 0\}$. Again, the face lattice of \mathcal{P} is inherited from \mathcal{K} , and the polar of \mathcal{K} induces the polar of \mathcal{P} . Hence, from the combinatorial point of view, there is no difference between spherical polytopes and Euclidean polytopes.

We usually identify \mathbb{E}^d with the fixed hyperplane $H_0 = \{\mathbf{x} \mid x_0 = 1\}$, so that the light cone \mathcal{L} appears as the standard unit ball in \mathbb{E}^d . We abuse the notation and denote the Euclidean unit ball by \mathcal{B} and its boundary by \mathcal{S} , as its spherical counterparts. Bounded Euclidean d -polytopes in \mathbb{E}^d correspond to spherical d -polytopes contained in the hemisphere $x_0 > 0$ of \mathbb{S}^d through central (gnomonic) projection from the origin. Furthermore, the polarity induced by the Lorentzian scalar product coincides with the classical polarity in Euclidean space. That is:

$$\mathcal{P}^* := \{\mathbf{x} \mid (\mathbf{x}, \mathbf{y}) \leq 1 \text{ for all } \mathbf{y} \in \mathcal{P}\}$$

where (\cdot, \cdot) denotes the Euclidean inner product. For an affine subspace $H \subset \mathbb{E}^d$, we use H^\perp to denote the *polar subspace*

$$H^\perp := \{\mathbf{x} \in \mathbb{E}^d \mid (\mathbf{x}, \mathbf{y}) = 1 \text{ for all } \mathbf{y} \in H\},$$

which corresponds to the orthogonal companion in $\mathbb{L}^{1,d}$.

The unit ball \mathcal{B} in the Euclidean space \mathbb{E}^d can also be seen as the Klein model of the hyperbolic space \mathbb{H}^d , then $\mathcal{P} \cap \mathcal{B}$ is a hyperbolic polytope. In the current paper, polytopes of interest have no vertex in the interior of \mathcal{B} , so they are not compact, or even of infinite volume in the hyperbolic space. The hyperbolic view is very useful for the study of stacked polytopes in Section 4. In particular, we will make use of hyperbolic reflection groups and hyperbolic dihedral angles for our proofs. Readers unfamiliar with hyperbolic polytopes are referred to [Vin93] or [Rat06].

Lorentz transformations are those linear transformations of \mathbb{R}^{d+1} that preserve \mathcal{L} . Lorentz transformations of $\mathbb{L}^{1,d}$ correspond to projective transformations of \mathbb{E}^d that preserve \mathcal{S} , or Möbius transformations of \mathbb{S}^d . If we regard the interior of \mathcal{B} as the hyperbolic space \mathbb{H}^d , then the Möbius transformations correspond to hyperbolic isomorphisms of \mathbb{H}^d .

Remark 1.4. The term “*Lorentz transformation*” is usually used to denote those linear transformations that preserve the Lorentzian inner product. What we call a Lorentz transformation here, i.e. those preserving \mathcal{L} , correspond to what is usually known as the *orthochronous Lorentz transformations*.

We use the notation $\text{span}(\mathcal{X})$ to denote the linear span in $\mathbb{L}^{1,d}$, the spherical span in \mathbb{S}^d , and the affine span in \mathbb{E}^d , depending on the context.

2. DEFINITIONS AND PROPERTIES

2.1. Strong k -scribability. The classical scribability problems go back to Steiner [Ste81], and were studied in full generality by Schulte [Sch87]. We will present them in terms of spherical polytopes, but as we will see soon, this formulation is equivalent to the classical setup.

Consider a polytope $\mathcal{P} \subset \mathbb{S}^d$ and let F be a face of \mathcal{P} . We say that F is *tangent* to \mathcal{S} if $\text{relint}(F) \cap \mathcal{S}$ consists of a single point, which is called the *tangency point* of F and denoted by t_F .

Definition 2.1. A spherical polytope \mathcal{P} is *(strongly) k -scribed* if every k -face of \mathcal{P} is tangent to \mathcal{S} , and *(strongly) k -scribable* if it has a k -scribed realization.

Here, the adjective *strong* is used to distinguish from the weak scribability, which will be defined later. We often omit the adjective since this type of scribability problem is of the earliest and greatest interest. We also say that a polytope \mathcal{P} is *inscribable*, *edge-scribable*, *ridge-scribable* or *circumscribable* if it is 0-, 1-, $(d-2)$ - or $(d-1)$ -scribable, respectively.

If $\mathcal{P} \subset \mathbb{S}^d$ is contained in the upper hemisphere $x_0 > 0$, then it corresponds to a bounded polytope in \mathbb{E}^d (identified with H_0), and our definition of “ k -scribed” coincides with that of Schulte [Sch87]. However, since not every spherical polytope is in $x_0 > 0$, it is not straightforward to see that every k -scribable spherical polytope has a k -scribed realization in Euclidean space.

Lemma 2.2. *If a d -polytope $\mathcal{P} \subset \mathbb{S}^d$ is k -scribable, then \mathcal{P} admits a k -scribed realization in the Euclidean space \mathbb{E}^d that is bounded and contains the center of \mathcal{S} in its interior.*

Remark 2.3. Before showing that our definition is indeed equivalent to that of Schulte [Sch87], let us first point out a related problem in Schulte’s paper.

In [Sch87, p. 507f.], Schulte uses a footnote of [Grü03, p. 285] which says that, for any point x in the interior of \mathcal{B} , there is a projective transformation T_x that preserves \mathcal{S} and sends x to the center of \mathcal{S} . Schulte argued that, if a polytope \mathcal{P} does not contain the center of \mathcal{S} , one can send a point $x \in \mathcal{P} \cap \mathcal{B}$ to the center of \mathcal{S} using T_x , and then $T_x \mathcal{P}$ is a polytope containing the center.

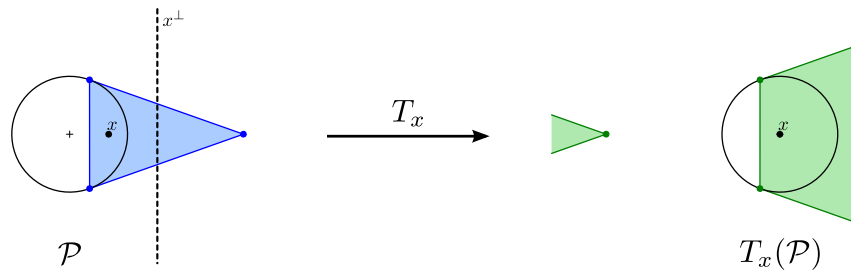


FIGURE 1. T_x destroys the boundedness of the polytope.

While this argument is correctly used in [Grü03], Schulte did not take precautions for the fact that, if the point x is not carefully chosen, $T_x \mathcal{P}$ might be unbounded (or even not connected). For example, consider the triangle \mathcal{P} in Figure 1, constructed by taking the convex hull of a point together with the intersections of its polar line with the circle. For any point $x \in \mathcal{P} \cap \mathcal{B}$, the *polar hyperplane* x^\perp is a line intersecting the triangle. As T_x sends x to the center, x^\perp is sent to infinity, which destroys the boundedness.

In our proof of Lemma 2.2, which uses the same idea as Schulte’s, we will carefully choose a suitable x for a k -scribed polytope.

Proof. Assume that \mathcal{P} is k -scribed and choose an arbitrary k -face F of \mathcal{P} with tangency point $t_F \in \mathcal{P}$. Observe that $F \subset H_F = t_F^\perp$ and $\mathcal{B} \subset H_F^- = t_F^{*+}$.

We claim that H_F^- is also a supporting half-space for \mathcal{P} . The k -scribedness implies that the interior of every $(k+1)$ -face of \mathcal{P} intersects \mathcal{B} . So every $(k+1)$ -face G of \mathcal{P} containing F has some

point in the open halfspace $H_F^- \setminus H_F$. Since $G \cap H_F = F$, this implies that H_F^- is supporting for all these faces, and hence also for \mathcal{P} .

Now, if x is a point sufficiently close to t_F on the segment connecting t_F and the center of \mathcal{B} , then $x \in \text{int}(\mathcal{P} \cap \mathcal{B})$ and the polar hyperplane x^\perp is disjoint from \mathcal{P} and \mathcal{B} . Thus the projective transformation T_x will send \mathcal{P} to a bounded k -scribed polytope containing the center of \mathcal{S} . \square

As a consequence, k -scribability for Euclidean polytopes is equivalent to k -scribability for spherical polytopes.

2.2. Weak k -scribability. Weak k -scribability problems were first asked for 3-polytopes by Grünbaum and Shephard [GS87], and then generalized to higher dimensions by Schulte [Sch87, Section 3]. By considering spherical polytopes, the notion of weak scribability is weakened, but has the desired properties with respect to polarity.

Consider a polytope $\mathcal{P} \subset \mathbb{S}^d$, and let F be a face of \mathcal{P} . We say that F is *weakly tangent* to \mathcal{S} if its spherical span is tangent to \mathcal{S} , i.e. if $\text{span}(F) \cap \mathcal{S}$ consists of a single point.

Definition 2.4. A spherical polytope \mathcal{P} is *weakly k -scribed* if every k -face of \mathcal{P} is weakly tangent to \mathcal{S} , and *weakly k -scribable* if it has a k -scribed realization.

Definition 2.4 is weaker than the Euclidean definition of Grünbaum–Shephard and Schulte. The two definitions of strong k -scribability were equivalent thanks to Lemma 2.2 which show that for every strongly k -scribed polytope \mathcal{P} , there is a hemisphere (e.g. H_F^-) containing both \mathcal{P} and \mathcal{S} . This is however not true for weakly k -scribed polytopes and in this case the spherical version is weaker.

For example, with the Grünbaum–Shephard definition, any weakly inscribed polytope is also strongly inscribed; see Schulte [Sch87]. This is not the case with Definition 2.4. The first example is, again, given by a stacked polytope. The *triakis tetrahedron*, which is the polytope obtained by stacking a vertex on top of every facet of a 3-dimensional simplex, is a well-known polytope that is not strongly inscribable [Ste28] (cf. [Grü03, Theorem 13.5.3], [GZ13]). However, it is weakly inscribable.

Example 2.5. The triakis tetrahedron is weakly inscribable (in the sense of Definition 2.4).

Proof. Consider the following eight vectors in \mathbb{R}^4 .

$$\begin{aligned} v_{1,2} &:= (+\sqrt{2}, 0, \pm 1, 1) & v_{3,4} &:= (+\sqrt{3}, \pm\sqrt{2}, 0, 1) \\ v_{5,6} &:= (-\sqrt{2}, \pm 1, 0, 1) & v_{7,8} &:= (-\sqrt{3}, 0, \pm\sqrt{2}, 1). \end{aligned}$$

They all satisfy $-x_0^2 + x_1^2 + x_2^2 + x_3^2 = 0$. Hence for all $1 \leq i \leq 8$, the intersection of the line $\text{span}(v_i)$ and the light cone $\mathcal{L} \subset \mathbb{R}^4$ is a single ray. This means that the intersection of $\mathcal{K} = \text{cone}(v_1, \dots, v_8)$ with \mathbb{S}^3 is a weakly inscribed 3-polytope \mathcal{P} . Its combinatorial type is that of the triakis tetrahedron. \square

Figure 2 illustrates the inscribed configuration. On the left, we visualize the intersection of \mathcal{K} with the hyperplane $x_3 = 1$; notice that then the intersection of $\mathcal{L} \cup -\mathcal{L}$ with the hyperplane appears as a 2-sheet hyperboloid. On the right, we visualize it by considering the intersection of $\mathcal{K} \cup -\mathcal{K}$ with the hyperplane $x_0 = 1$; then we see two connected components, corresponding to \mathcal{K} and $-\mathcal{K}$, respectively.

Nevertheless, Definition 2.4 has the desired property: the polar of a weakly k -scribable d -polytope is weakly $(d - 1 - k)$ -scribable; see the upcoming Lemma 2.12(ii). This is precisely the missing piece that prevented Schulte from proving Theorem 3.

2.3. Strong and weak (i,j) -scribability. In this section, we present the new concept of (i,j) -scribability, which generalizes the concept of k -scribability presented above. Instead of asking for realizations with the k -faces tangent to the sphere, we are interested in realizations with the i -faces “avoiding” the sphere and the j -faces “cutting” it, in such a way that (i,j) -scribability reduces to i -scribability when $i = j$. As before, the definitions come in strong and weak forms.

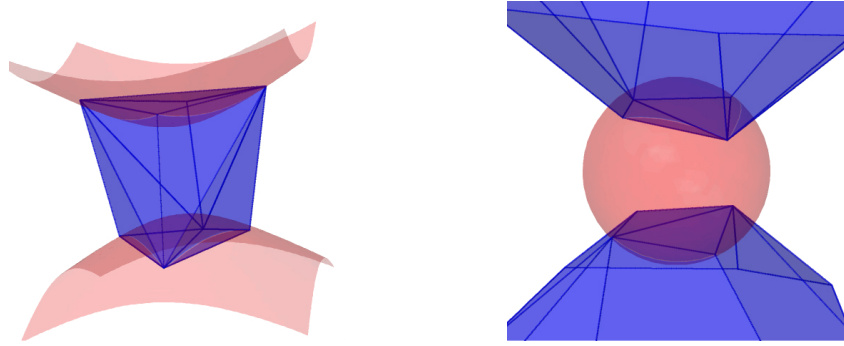


FIGURE 2. The inscribed triakis tetrahedron \mathcal{P} , view of $\pm\mathcal{P}$ and $\pm\mathcal{S}$ projected on the hyperplane $x_3 = 1$ (left), and on $x_0 = 1$ (right).

Definition 2.6. Consider a spherical polytope $\mathcal{P} \subset \mathbb{S}^d$, and let F be a proper face of \mathcal{P} .

We say that F

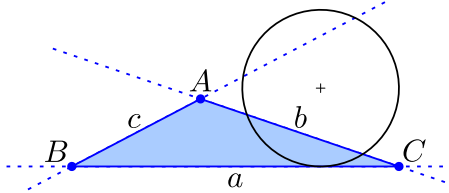
- *strongly cuts* \mathcal{S} if $\text{relint}(F) \cap \mathcal{B} \neq \emptyset$;
- *weakly cuts* \mathcal{S} if $\text{span}(F) \cap \mathcal{B} \neq \emptyset$;

We say that F

- *strongly avoids* \mathcal{S} if there is a supporting hyperplane H of \mathcal{P} such that $F = H \cap \mathcal{P}$ and $\mathcal{B} \subset H^-$.
- *weakly avoids* \mathcal{S} if $\text{span}(F) \cap \text{int } \mathcal{B} = \emptyset$;

where $\text{int } \mathcal{B} = \mathcal{B} \setminus \mathcal{S}$ is the interior of the ball \mathcal{B} .

Example 2.7. Consider the following triangle.



The edge a strongly avoids and cuts \mathcal{S} . The edge b strongly cuts \mathcal{S} and does not avoid \mathcal{S} in any sense. The edge c weakly cuts \mathcal{S} as shown by the dashed line. The vertex A weakly avoids \mathcal{S} . The vertices B and C strongly avoid \mathcal{S} and do not cut \mathcal{S} in any sense.

In the following, in order to ease the text, the phrase “in the strong (resp. weak) sense” means that the adverb “strongly” (resp. “weakly”) is implied wherever applicable in the context.

Definition 2.8. Let $0 \leq i \leq j \leq d - 1$. In the *strong* or *weak* sense, a spherical d -polytope $\mathcal{P} \subset \mathbb{S}^d$ is *i-avoiding* if every i -face of \mathcal{P} avoids \mathcal{S} , and *j-cutting* if every j -face of \mathcal{P} cuts \mathcal{S} . We say that \mathcal{P} is *(i, j)-scribed* if it is i -avoiding and j -cutting, and *(i, j)-scribable* if it has an (i, j) -scribed realization.

Remark 2.9. These notions should not be confused with a (m, d) -scribable polytope in the sense of Schulte [Sch87], which means a d -polytope that is m -scribable.

Remark 2.10. There is a third even weaker version of scribability that seems reasonable at first sight, where faces are *feeble cutting* if they are not strongly avoiding and *feeble avoiding* if they are not strongly cutting. However, observe that we can always find such a feeble $(d - 1, 0)$ -scribed realization of any polytope P by simply taking a realization of P with all the vertices in $-\mathcal{B} \subset \mathbb{S}^d$, and thus this feeble version of scribability is trivial.

2.4. Properties of (i, j) -scribability. A first easy observation is that the strong versions are indeed stronger than the weak versions. That is, the strong forms of cutting, avoiding and scribability imply the weak forms.

Lemma 2.11. *In the strong or weak sense, a face that cuts and avoids \mathcal{S} is tangent to \mathcal{S} . Consequently, a (k, k) -scribed polytope is k -scribed.*

We say that a face is *strictly* cutting (resp. avoiding) \mathcal{S} if it is cutting (resp. avoiding) \mathcal{S} but not tangent to \mathcal{S} . In the strong sense, it is possible that a face is neither cutting nor avoiding \mathcal{S} at the same time. This is however not possible in the weak sense.

The following lemma collects the essential properties of (i, j) -scribability, which are repeatedly used in the upcoming proofs. It is a generalized version of the main results in [Sch87], Theorems 1 and 2. It implies also the weak version of [Sch87, Theorem 1], needed for proving Theorem 3.

Lemma 2.12. *Let $d \geq 1$ and $0 \leq i, j \leq d - 1$. In the strong or weak sense, if a d -polytope \mathcal{P} is (i, j) -scribable, then:*

- (i) \mathcal{P} is (i', j') -scribable for any $i' \leq i$ and $j' \geq j$;
- (ii) the polar polytope \mathcal{P}^* is $(d - 1 - j, d - 1 - i)$ -scribable;
- (iii) if $j \leq d - 2$, each facet of \mathcal{P} is an (i, j) -scribable $(d - 1)$ -polytope;
- (iv) if $i \geq 1$, each vertex-figure of \mathcal{P} is an $(i - 1, j - 1)$ -scribable $(d - 1)$ -polytope.

Proof.

- (i) Assume that \mathcal{P} is strongly j -cutting, we need to prove that \mathcal{P} is also j' -cutting for any $j' \geq j$. Indeed, for any $(j + 1)$ -face F , take a point in $\text{relint } F' \cap \mathcal{B}$ for each j -face F' incident to F , then the barycenter of these points is in $\text{relint } F \cap \mathcal{B}$. By polarity we see that if \mathcal{P} is strongly i -avoiding, then \mathcal{P} is also i' -avoiding for any $i' \leq i$. This proves the strong version of the statement. The weak version follows similarly, just replace relint by span .
- (ii) The weak version follows directly from Lemma 1.2. For the strong version, one also needs Lemma 1.3.
- (iii) For either strong or weak version, notice from the proof of (i) that \mathcal{P} is strictly $(d - 1)$ -cutting in the weak sense. Let F be a facet. If we identify $\text{span } F \subset \mathbb{S}^d$ with \mathbb{S}^{d-1} , then $F \subset \mathbb{S}^{d-1}$ is an (i, j) -scribed $(d - 1)$ -polytope with respect to the sphere $\text{span } F \cap \mathcal{S}$.
- (iv) By polarizing (iii). □

In the remaining of the paper, our mission is two-fold: for each triple (d, i, j) we either try to prove that every d -polytope is (i, j) -scribable, or we try to construct an example of a d -polytope that is not (i, j) -scribable. In view of Lemma 2.12(i), we seek to construct polytopes that are not (i, j) -scribable with $j - i$ as large as possible, or to prove that every d -polytope is (i, j) -scribable for $j - i$ as small as possible. The remaining items of Lemma 2.12 are used to do induction on the dimension d .

We end this section by proving that the Euclidean and spherical definitions of strong (i, j) -scribability are equivalent. When $i < j$, the analogue of Lemma 2.2 does not guarantee simultaneously that \mathcal{P} is bounded and contains the origin. However, boundedness suffices for the equivalence between the Euclidean and the spherical setup.

Lemma 2.13. *If a d -polytope \mathcal{P} is strongly (i, j) -scribable, with $0 \leq i \leq j \leq d - 1$ then \mathcal{P} admits a strongly (i, j) -scribed bounded realization in Euclidean space \mathbb{E}^d .*

Proof. We prove the dual statement, i.e. \mathcal{P} admits a strongly (i, j) -scribed realization with the center of \mathcal{S} in its interior. Since \mathcal{P} is strongly (i, j) -scribed, each facet contains a point of \mathcal{B} . The barycenter of these points is interior to both \mathcal{P} and \mathcal{B} , and can be sent to the center of \mathcal{S} with a Möbius transformation. This gives a realization of \mathcal{P} containing the center, then the polarity yields a bounded realization of \mathcal{P}^* . □

3. WEAK SCRIBABILITY

In this section we concentrate on the investigation of weak (i, j) -scribability. On the one hand, we show in Theorem 3 that there are d -polytopes that are not weakly k -scribable except for $d = 3$ and $k = 1$ or $d \leq 2$, since a 3-polytope is already strongly 1-scribable. On the other hand, we show in Theorem 4 that when $i < j$, every polytope is weakly (i, j) -scribable.

3.1. Weak k -scribability. Despite Example 2.5, there are 3-polytopes that are not weakly inscribable. We provide two constructions.

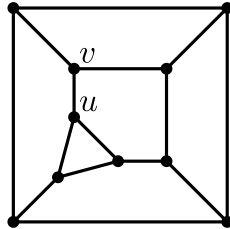


FIGURE 3. The truncated cube is not weakly inscribable.

Example 3.1. The 3-polytope \mathcal{P} obtained by truncating one vertex of a 3-cube is not weakly inscribable.

Proof. Let \mathcal{K} be the polyhedral cone spanned by a spherical realization of \mathcal{P} and let H be a transversal hyperplane of \mathcal{K} . If we identify the Euclidean space \mathbb{E}^d with H (instead of with H_0 as usual), the polytope $\mathcal{P}' = H \cap \mathcal{K}$ is a bounded polytope, and the “sphere” $\mathcal{S} = H \cap (\partial\mathcal{L} \cup -\partial\mathcal{L})$ appears as a quadric in \mathbb{E}^d . Since \mathcal{P} is weakly inscribed, the vertices of \mathcal{P}' are all on the quadric \mathcal{S} .

It is well known that if seven vertices of a (combinatorial) 3-cube lie on a quadric, so does the eighth one [BS08, Section 3.2]. We can recover a 3-cube by removing the truncating facet of \mathcal{P}' . Let w be the 8th vertex of this cube (the one that does not belong to \mathcal{P}'). Then w and the points u and v from Figure 3 all lie on the quadric. If a quadric contains 3 collinear points, then it contains a whole line (see [BS08, Ex 3.7]). However, since $0 \notin H$, our conic section does not contain lines; a contradiction. \square

We are now ready to prove Theorem 3, which we repeat below.

Theorem 3. *Except for the case $d = 3, k = 1$, for every $d \geq 3$ and $0 \leq k \leq d - 1$, there is a d -polytope that is not weakly k -scribable.*

Schulte [Sch87, Sec. 3] gave the proof for $k \leq d - 3$, but remarked that the remaining cases would follow from the existence of polytopes that are not weakly circumscribable. The polar of the truncated cube is such a polytope.

Proof. The proof is by induction on d and follows the same steps as Schulte’s.

In dimension 3, the truncated cube is not weakly inscribable, and its polar is not circumscribable by 2.12(i) (the weak version with $i = j = k$). The pyramid over the truncated cube is a 4-polytope that has a truncated cube as a facet and as a vertex figure, so it is not weakly k -scribable for $k = 0, 1$ by Lemma 2.12(ii) and (iii) (the weak version with $i = j = k$). Its polar has a stacked octahedron as a facet and as a vertex figure, so it is not weakly k -scribable for $k = 2, 3$.

In higher dimensions, the pyramid over a $(d - 1)$ -polytope that is not weakly k -scribable gives a d -polytope that is neither k - nor $(k + 1)$ -scribable. So the theorem follows by induction. \square

Recall that although we work in spherical space, our definition of weak k -scribability is weaker than the one for the Euclidean setting used by Schulte. Consequently, examples for Theorem 3 are not weakly k -scribable in Euclidean space, neither. This finishes Schulte’s work.

We now present an alternative construction. Despite the absence of Lemma 2.12(ii) in Euclidean space, it is possible to bypass the spherical geometry, and construct polytopes that are not weakly circumscribable directly within the Euclidean setup of [Sch87]. Our construction is based on the following lemma:

Lemma 3.2. *Any weakly circumscribed Euclidean polygon with more than 4 edges is also strongly circumscribed.*

Proof. Let \mathcal{P} be a weakly circumscribed polygon in Euclidean space. A half-plane L^- supporting an edge of \mathcal{P} is either of the form $\{\langle a, x \rangle \leq -1\}$ for some unit vector a , in which case we call the edge *separating* because \mathcal{P} and \mathcal{B} lie at opposite sides of the supporting line, or of the form $\{\langle a, x \rangle \leq 1\}$, and then $\mathcal{B} \cup \mathcal{P} \subset L^-$ and we call the edge *non-separating*. Observe that \mathcal{P} is not strongly circumscribed if and only if it has a separating edge.

Assume that \mathcal{P} has three separating edges. If the unit normal vectors were positively dependent, the intersection of the half-planes would be empty. Hence, we may assume that one of them can be written as a linear combination of the other two with positive coefficients, but then one can easily see that this inequality is redundant.

We also claim that, with the presence of a separating edge, \mathcal{P} can have at most two non-separating edges. To see this, consider one separating edge with unit vector a_0 and two non-separating edges with vectors a_1, a_2 . A linear relation of the form $a_1 = \lambda a_0 + \mu a_2$ with positive coefficients is not possible. Otherwise, a small computation shows that the inequality defined by a_1 is redundant. The forbidden linear relation is however inevitable if \mathcal{P} has three non-separating edges.

Hence, if \mathcal{P} has a separating edge, then it can have at most four edges, two of each kind. The different situations are illustrated in Figure 4. \square

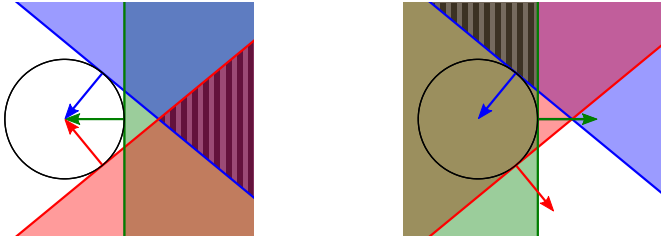


FIGURE 4. Redundant inequalities for the proof of Lemma 3.2. The depicted vectors are outer normal vectors and point away from the half-space. The striped region is the intersection of all the half-spaces. Notice that in both situations there is a half-space containing the intersection of the other two.

The same proof carries over almost directly to spherical polytopes. The correct statement in the spherical setting would be: If $\mathcal{P} \subset \mathbb{S}^2$ is a weakly circumscribed spherical polygon with more than 4 edges, then either \mathcal{P} or $-\mathcal{P}$ is strongly circumscribed.

Example 3.3. Let \mathcal{P} be the polytope obtained by truncating all the vertices of a tetrahedron, then stacking on each of the newly created facets, and then stacking again on each of the newly created facets (Figure 5). Then \mathcal{P} is not weakly circumscribable.

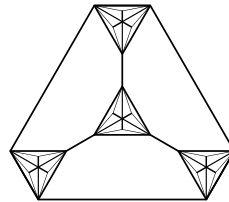


FIGURE 5. This polytope is not weakly circumscribable.

Proof. We start by showing that \mathcal{P} is not strongly circumscribable. First of all, the truncated tetrahedron is not strongly circumscribable (it is polar to the triakis tetrahedron). For any facet arising from the truncation, we can replace the supporting half-space by any supporting half-space of one of the simplices stacked on the facet, and the result is still a truncated tetrahedron. Hence \mathcal{P} is not strongly circumscribable.

Now assume that \mathcal{P} is weakly circumscribed but not strongly circumscribed. Then there is a facet F whose supporting half-space does not contain \mathcal{B} . Every facet is incident to a vertex of degree 6. Let v be such a vertex incident to F , then the vertex figure at v is a weakly circumscribed hexagon that is not strongly circumscribed, contradicting Lemma 3.2. \square

The same method can be applied to many other 3-polytopes proven to be non-circumscribable by Steinitz (cf. [Griü03, Theorem 13.5.2]) to get an infinite family of 3-polytopes that are not weakly circumscribable. More specifically, if a simple 3-polytope has more vertices than facets, then truncating the vertices yields a polytope that is not strongly circumscribable, and stacking twice on the truncated facets provides a polytope that is not weakly circumscribable.

3.2. Weak (i, j) -scribability. We end by dealing with the remaining cases and showing that weak (i, j) -scribability is indeed very weak.

Theorem 4. *Every d -polytope is weakly (i, j) -scribable for $0 \leq i < j \leq d - 1$.*

Proof. It suffices to show that every d -polytope \mathcal{P} is weakly $(i, i+1)$ -scribable for all $0 \leq i \leq d-2$. Consider a Euclidean realization of \mathcal{P} and a generic affine subspace L of dimension $d-i$ that does not intersect \mathcal{P} . Then L intersects the affine span of every $(i+1)$ -face of \mathcal{P} at a single point, but does not intersect the affine span of any i -face. We can find, in the neighborhood of L , an ellipsoid \mathcal{E} that contains all these intersection points but remains disjoint from the affine span of every i -face. The affine transformation that sends \mathcal{E} to the unit ball \mathcal{B} sends \mathcal{P} to a weakly $(i, i+1)$ -scribed realization. \square

4. STACKED POLYTOPES

From now on, we focus only on strong scribability. In the remaining of the paper, we often omit the adjective “*strong*”, which has to be understood whenever we talk about (i, j) -scribability unless explicitly stated otherwise.

The goal of the current section is to answer the scribability problems for stacked polytopes. That is, we want to know which are the values of k such that every stacked d -polytope is k -scribable.

We recall the definitions of stacking and stacked polytope. For a d -polytope \mathcal{P} with a simplicial facet F , we *stack* a vertex onto F by taking the convex hull of $\mathcal{P} \cup p$ for some point p close enough to the barycenter of F . In terms of the *connected sum* (cf. Section 4.2), this corresponds to gluing \mathcal{P} and a simplex d -simplex Δ along F . A *stacked polytope* is any polytope obtained from a simplex by repeatedly stacking vertices onto facets. The dual of a stacked polytope is a *truncated polytope*, obtained from a simplex by repeatedly cutting off vertices.

A stacked polytope \mathcal{P} of dimension $d \geq 3$ has a unique triangulation \mathcal{T} with no interior faces of dimension $< d-1$, the *stacked triangulation*. The *dual tree* of \mathcal{T} takes the maximal simplices in \mathcal{T} as vertices and connects two vertices if they share a face of dimension $d-1$.

Already in dimension 3, stacked polytopes provide the first examples of polytopes that are not inscribable [Ste28]. Gonska and Ziegler [GZ13] proved that a stacked polytope is inscribable if and only if all the nodes of its dual tree have degree ≤ 3 . In higher dimensions, Eppstein, Kuperberg and Ziegler [EKZ03] proved that no stacked 4-polytope on more than 6 vertices is edge-scribable.

While it is well known stacked polytopes present obstructions to inscribability and edge-scribability, the other side of the story seems to have escaped the attention of the community. In this section, we show that stacked polytopes are actually always circumscribable and ridge-scribable. On the other hand, stacked polytopes that are not k -scribable exist for any other smaller k .

Proposition 4.1. *For any $d > 3$ and $0 \leq k \leq d-3$, there is a stacked d -polytope that is not k -scribable.*

Proof. In [GZ13] it is proved that, for every $d \geq 3$, there is a stacked d -polytope that is not inscribable, which solves the case $k = 0$. We conclude the proposition by induction using Lemma 2.12(ii) and the fact that every stacked d -polytope is the vertex-figure of a stacked $(d+1)$ -polytope, and a k -face figure of a stacked $(d+1+k)$ -polytope. \square

We can strengthen this statement for the case $d > 3$ and $k = d - 3$.

Proposition 4.2. *For $d > 3$, no stacked d -polytope with more than $d + 2$ vertices is $(d - 3)$ -scribable.*

Proof. Any stacked d -polytope \mathcal{P} with more than $d + 2$ vertices admits a vertex figure with the combinatorial type of a stacked $(d - 1)$ -polytope with more than $d + 1$ vertices. To see this, first notice that the vertex figure at any vertex of \mathcal{P} has the combinatorial type of a stacked $(d - 1)$ -polytope. Since \mathcal{P} has more than $d + 2$ vertices, it is not a simplex nor a bypyramid, hence the dual tree of \mathcal{P} has a node of degree ≥ 2 . Thus there are three simplices in the stacked triangulation sharing a ridge of \mathcal{P} . For any vertex in this ridge, the vertex figure contains at least $d + 2$ vertices.

By Lemma 2.12(ii), if \mathcal{P} is $(d - 3)$ -scribable, its vertex figures are all $(d - 4)$ -scribable. The theorem then follows by induction since no 4-polytope on more than 6 vertices is edge-scribable [EKZ03, Corollary 9]. \square

4.1. Circumscribability.

Proposition 4.3. *Every stacked polytope is circumscribable.*

Proof. We prove by explicit construction the dual version of the proposition, namely that every truncated polytope is inscribable.

Let \mathcal{P} be a truncated polytope, obtained from a d -simplex \mathcal{P}_0 by repeatedly truncating vertices. We start with an inscribed realization of \mathcal{P}_0 .

In the first step, we perform simultaneously all the truncations that remove vertices of \mathcal{P}_0 . This is carried out as follows: For every vertex v to be truncated, we pull v towards the exterior of \mathcal{S} by a sufficiently small distance. Let \mathcal{P}'_0 be the adjusted simplex. Then the sphere \mathcal{S} intersects the edges of \mathcal{P}'_0 near the adjusted vertices, while the other vertices remain on the sphere. The convex hull of these intersection points gives the desired truncated polytope \mathcal{P}_1 with all its vertices on \mathcal{S} . Observe that every vertex not present in \mathcal{P}_0 is incident to a (essentially unique) simplicial facet of \mathcal{P}_1 .

Now, let \mathcal{P}_k be the truncated polytope we obtain after the first k steps. In the $(k + 1)$ -th step, we perform simultaneously all the truncations that remove vertices of \mathcal{P}_k . The proof is by induction on k . We assume that all the vertices of \mathcal{P}_k are situated on the sphere \mathcal{S} , and that every vertex v not present in \mathcal{P}_{k-1} is incident to a simplicial facet F_v of \mathcal{P}_k . These assumptions have been verified for $k = 1$.

Consider all the vertices v of \mathcal{P}_k to be truncated in the $(k + 1)$ -th step. We pull every such v by a sufficiently small distance towards the exterior of the sphere \mathcal{S} along the edge e_v that is incident to v but does not belong to F_v . These movements do not change the combinatorial type of \mathcal{P}_k . Let \mathcal{P}'_k be the adjusted polytope. Then the sphere \mathcal{S} intersects the 1-skeleton of \mathcal{P}'_k near the adjusted vertices, while the other vertices remain on the sphere. The convex hull of these intersection points gives the desired truncated polytope \mathcal{P}_{k+1} with all its vertices on \mathcal{S} , and every newly created vertex is incident to a (essentially unique) simplicial facet of \mathcal{P}_{k+1} .

It then follows by induction that \mathcal{P} has an inscribed realization. The procedure is sketched in Figure 6. \square

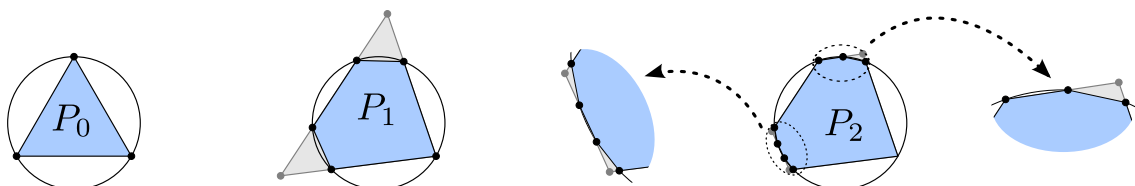


FIGURE 6. Steps of the proof of Proposition 4.3

The fact that every newly created vertex is incident to a simplex facet is critical for this proof. It allows us to pull the vertices independently without changing the combinatorial type of the polytope.

Observe that this proof also works if we replace the sphere by any strictly convex surface. This means that truncated polytopes are *universally inscribable* in the sense of [GP15].

Proposition 4.4. *Every truncated polytope has a realization with all its vertices on any given strictly convex surface.*

And the construction also works in more general settings. For example, it works if \mathcal{P}_0 is an inscribable simple polytope (e.g. cube) and every vertex of \mathcal{P}_0 is truncated in the first step. In this case, the first step can be carried out by shrinking the sphere by a sufficiently small amount. From this moment, every vertex is adjacent to a simplex facet and the remaining steps remain as described in the proof.

4.2. Ridge-scribability.

Proposition 4.5. *Every stacked polytope is ridge-scribable.*

Proof. Let Δ be a ridge-scribed realization of the simplex. The interior of \mathcal{B} can be regarded as the Klein model of d -dimensional hyperbolic space. The tangency points of the ridges are all ideal in hyperbolic space, so the facets are all parallel or ultraparallel. Then the hyperbolic reflections in the facets of \mathcal{P} generate a universal Coxeter group W . The associated Coxeter diagram is a complete graph with label ∞ on all the edges. The fundamental domain of W is Δ . See [Vin67, Vin71] for more details on hyperbolic Coxeter groups. Simplices in the orbit $W(\Delta)$ form a simplicial complex called the *Coxeter complex*; see [AB08].

Stacked polytopes can be seen as strongly connected subcomplexes of the Coxeter complex. To see this, notice that for any $w \in W$, the simplex $w(\Delta)$ is a ridge-scribed simplex in the Euclidean view. The dual graph of $W(\Delta)$ is the Cayley graph of W , which is a tree. The convexity is guaranteed by the fact that, for any hyperplane H that is tangent to \mathcal{B} and contains a ridge of $W(\Delta)$, $W(\Delta)$ is contained in the halfspace H^- . Ridge-scribed realizations for stacked polytopes are therefore given by the Coxeter complex. \square

Inspired by this proof, we now extend the proof to a generalization of stacked polytopes. Let \mathcal{P} be a ridge-scribed polytope. The reflections in the facets of \mathcal{P} again form a hyperbolic Coxeter group. The Coxeter complex is a polytopal cell complex, each cell being a copy of \mathcal{P} . Every strongly connected subcomplex of the Coxeter complex again forms a convex polytope, which we call a *stacked \mathcal{P} -polytope*. Then the same argument proves that

Proposition 4.6. *Stacked \mathcal{P} -polytopes are ridge-scribable if \mathcal{P} is.*

We can further extend the proof to connected sums of polytopes. Recall that two polytopes are *projectively equivalent* if there is a projective transformation that sends one to the other. Let \mathcal{P} and \mathcal{Q} be two polytopes with facets projectively equivalent to F , then the *connected sum* of \mathcal{P} and \mathcal{Q} through F , denoted $\mathcal{P} \#_F \mathcal{Q}$, is obtained by “gluing” \mathcal{P} and \mathcal{Q} by identifying the projectively equivalent facets (see [RG96, Section 3.2]). So the operation of stacking is actually taking connected sum with a simplex.

We say that two polytopes are *Möbius equivalent* if there is a Möbius transformation (projective transformation preserving \mathcal{S}) that sends one to the other. Then

Proposition 4.7. *Let \mathcal{P} and \mathcal{Q} be ridge-scribed polytopes with facets Möbius equivalent to F , then the connected sum $\mathcal{P} \#_F \mathcal{Q}$ is ridge-scribable.*

Proof. With a Möbius transformation if necessary, we may assume that \mathcal{P} and \mathcal{Q} are ridge-scribed and $\mathcal{P} \cap \mathcal{Q} = F$. For any ridge R adjacent to F , the hyperplane that is tangent to \mathcal{S} and contains R is supporting both for \mathcal{P} and for \mathcal{Q} (see the proof of Lemma 2.2). So the polytope $\mathcal{P} \#_F \mathcal{Q} = \mathcal{P} \cup \mathcal{Q}$ is convex and ridge-scribed by construction. \square

Ridge-scribed simplices are all Möbius equivalent; see [EKZ03, Lemma 7] for the dual statement. We can therefore regard Proposition 4.5 as a special case of Proposition 4.7.

Finally, we prove an interpretation of Proposition 4.5 in terms of ball packings. For every point $\mathbf{x} \in \mathbb{E} \setminus \mathcal{B}$, the part of \mathcal{S} visible from \mathbf{x} is a spherical cap on \mathcal{S} . For an edge-scribed polytope, the

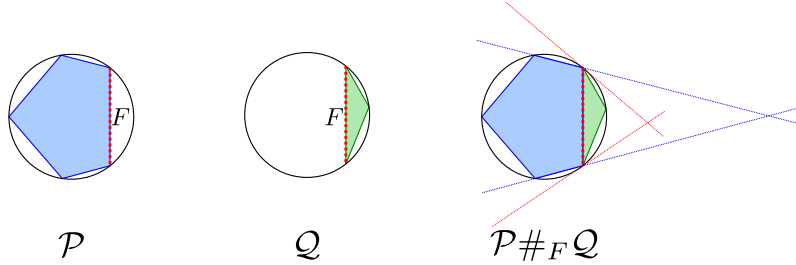


FIGURE 7. The relevant tangent hyperplanes and facet defining hyperplanes in a connected sum of ridge-scribed polytopes through a Möbius equivalent facet.

caps corresponding to the vertices have disjoint interiors. After a stereographic projection, they form a ball packing in Euclidean space whose tangency graph is isomorphic to the 1-skeleton of the polytope; see [Che13]. The dual version of Proposition 4.5 says that every truncated polytope is edge-scribable. Therefore,

Corollary 4.8. *The 1-skeleton of every truncated d -polytope is the tangency graph of a ball packing in dimension $d - 1$.*

Here we provide a self-consistent proof independent to Proposition 4.5. In fact, the two proofs are essentially the same, as inversions correspond to hyperbolic reflections; see [Che14].

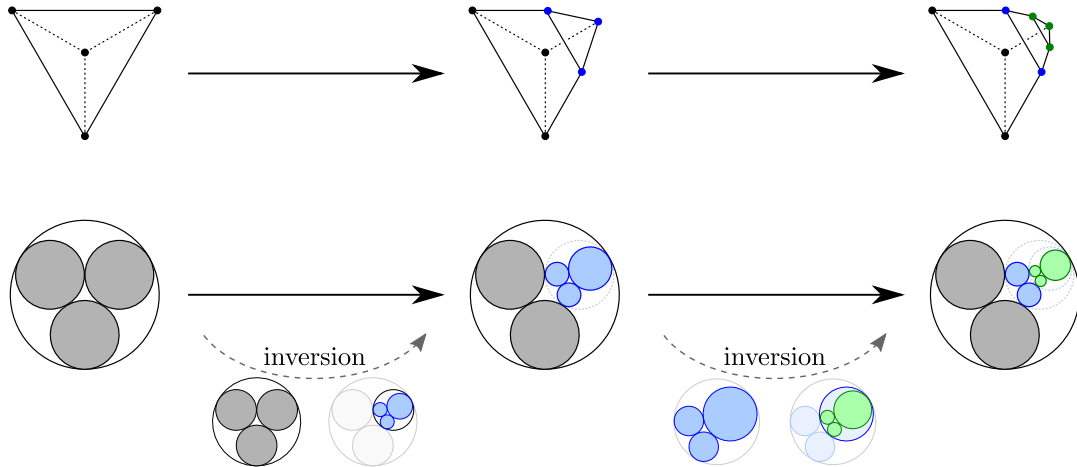


FIGURE 8. The graph of a truncated polytope as a ball packing through a series of inversions.

Proof. We construct the truncated polytope and the ball packing in parallel, and keep the 1-skeleton and the tangency graph isomorphic. We begin with an edge-tangent d -simplex Δ and the corresponding configuration of $d + 1$ pairwise tangent balls B_0, \dots, B_d of dimension $d - 1$.

We now proceed by induction, truncating the vertices one by one. Let B be the ball corresponding to the vertex to be truncated.

If B is in the initial packing of $d + 1$ balls, say $B = B_0$, then the inversion in ∂B sends B_1, \dots, B_d into pairwise tangent balls B'_1, \dots, B'_d in the interior of B , and B'_i is tangent to B_i , $1 \leq i \leq d$. Since the tangency points are preserved, replacing B by these primed balls gives the desired packing.

Otherwise, B appeared in some latter truncation step, when a ball B'_d was replaced by d pairwise tangent balls B'_0, \dots, B'_{d-1} . Say $B = B'_0$. They are all tangent from the interior to $\partial B'_d$, which we can regard the exterior of B'_d as a ball of negative curvature. The inversion in ∂B sends B'_1, \dots, B'_d into pairwise tangent balls B''_1, \dots, B''_d in the interior of B . Again, the tangency points of these

balls with B coincide with those of B with its neighbors. Replacing B by these doubly primed balls gives the desired packing.

The corollary then follows by induction. See also Figure 8. \square

4.3. The $(i, i+1)$ scribability. Finally, we prove Theorem 7 by constructing stacked d -polytopes that are not $(i, i+1)$ -scribed for $0 \leq i \leq d-4$.

We still regard the interior of $\mathcal{B} \subset \mathbb{E}^d$ as the Klein model of the hyperbolic space \mathbb{H}^d . To study the vertex figure \mathcal{P}/v , consider a surface Σ that intersects perpendicularly all the hyperbolic geodesics that passes through v (in \mathbb{E}^d). There are three cases: If v is a point of \mathbb{H}^d (in the interior of \mathcal{B}), Σ is a $(d-1)$ -sphere \mathbb{S}^{d-1} centered at v ; this is more clear if we assume v is the center of \mathcal{B} , or simply use the Poincaré ball model for \mathbb{H}^d . If v is an ideal point of \mathbb{H}^d (on the boundary of \mathcal{B}), then Σ is a horosphere based at v , which can be identified to the Euclidean space \mathbb{E}^{d-1} ; this can be easily seen with Poincaré half-space model, cf. [Rat06, § 6.4]. Finally, if v is hyperideal for \mathbb{H}^d (in the exterior of \mathcal{B}), then Σ is the totally geodesic surface given by the intersection $\mathcal{B} \cap v^\perp$, which can be identified to the hyperbolic space \mathbb{H}^{d-1} .

Now the vertex figure \mathcal{P}/v can be realized as the polytope $\mathcal{P} \cap \Sigma$, which lies in \mathbb{S}^{d-1} , \mathbb{E}^{d-1} or \mathbb{H}^{d-1} if v is in the interior, boundary or exterior of \mathcal{B} , independently. Since Σ is perpendicular to all the hyperbolic geodesics through v , the dihedral angles of \mathcal{P} is preserved in $\mathcal{P} \cap \Sigma$; cf. [Rat06]. More generally, a face figure \mathcal{P}/F can be obtained by consecutively taking vertex figures at each vertices of F . So we can realize \mathcal{P}/F as a spherical, Euclidean or hyperbolic polytope if F is (in the strong sense) strictly cutting, tangent or strictly avoiding \mathcal{S} , independently.

We will need the following lemma:

Lemma 4.9. *Let \mathcal{P} be a $(0, d-3)$ -scribed d -simplex, and F be a facet of \mathcal{P} . If we regard \mathcal{B} as the Klein model of the hyperbolic space \mathbb{H}^d , then the hyperbolic dihedral angles at the ridges incident to F sum up to at least π .*

Proof. Since the $(d-3)$ -faces cut \mathcal{S} , their links are spherical or Euclidean triangles, i.e. the dihedral angles at the ridges incident to a $(d-3)$ -face sum up to at least π . If we consider only the $(d-3)$ -faces incident to F , the dihedral angles at the ridges incident to them sum up to at least $\binom{d}{2}\pi$.

However, this summation also includes some ridges not incident to F . These ridges are all incident to the vertex v that is not in F . Since v avoids \mathcal{S} , the vertex figure is a hyperbolic or Euclidean $(d-1)$ -simplex. By a result of Höhn [Höh53] (see also [Gad56]) and [ALS08]), the dihedral angles of these ridges sum up to at most $\binom{d-1}{2}\pi$. Subtracting this from the summation above yields at least $\binom{d}{2}\pi - \binom{d-1}{2}\pi = (d-1)\pi$.

Furthermore, every ridge is counted $d-1$ times, which is the number of $(d-3)$ -faces incident to each ridge. So the sum of the dihedral angles at the ridges incident to F sum up to at least π . \square

By Lemma 2.12, Theorem 7 is derived from the following proposition.

Proposition 4.10. *There is a stacked 4-polytope that is not $(0, 1)$ -scribable.*

Proof. Consider the stacked 4-polytope obtained by stacking on every facet of a simplex, and then stacking again on every facet. The stacked triangulation of the resulting polytope consists of $1+5+20=26$ 4-simplices. Twenty of them have boundary facets, we call them *exterior simplices*. The remaining six only have interior facets, we call them *interior simplices*.

There are 40 ridges incident to the interior facets, and we want to estimate the sum of the hyperbolic dihedral angles at these ridges. Each interior simplex contributes at least $10\pi/3$. To see this, notice that the link of each edge is a spherical or Euclidean triangle, and so the adjacent dihedral angles sum up to at least π , and that each ridge is incident to 3-edges, so each angle is counted three times. On the other hand, each exterior simplex shares a facet with an interior simplex. Hence, by Lemma 4.9, it contributes with at least π to the sum of the dihedral angles of ridges incident to interior simplices. Hence, the dihedral angles at these 40 ridges sum up to at least 40π .

Therefore, there is at least one ridge at which the hyperbolic dihedral angle is at least π , which destroys the convexity of the polytope. \square

Dihedral angles for $(0, 1)$ -scribed 3-polytopes are fully characterized by Bao and Bonahon [BB02], who refer these polytopes as “hyperideal polyhedra”, and also proved the uniqueness up to hyperbolic isometry; see also [Sch05] for the connection to circle configurations.

5. CYCLIC POLYTOPES

The main result of this section is that even-dimensional cyclic polytopes with sufficiently many vertices are not $(1, d - 1)$ -scribable. We also investigate odd-dimensional cyclic polytopes and neighborly polytopes in general.

A d -polytope is *k -neighborly* if every k vertices form a face. Since the only k -neighborly d -polytope with $k > \lfloor d/2 \rfloor$ is the simplex, we call a d -polytope simply *neighborly* if it is $\lfloor d/2 \rfloor$ -neighborly.

The most important examples of neighborly polytopes are cyclic polytopes. Consider a curve γ of *order d* , which means that each hyperplane intersects γ in at most d points, such as the d -dimensional moment curve (t, t^2, \dots, t^d) . Take the convex hull of n distinct points on γ . That is,

$$\text{conv}(\gamma(t_1), \gamma(t_2), \dots, \gamma(t_n))$$

for n distinct parameters $t_1 < t_2 < \dots < t_n$. Then the combinatorial type of this polytope (and, even more, the oriented matroid defined by the points $\gamma(t_i)$) does not depend on the choice of the parameters t_i . We call any polytope of this combinatorial type a *cyclic d -polytope* with n vertices, and denote it by $\mathcal{C}_d(n)$. If we identify the vertices of $\mathcal{C}_d(n)$ with the indices $[n] = \{1, \dots, n\}$, the combinatorics of $\mathcal{C}_d(n)$ are described by the followed criterion, called *Gale's evenness condition* (cf. [Grü03, Section 4.7], [Zie95, Theorem 0.7]).

Proposition 5.1. *Let $I \subset [n]$ be a set of d vertices. Then I indexes a facet of $\mathcal{C}_d(n)$ if and only if for any two vertices $j < k$ in $[n] \setminus I$, the set $\{i \in I \mid j < i < k\}$ contains an even number of vertices.*

It is well-known that cyclic polytopes are inscribable; see [Car11] [GS87, p. 67] [Sei91, p. 521] [GZ13, Proposition 17]. This implies that they are $(0, j)$ -scribable for any $j \geq 0$. We will however see that, in even dimensions, cyclic polytopes provide non-examples for (i, j) -scribability with $i > 0$. In particular, cyclic polytopes behave poorly with respect to k -scribability, as indicated by Theorem 2, which we recall below.

Theorem 2. *For any $1 \leq k \leq d - 1$, a cyclic d -polytope with sufficiently many vertices is not k -scribable.*

This follows from the main results of this section, namely Propositions 5.6 for even dimensions, Corollary 5.8 for odd dimensions and $k > 1$, and Proposition 5.12 for $k = 1$.

5.1. k -ply systems and k -sets. As we have already mentioned in Section 4, any point \mathbf{x} in $\mathbb{E}^d \setminus \mathcal{B}$ can be associated with a closed spherical cap on \mathcal{S} , namely the set of points of \mathcal{S} that are visible from \mathbf{x} . A set of spherical caps on \mathcal{S} is said to be a *k -ply system* if no point of \mathcal{S} is in the interior of k caps. These systems were studied by Miller et al. [MTTV97], who proved the following Separation Theorem. Here, the *intersection graph* is the graph where every vertex represents a cap, and two caps form an edge if they intersect.

Proposition 5.2 (Sphere Separator Theorem). *The intersection graph of a k -ply system consisting of n caps on a d -dimensional sphere can be separated into two disjoint parts, each of size at most $\frac{d+1}{d+2}n$, by removing $O(k^{1/d}n^{1-1/d})$ vertices.*

To the knowledge of the authors, the best known constant factor in the proposition is

$$c_2 = \sqrt{\frac{2\pi}{\sqrt{3}}} \left(\frac{1 + \sqrt{k}}{\sqrt{2(1+k)}} + o(1) \right)$$

for $d = 2$ and

$$c_d = \frac{2A_{d-1}}{A_d^{1-1/d} V_d^{1/d}} + o(1)$$

for $d > 2$; see [ST96]. Here V_d is the volume of a unit d -ball and A_d is the area of a unit d -sphere, so $A_{d-1} = dV_d$.

For a point set $V \subset \mathbb{E}^d$, a subset I of cardinality k is said to be a *k-set* if there is a hyperplane strictly separating I and $V \setminus I$. We will define the k -sets of a polytope to be the k -sets of its set of vertices, and say that a k -set intersects \mathcal{S} if its convex hull intersects \mathcal{S} . The following lemma relates k -sets and k -ply systems.

Lemma 5.3. *A point set $V \subset \mathbb{E}^d \setminus \mathcal{B}$ corresponds to a k -ply system on \mathcal{S} if and only if every k -set intersects the sphere \mathcal{S} .*

Proof. Assume that there is a k -set I such that $\text{conv } I \cap \mathcal{S} = \emptyset$. Then there is a hyperplane tangent to \mathcal{S} separating I and the interior of \mathcal{B} . The tangency point is visible from every point in I . In other words, it is in the interior of at least k of the associated caps, so the set of caps corresponding to V is not a k -ply system. The other direction is obtained by reversing the argument. \square

The following obvious fact can be regarded as a special case of this lemma.

Corollary 5.4. *The caps of \mathcal{S} corresponding to $v, w \in \mathbb{E}^d \setminus \mathcal{B}$ have disjoint interiors if and only if the segment $[v, w]$ strongly cuts \mathcal{S} .*

5.2. Even dimensional cyclic polytopes. The following is the key for proving our main result. It uses that all even-dimensional cyclic polytopes have the same oriented matroid to make statements about the k -sets of any realization of $\mathcal{C}_d(n)$ (which fail for odd dimensions, cf. Section 5.3).

Lemma 5.5 (*k*-set Lemma). *For even d and $k \geq 3d/2 - 1$, every k -set of $\mathcal{C}_d(n)$ contains a facet of $\mathcal{C}_d(n)$.*

Proof. Without loss of generality, we can assume that $k = 3d/2 - 1$. Let I be a k -set of $\mathcal{C}_d(n)$.

Every even-dimensional cyclic polytope has its vertices on a order- d curve γ [Stu87]. Every hyperplane H intersects γ in at most d points, and hence there can be at most d changes of sides of H between I and $[n] \setminus I$. So I can be decomposed into at most $d/2 + 1$ consecutive segments of $[n]$. If we ignore the external segments (the ones containing 1 or n), there are at most $d/2 - 1$ internal segments.

Since $k = 3d/2 - 1 \not\equiv d/2 \pmod{2}$, at most $d/2 - 1$ of these internal segments have odd length. By removing a vertex from the boundary of each of the odd internal segments, we obtain a set J of at least $k + 1 - d/2$ vertices satisfying Gale's evenness condition. As $k \geq 3d/2 - 1$, J contains at least d vertices. Finally, we take a d -element subset of J by taking even-length subsegments from the internal segments together with external subsegments from the external segments. This set corresponds to a facet since it still fulfills Gale's evenness condition. \square

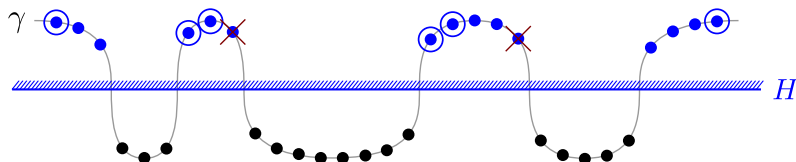


FIGURE 9. Sketch of a 15-set of a cyclic 6-polytope. The curve γ intersects the hyperplane H in 6 points, separating them into the k -set (above) and its complement (below).

The proof of the k -set Lemma is illustrated in Figure 9. It shows a 15-set of a cyclic 6-polytope, which consists of 4 segments, of lengths 3, 3, 5 and 4, respectively. The second and third segments are internal. We remove one extreme point from every internal odd segment (marked with a cross). Then we can select a subset that forms a facet (circled elements).

We are finally ready to prove the main result of this part.

Proposition 5.6. *Let $d \geq 4$ be an even integer and*

$$n > (c_{d-1}(d+1))^{d-1}(3d/2 - 1),$$

then the cyclic polytope $\mathcal{C}_d(n)$ is not $(1, d-1)$ -scribable.

By Lemma 2.12(i), this implies that, in even dimensions, $\mathcal{C}_d(n)$ is not (i, j) -scribable for $1 \leq i \leq j \leq d-1$ if n is large enough. In particular, we have proved Theorem 2 for even dimensions.

Proof. It is enough to prove that $\mathcal{C}_d(n)$ is not $(1, d-1)$ -scribable when n is sufficiently large. Assume that \mathcal{P} is a $(1, d-1)$ -scribed cyclic polytope with n vertices. Let $k = 3d/2 - 1$. By the k -set Lemma 5.5, every k -set of the vertices of \mathcal{P} contains a facet. Since every facet of \mathcal{P} cuts the sphere \mathcal{S} , this implies that every k -set intersects \mathcal{S} . Hence, the collection spherical caps corresponding to the vertices of \mathcal{P} form a k -ply system. By the Sphere Separator Theorem 5.2, the intersection graph of the caps admits a separator of size

$$c_{d-1} \lfloor d/2 \rfloor^{\frac{1}{d-1}} n^{\frac{d-2}{d-1}} < \frac{n}{d+1}.$$

However, since all the edges of \mathcal{P} strongly avoid the sphere, the intersection graph is a complete graph by Lemma 5.4, and the removal of the separator leaves a complete graph of more than $\frac{d}{d+1}n$ vertices, contradicting Proposition 5.2. \square

By Lemma 2.12(iii) and (iv), we obtain the following corollary, which provides the final counterexamples to (i, j) -scribability for the proof of Theorem 5.

Corollary 5.7. *For odd d , the pyramid over a cyclic $(d-1)$ -polytope with sufficiently many vertices is a d -polytope that is neither $(1, d-2)$ -scribable nor $(2, d-1)$ -scribable.*

5.3. Odd dimensional cyclic polytopes. The proof of the k -set Lemma 5.5 fails dramatically in odd dimensions. When d is odd, different realizations of $\mathcal{C}_d(n)$ may have different oriented matroids and hence different k -set structures. In particular, the vertices do not necessarily lie on any order- d curve. In fact, the k -set Lemma 5.5 does not hold in odd dimensions, as we will see in Remark 5.11.

Nevertheless, since $\mathcal{C}_d(n)$ has $\mathcal{C}_{d-1}(n-1)$ as a vertex-figure, we obtain the following corollary by Lemma 2.12(iv).

Corollary 5.8. *Let $d \geq 5$ be an odd integer and*

$$n > (c_{d-1}(d+1))^{d-1}(\lfloor 3d/2 \rfloor - 1),$$

then the cyclic polytope $\mathcal{C}_d(n)$ is not $(2, d-1)$ -scribable.

By Lemma 2.12(i), this implies that, in odd dimensions, $\mathcal{C}_d(n)$ is not (i, j) -scribable with $2 \leq i \leq j \leq d-1$ if n is large enough. This proves Theorem 2 for $1 < k \leq d-1$. The 1-scribability of odd-dimensional cyclic polytopes will be taken care of in Section 5.4.

However, odd-dimensional cyclic polytopes are $(1, d-1)$ -scribable, in contrast to the situation in even dimensions.

Proposition 5.9. *For odd d , the cyclic polytope $\mathcal{C}_d(n)$ is $(1, d-1)$ -scribable.*

Proof. Take a realization of $\mathcal{C}_{d-1}(n-1)$ in \mathbb{R}^{d-1} that is inscribed with respect to a sphere \mathcal{S}' , and fix a vertex v of $\mathcal{C}_{d-1}(n-1)$. Shrink \mathcal{S}' to \mathcal{S}'' with respect to v such that any edge of $\mathcal{C}_{d-1}(n-1)$ that is disjoint from v avoids \mathcal{S}'' .

Embed \mathbb{R}^{d-1} into \mathbb{R}^d as the hyperplane $x_0 = 0$, and extend \mathcal{S}'' to a sphere \mathcal{S} in \mathbb{R}^d so that \mathcal{S}'' is the equator of \mathcal{S} . Then we split the vertex v into two vertices $v_{\pm} = (\pm h, v)$. The ‘height’ h is chosen such that, if a light source is placed at v_{\pm} , then the shadow of \mathcal{S} on \mathbb{R}^{d-1} is exactly \mathcal{S}' .

The convex hull of v_{\pm} and the remaining vertices of $\mathcal{C}_{d-1}(n-1)$ is a realization of $\mathcal{C}_d(n)$ (cf. [CD00] and Remark 5.10). One then easily checks that, in this realization, edges incident to v_{\pm} are tangent to \mathcal{S} ; the other edges, belonging to $\mathcal{C}_{d-1}(n-1)$, avoid \mathcal{S} by construction. On the other hand, all the facets are adjacent to either v_+ or v_- and cut \mathcal{S} . The construction is sketched in Figure 10. \square

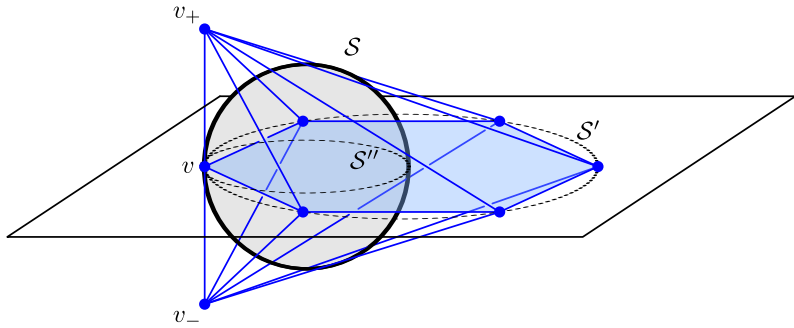


FIGURE 10. Sketch of the construction of Proposition 5.9.

Remark 5.10. Cordovil and Duchet [CD00] proposed a process that can realize any oriented matroid for $\mathcal{C}_d(n)$ when d is odd, but their description does not quite work. They first stack a vertex onto $\mathcal{C}_{d-1}(n-1)$, then split it into an extra dimension, followed by a perturbation. This process does not in general give a cyclic polytope. The correct construction consists of splitting a vertex of $\mathcal{C}_{d-1}(n-1)$ into an extra dimension, as we did in the proof above, and then a perturbation.

Remark 5.11. There can be arbitrarily large k -sets of an odd dimensional cyclic polytope that do not contain a facet. To see this, take the realization of $\mathcal{C}_d(n)$ from Proposition 5.9. From the copy of $\mathcal{C}_{d-1}(n-1)$ lying in $x_0 = 0$ take a subset of vertices not containing any facet, and lift them to height $x_0 = \varepsilon > 0$; and descend the remaining vertices of $\mathcal{C}_{d-1}(n-1)$ to $x_0 = -\varepsilon$. If ε is sufficiently small, then this does not change the combinatorial type, and the points in the open half-space $x_0 > 0$ form a k -set not containing any facet.

5.4. Neighborly polytopes. In this part, we apply the ideas leading to Proposition 5.6 to general neighborly polytopes. However, the lack of an analogue to Lemma 5.5 does not allow us to carry over the argument in full generality.

Let \mathcal{P} be a j -neighborly d -polytope. Since every j -set of \mathcal{P} forms a $(j-1)$ -face, the argument for Proposition 5.6 proves that if \mathcal{P} has sufficiently many vertices then it is not $(1, j-1)$ -scribable. In particular, neighborly polytopes with sufficiently many vertices are not edge-scribable. This provides the last missing piece (namely $k=1$) for Theorem 2.

We will however prove a slightly stronger result

Proposition 5.12. *For $d \geq 4$, a k -neighborly d -polytope \mathcal{P} with sufficiently many vertices is not $(1, k)$ -scribable.*

For a proof, the argument for Proposition 5.6 applies almost directly. But in place of Lemma 5.5, we need the following k -set lemma.

Lemma 5.13 (k -set lemma for neighborly polytopes). *Every $(k+1)$ -set of a k -neighborly d -polytope is a k -face.*

For a polytope, a set I of vertices is a *missing face* if I is not a face but every proper subset I is. For a k -neighborly polytope, every $(k+1)$ -set either forms a face or a missing face. The k -set Lemma 5.13 is then a special case of the following more general lemma.

Lemma 5.14. *The k -sets of a polytope are not missing faces.*

Proof. Let V be the vertex set of the polytope, and I be a subset of k vertices. If I is a k -set, then $\text{conv}(I) \cap \text{conv}(V \setminus I) \neq \emptyset$. But if I is a missing face, then $\text{conv}(I) \cap \text{conv}(V \setminus I) = \emptyset$. \square

Neighborliness is a property that only depends on the f -vector. Hence Proposition 5.12 implies Theorem 6, which we restate here:

Theorem 6. *For $d \geq 4$ and any $1 \leq k \leq d-2$, there are f -vectors such that no d -polytope with those f -vectors are k -scribable.*

Proof. For $1 \leq k \leq \lfloor d/2 \rfloor$, the theorem follows by taking $j = \lfloor d/2 \rfloor$ in Proposition 5.12. The remaining cases, i.e. $\lceil d/2 \rceil \leq k \leq d-2$, are obtained by taking the polar. \square

6. STAMPS

Polytopes that are not $(0, d-3)$ -scribable can be obtained by taking the polar of cyclic polytopes. Here we present another alternative construction based on projectively prescribed faces.

Lemma 6.1. *For every $d \geq 2$, there is a polytope \mathcal{P} with no $(0, d-1)$ -scribed projectively equivalent realization.*

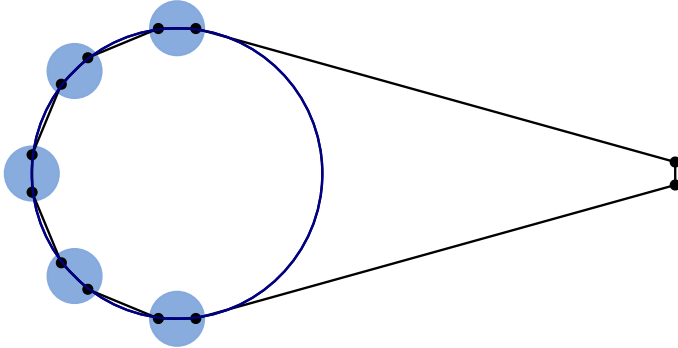


FIGURE 11. The construction of Lemma 6.1. Any polygon projectively equivalent to this polygon is not $(0, 1)$ -scribed.

Proof. Consider $N = \binom{n+2}{2} - 1$ generic points p_1, \dots, p_N lying on the $x_0 < 0$ hemisphere of \mathcal{S} . There is a unique quadric going through $\binom{n+2}{2} - 1$ generic points, and this dependence is continuous since the coefficients of the quadric are the solution of a linear system of equations on the points' coordinates. Hence, there exists an $\varepsilon > 0$ such that for any q_1, \dots, q_N with $q_i \in B_\varepsilon(p_i)$, the unique quadric that goes through these q_i 's is an ellipsoid contained in $2\mathcal{B}$.

Now, consider dN distinct points p_i^j for $1 \leq i \leq N$ and $1 \leq j \leq d$ with $p_i^j \in \mathcal{S} \cap B_\varepsilon(p_i)$. Choose d additional points p_0^j , $1 \leq j \leq d$, on the hyperplane $x_0 = 3$ in the neighborhood $B_\varepsilon(p_0)$ where $p_0 = (3, 0, \dots, 0)$, such that all the $d(N + 1)$ points are in convex position. Let \mathcal{P} be the convex hull of all these points. If ε is small enough, then for each $0 \leq i \leq N$, the corresponding p_i^j 's form a facet F_i of \mathcal{P} .

For the sake of contradiction, assume a projective transformation T such that $T\mathcal{P}$ is $(0, d-1)$ -scribed, then $T^{-1}\mathcal{S}$ is a quadric that intersects all the facets of \mathcal{P} . Since $T^{-1}\mathcal{S}$ contains a point $q_i \in B_\varepsilon(p_i)$ for each $1 \leq i \leq N$, the quadric is contained in $2\mathcal{B}$ and hence does not intersect F_0 . Hence, such a transformation T cannot exist.

This construction is sketched in Figure 11. \square

We need the following result, found by Below [Bel02] and by Dobbins [Dob11, Dob15].

Proposition 6.2 ([Bel02, Ch. 5], see also [Dob11, Thm. 4.1] and [Dob15, Thm. 1]). *Let \mathcal{P} be a d -dimensional polytope with algebraic vertex coordinates. Then there is a polytope $\widehat{\mathcal{P}}$ of dimension $d + 2$ that contains a face F that is projectively equivalent to \mathcal{P} in every realization of $\widehat{\mathcal{P}}$.*

Such a polytope $\widehat{\mathcal{P}}$ is called a *stamp* for \mathcal{P} in [Dob11, Dob15]. We are now ready to prove the main result of this part.

Proposition 6.3. *A stamp for a $(d-2)$ -polytope with no $(0, d-3)$ -scribed projectively equivalent realization is not $(0, d-3)$ -scribable.*

Proof. Let \mathcal{P} be a $(d-2)$ -polytope with no $(0, d-3)$ -scribed projectively equivalent realization, whose existence is guaranteed by Lemma 6.1. Observe that in the construction of Lemma 6.1 we can impose that it has algebraic coordinates (and even rational). Now let $\widehat{\mathcal{P}}$ be the stamp polytope from Theorem 6.2. We claim that $\widehat{\mathcal{P}}$ is not $(0, d-3)$ -scribable. Otherwise, its $(d-2)$ -dimensional face F , which is projectively equivalent to \mathcal{P} in every realization of $\widehat{\mathcal{P}}$, is also $(0, d-3)$ -scribed, contradicting our assumption. \square

7. OPEN PROBLEMS

Several natural questions arise from our results. The most intriguing is probably the existence of d -polytopes that cannot be $(0, d - 1)$ -scribed.

Conjecture 7.1. *For $d > 3$, there are d -polytopes that are not $(0, d - 1)$ -scribable.*

Although we strongly believe that the conjecture is true, we did not manage to construct examples. A promising strategy to find such a polytope would be using projectively unique polytopes, or polytopes with a very constrained realization space. So far, the largest family of projectively unique polytopes that we know of are those constructed by Adiprasito and Ziegler [AZ15, Section A.5.2]. However, they are essentially inscribable, and hence they do not provide counterexamples directly.

Even for the case of $(1, d - 1)$ -scribability, our results are not complete. We only managed to find polytopes that are not $(1, d - 1)$ -scribable in even dimensions: for odd dimensions $d \geq 5$, cyclic polytopes do not provide examples; see Proposition 5.9.

Conjecture 7.2. *For every odd $d \geq 3$, there are d -polytopes that are not $(1, d - 1)$ -scribable.*

For odd dimensional cyclic polytopes, we know that they are $(1, d - 1)$ -scribable (Proposition 5.9) but not $(1, \lfloor d/2 \rfloor)$ -scribable (Proposition 5.12). We would like to know

Question 7.3. *For odd $d \geq 5$ and $\lfloor d/2 \rfloor < k < d - 1$, is every cyclic d -polytope $(1, k)$ -scribable?*

We showed that cyclic polytopes with sufficiently many vertices are not circumscribable. We conjecture that this holds for any neighborly polytope.

Conjecture 7.4. *Neighborly polytopes with sufficiently many vertices are not circumscribable.*

If the conjecture is true, the dual of cyclic polytopes would give the first examples of f -vectors that are not inscribable (see also [GZ13]), completing our Theorem 6.

On the other hand, every cyclic polytope is inscribable, and so are all neighborly polytopes of a large family [GP15]. Computational results of Moritz Firsching show that every neighborly 4-polytope with at most 11 vertices is inscribable (personal communication). In [GP15] the following question is posed.

Question 7.5. *Is every neighborly polytope inscribable?*

For stacked polytopes, we do not have results on (i, j) -scribability for $j - i \geq 2$. Unfortunately, the angle-sum technique that proves Theorem 7 does not work for dimension 5 or higher.

Question 7.6. *Given i, j such that $j - i \geq 2$, is every stacked d -polytope (i, j) -scribable?*

REFERENCES

- [AB08] P. Abramenko and K. S. Brown, *Buildings*, GTM, vol. 248, Springer, New York, 2008.
- [ALS08] T. K.-K. Au, F. Luo, and R. Stong, *Comparing corresponding dihedral angles on classical geometric simplices*, Asian J. Math. **12** (2008), no. 2, 203–212.
- [AZ15] K. A. Adiprasito and G. M. Ziegler, *Many projectively unique polytopes*, Invent. Math. **199** (2015), no. 3, 581–652.
- [Bar71] D. W. Barnette, *The minimum number of vertices of a simple polytope*, Israel J. Math. **10** (1971), 121–125.
- [Bar73] D. Barnette, *A proof of the lower bound conjecture for convex polytopes*, Pacific J. Math. **46** (1973), 349–354.
- [BB02] X. Bao and F. Bonahon, *Hyperideal polyhedra in hyperbolic 3-space*, Bull. Soc. Math. France **130** (2002), no. 3, 457–491.
- [Bel02] A. Below, *Complexity of triangulation*, Ph.D. Thesis, Zürich, CH, 2002. <http://dx.doi.org/10.3929/ethz-a-004420540>.
- [BS08] A. I. Bobenko and Y. B. Suris, *Discrete differential geometry: Integrable structure*, Graduate Studies in Mathematics, vol. 98, American Mathematical Society, Providence, RI, 2008.
- [Car11] C. Carathéodory, *Über den Variabilitätsbereich der Fourierschen Konstanten von positiven harmonischen Funktionen.*, Rend. Circ. Mat. Palermo **32** (1911), 193–217 (German).
- [CD00] R. Cordovil and P. Duchet, *Cyclic polytopes and oriented matroids*, European J. Combin. **21** (2000), no. 1, 49–64. Combinatorics of polytopes.
- [Che13] H. Chen, *Apollonian ball packings and stacked polytopes* (2013). Preprint, 18 pp., [arXiv:1306.2515v2](https://arxiv.org/abs/1306.2515v2).

- [Che14] H. Chen, *Even more infinite ball packings from Lorentzian Coxeter systems* (2014). Preprint, 22 pp., [arXiv:1408.2439v1](https://arxiv.org/abs/1408.2439v1).
- [Dob11] M. G. Dobbins, *Representations of Polytopes*, Ph.D. Thesis, Philadelphia, US, 2011. <http://math.temple.edu/graduate/recentphdtheses/mgdtudissf.pdf>.
- [Dob15] M. G. Dobbins, *Antiprismless, or: Reducing Combinatorial Equivalence to Projective Equivalence in Realizability Problems for Polytopes* (2015). Preprint, 33 pp., [arXiv:1307.0071v3](https://arxiv.org/abs/1307.0071v3).
- [DS96] M. B. Dillencourt and W. D. Smith, *Graph-theoretical conditions for inscribability and Delaunay realizability*, Discrete Mathematics **161** (1996), no. 1–3, 63–77.
- [EKZ03] D. Eppstein, G. Kuperberg, and G. M. Ziegler, *Fat 4-polytopes and fatter 3-spheres*, Discrete geometry: In honor of W. Kuperberg's 60th birthday, 2003, pp. 239–265.
- [Gad56] J. W. Gaddum, *Distance sums on a sphere and angle sums in a simplex*, Amer. Math. Monthly **63** (1956), 91–96.
- [GP15] B. Gonska and A. Padrol, *Neighborly inscribed polytopes and Delaunay triangulations* (2015). Preprint, 15 pp., [arXiv:1308.5798v2](https://arxiv.org/abs/1308.5798v2).
- [Grü03] B. Grünbaum, *Convex polytopes*, 2nd ed., Graduate Texts in Mathematics, vol. 221, Springer-Verlag, New York, 2003.
- [GS87] B. Grünbaum and G. C. Shephard, *Some problems on polyhedra*, J. Geom. **29** (1987), no. 2, 182–190.
- [GZ13] B. Gonska and G. M. Ziegler, *Inscribable stacked polytopes*, Adv. Geom. **13** (2013), no. 4, 723–740.
- [Höh53] W. Höhn, *Winkel und Winkelsumme im n-dimensionalen euklidischen Simplex*, Ph.D. Thesis, Zürich, CH, 1953 (German). <http://dx.doi.org/10.3929/ethz-a-000089763>.
- [HRS92] C. D. Hodgson, I. Rivin, and W. D. Smith, *A characterization of convex hyperbolic polyhedra and of convex polyhedra inscribed in the sphere*, Bull. Amer. Math. Soc. (N.S.) **27** (1992), no. 2, 246–251.
- [McM70] P. McMullen, *The maximum numbers of faces of a convex polytope*, Mathematika **17** (1970), 179–184.
- [MTTV97] G. L. Miller, S.-H. Teng, W. Thurston, and S. A. Vavasis, *Separators for sphere-packings and nearest neighbor graphs*, J. ACM **44** (1997), no. 1, 1–29.
- [Rat06] J. G. Ratcliffe, *Foundations of hyperbolic manifolds*, 2nd ed., Graduate Texts in Mathematics, vol. 149, Springer, New York, 2006.
- [RG96] J. Richter-Gebert, *Realization Spaces of Polytopes*, Lecture Notes in Mathematics, vol. 1643, Springer-Verlag, Berlin, 1996.
- [Riv03] I. Rivin, *Combinatorial optimization in geometry*, Adv. Appl. Math. **31** (2003), no. 1, 242–271.
- [Riv93] I. Rivin, *On geometry of convex ideal polyhedra in hyperbolic 3-space*, Topology **32** (1993), no. 1, 87–92.
- [Riv94] I. Rivin, *Euclidean structures on simplicial surfaces and hyperbolic volume*, Ann. Math. (2) **139** (1994), no. 3, 553–580.
- [Riv96] I. Rivin, *A characterization of ideal polyhedra in hyperbolic 3-space*, Ann. of Math. (2) **143** (1996), no. 1, 51–70.
- [Sch05] J.-M. Schlenker, *Hyperideal circle patterns*, Math. Res. Lett. **12** (2005), no. 1, 85–102.
- [Sch87] E. Schulte, *Analogues of Steinitz's theorem about non-inscribable polytopes*, Intuitive geometry (Siófok, 1985), 1987, pp. 503–516.
- [Sei91] R. Seidel, *Exact upper bounds for the number of faces in d-dimensional Voronoi diagrams*, Applied geometry and discrete mathematics, 1991, pp. 517–529.
- [ST96] D. A. Spielman and S.-H. Teng, *Disk packings and planar separators*, Proceedings of the Twelfth Annual Symposium on Computational Geometry, 1996, pp. 349–358.
- [Ste28] E. Steinitz, *Über isoperimetrische Probleme bei konvexen Polyedern*, J. Reine Angew. Math. **159** (1928), 133–143.
- [Ste81] J. Steiner, *Systematische Entwicklung der Abhängigkeit geometrischer Gestalten von einander*, Reimer, Berlin, 1832, J. Steiner's Collected Works, 1881, pp. 229–458.
- [Stu87] B. Sturmfels, *Cyclic polytopes and d-order curves*, Geom. Dedicata **24** (1987), no. 1, 103–107.
- [Vin67] È. B. Vinberg, *Discrete groups generated by reflections in Lobachevskii spaces*, Mat. Sb. (N.S.) **72**(144) (1967), no. 3, 471–488; correction, ibid. **73** (115) (1967), 303. English translation: Math. USSR Sb. **1** (1967), no. 3, 429–444.
- [Vin71] È. B. Vinberg, *Discrete linear groups generated by reflections*, Izv. Akad. Nauk SSSR Ser. Mat. **35** (1971), no. 5, 1072–1112. English translation: Math. USSR Izv. **5** (1971), no. 5, 1083–1119.
- [Vin93] È. B. Vinberg (ed.), *Geometry. II: spaces of constant curvature*, Encyclopaedia of Mathematical Sciences, Springer-Verlag, Berlin, 1993.
- [Zie07] G. M. Ziegler, *Convex polytopes: extremal constructions and f-vector shapes*, Geometric combinatorics, 2007, pp. 617–691.
- [Zie95] G. M. Ziegler, *Lectures on polytopes*, Graduate Texts in Mathematics, vol. 152, Springer-Verlag, New York, 1995.

FREIE UNIVERSITÄT BERLIN, INSTITUT FÜR MATHEMATIK, ARNIMALLEE 2, 14195 BERLIN, GERMANY
 E-mail address: haochen@math.fu-berlin.de

E-mail address: arnau.padrol@fu-berlin.de